MODELLING AND DELAY ANALYSIS OF INTERMITTENTLY CONNECTED ROADSIDE COMMUNICATION NETWORKS

Maurice Khabbaz

A thesis

in

The Department

of

Electrical and Computer Engineering

Presented in Partial Fulfillment of the Requirements

For the Degree of Doctor of Philosophy

Concordia University

Montréal, Québec, Canada

September 2012

Concordia University

Engineering and Computer Science

This is to certify that the thesis prepared

By: **Maurice Khabbaz**

Entitled: **MODELLING AND DELAY ANALYSIS OF INTERMITTENTLY CONNECTED ROADSIDE COMMUNICATION NETWORKS**

and submitted in partial fulfillment of the requirements for the degree of

Doctor of Philosophy (Electrical and Computer Engineering)

complies with the regulations of this University and meets the accepted standards with respect to originality and quality.

Signed by the final examining committee:

Dr. Catherine Mulligan
_____ Chair

Dr. Raouf Boutaba
_____ External Examiner

Dr. Ciprian Alecsandru
_____ External to Program

Dr. Mustafa Mehemet Ali
_____ Examiner

Dr. Dongyu Qiu
_____ Examiner

Dr. Chadi Assi
_____ Thesis Co-Supervisor

Dr. Wissam Fawaz
_____ Thesis Co-Supervisor

Approved by

_____

Chair of Department or Graduate Program Director

_____ _____

Dean of Faculty

Abstract

MODELLING AND DELAY ANALYSIS OF INTERMITTENTLY CONNECTED ROADSIDE COMMUNICATION NETWORKS

Maurice Khabbaz, Ph.D.
Concordia University, 2012

During the past decade, consumers all over the world have been showing an incremental interest in vehicular technology. The world's leading vehicle manufacturers have been and are still engaged in continuous competitions to present for today's sophisticated drivers, vehicles that gratify their demands. This has lead to an outstanding advancement and development of the vehicular manufacturing industry and has primarily contributed to the augmentation of the twenty first century's vehicle with an appealing and intelligent personality. Particularly, the marriage of information technology to the transport infrastructure gave birth to a novel communication paradigm known as *Vehicular Networking*. More precisely, being equipped with computerized modules and wireless communication devices, the majority of today's vehicles qualify to act as typical mobile network nodes that are able to communicate with each other. In addition, these vehicles can as well communicate with other wireless units such as routers, access points, base stations and data posts that are arbitrarily deployed at fixed locations along roadways. These fixed units are referred to as Stationary Roadside Units (SRUs). As a result, ephemeral and self-organized networks can be formed. Such networks are known as *Vehicular Networks* and constitute the core of the latitudinarian *Intelligent Transportation System* (ITS) that embraces a wide variety of applications including but not limited to: traffic management, passenger and road safety, environment monitoring and road surveillance, hot-spot guidance, on the fly Internet access, remote region connectivity, information

sharing and dissemination, peer-to-peer services and so forth.

This thesis presents an in-depth investigation on the possibility of exploiting mobile vehicles to establish connectivity between isolated SRUs. A network of intercommunicating SRUs is referred to as an Intermittently Connected Roadside Communication Network (ICRCN). While inter-vehicular communication as well as vehicle-to-SRU communication has been widely studied in the open literature, the inter-SRU communication has received very little attention. In this thesis, not only do we focus on inter-SRU connectivity establishment through the transport infrastructure but also on the objective of achieving delay-minimal data delivery from a source SRU to a destination SRU in. This delivery process is highly dependent on the vehicular traffic behaviour and more precisely on the arrival times of vehicles to the source SRU as well as these vehicles' speeds. Vehicle arrival times and speeds are, in turn, highly random and are not available *a priori*. Under such conditions, the realization of the delay-minimal data delivery objective becomes remarkably challenging. This is especially true since, upon the arrival of vehicles, the source SRU acts on the spur of the moment and evaluates the suitability of the arriving vehicles. Data bundles are only released to those vehicles that contribute the most to the minimization of the average bundle end-to-end delivery delays. Throughout this thesis, several schemes are developed for this purpose. These schemes differ in their enclosed vehicle selection criterion as well as the adopted bundle release mechanism. Queueing models are developed for the purpose of capturing and describing the source SRU's behaviour as well as the contents of its buffer and the experienced average bundle queueing delay under each of theses schemes. In addition, several mathematical frameworks are established for the purpose of evaluating the average bundle transit delay. Extensive simulations are conducted to validate the developed models and mathematical analyses.

Acknowledgments

"Every long and beautiful journey must finally come to an end."

(Wissam F. Fawaz)

Indeed, pursuing a four-year Ph.D. track was, to me, *beautiful pain*. It was a painful but yet an enjoyable experience. It was exactly similar to climbing a tough mountain, one step at a time, escorted by bitterness, hardships, frustration, the motivations, encouragements, trust and kind help of so many people around. Only at the moment where I have reached the peak of that mountain and started enjoying the beautiful scenery that I realized the fact that what got me there were *The Almighty Lord* and *teamwork*. Praised is your name *Jesus* and though words will never be enough to express my sincere gratitudes to all those people who helped me, I would still like to give it a try.

First and foremost, I would like to express my sincere thanks to my honorific supervisor, Professor *Chadi M. Assi*, who, without hesitation, has admitted me to the program as his advisee. Professor Assi, is one example of a person characterized by *sweet toughness*, superlative ethics, dedication and devotion. As challenging as he is, he is also one of those rare humble professors who actually *care*. Above all, he has never looked over my shoulder. Instead, he has wisely challenged me and surprisingly, he had this amazing skill in turning almost all my attacks of raging fury into screaming laughter. He offered me loads of advices while patiently supervising

me, motivating me and always leading me to the right path. I have learned so much from him. Truly, his role was vital and this dissertation would have never observed light without his continuous support. Professor Assi, it will always be insufficient to express my thanks to you with a few words. However, *Thank You*.

Second, words will also not be enough to express how grateful and thankful I am to my illustrious and scrupulous co-supervisor, Professor *Wissam F. Fawaz*. I am enormously proud of being Professor Fawaz's advisee for the past seven years, ever since I was pursuing the M.Sc. in Engineering program at the Lebanese American University. He has highly contributed in shaping my academic career and my personality on an equal level. Our relationship was not the typical limited student-professor one. It was, indeed, brotherhood. On the academic level, Professor Fawaz is characterized by a highly professional advisory skill that is complemented by a very strong and comprehensive knowledge in Queueing Theory, a field that the international research community classifies as one of the most difficult. He was the one to press the *launch* button of all my contributions done throughout my Ph.D. track. His advices were indispensable and he was able to maintain a sound and high quality supervision irrespective of the long distances that separated us. "No fear Wissam is here," he always repeated. I learned from him heaps and his motivating words and supporting actions came always at the right time to incentivize me to move forward and help me bypass the difficulties. As a matter of fact, he was the one to help me get enrolled at Concordia as he introduced me to Professor Assi. Professor Fawaz, *Many Thanks*.

Third, the final stage of my Ph.D. track has witnessed a wonderful collaboration with Professor *Hamed M. K. Alazemi*. This collaboration fruitfully lead to the publication of highly prestigious and well reputed journal and conference articles. Although I have not had enough time to further get to know Professor Alazemi, but our almost-daily meetings during his seven-months visit to Concordia were enough for me

to discover his wonderful personality, humbleness and sense of humour. Academically, Professor Alazemi is a highly professional researcher touched by a remarkable wisdom and ability to perform in-depth problem analysis. Our long discussions together with Professor Assi were very fruitful and have lead to broadening my knowledge on Stochastic Theory. Professor Alazemi, it was indeed a great pleasure to get to know you, *Thank You*.

Fourth, I would like to express my sincere gratitude to the members of my examining committee, Professor *Raouf Boutaba*, Professor *Mustafa M. Ali*, Professor *Dongyu Qiu*, Professor *Ciprian Alecsandru* and Professor *Pin-Han Ho*, first, for accepting to serve on my committee and, second, for their critical comments and suggestions for improving my doctoral thesis. *Thank you all.*

Fifth, I would like to express my sincere thanks to the Computer Systems Odessa (CSODESSA) for their collaboration on the development of a novel ConceptDRAW Vehicular Networking Solution that will provide researchers in the field with a new diagramming dimension for the purpose of illustrating and visualizing the future new vehicular data networking concepts. *Thank You.*

Sixth, I cannot but express my appreciation and my heartfelt thanks to my home university and Alma Matter, the *Lebanese American University*, as well as to all my professors there and particularly the chairperson of the Electrical and Computer Engineering (ECE) Department, Professor *Samer S. Saab*. It was, indeed, Professor Saab who, more than nine years ago, had initially prepared the ground for me to become what I am today. Back then, I was a student in one of his classes. He strongly believed in my capabilities. He taught me and then adopted me as his assistant for five consecutive years. During all these years I have learned a lot from him. He has opened the gates of success for me and welcomed me in. As I closely worked under his supervision, I couldn't but notice how much hard working he is

and how much effort he invests with all enthusiasm and passion in doing what he believes is best for his students. Ever since he became the chairperson of the ECE department, that department never ceased to advance and develop both on academic and reputation levels. He, in fact, was the *dynamo* of the ECE department. Wherever he walks, he throws positive energy, motivation and plants courage and will in the hearts and minds of his faculty and students. I cannot be more proud that once I have served him as assistant, was his student in four courses and learned from him on both academic and humanitarian levels based on which I am building my professional career and life. Professor Saab, *Million Thanks*.

Seventh, I would like to express my profound gratitude to my ever spiritual guide, Father *Richard R. Daher*. Truly, ever since I was first introduced to Father Richard, I felt that life, in Montreal, was going to be much more beautiful and indeed it was. Father Richard is a distinguished priest who speaks in the name of the *Love and Peace of Jesus Christ*. He is Humble, pure, loving, caring and much more. Above all, he is full of faith in *Jesus*, our Lord. He has played a major role and rendered my life, in Montreal, as easy and happy as it can be. He adopted me and named me his *miraculous child*. In all what the word has in meaning, he, indeed, was to me the father who offered me his shoulder and hands when I was in need. He, his wife *Gisele* and their children *Myriam* and *Raymond*, constituted my second family in Canada. As a matter of fact, after I got to know them, I never felt alone anymore. His home was to me the second roof under which I was warmly received. All throughout my stay in Montreal, Father Richard was always there when I needed to talk to someone. He was my secret holder and his advices and guidance were always in their right place at the right time. No matter how much I try father, these words will never be enough to thank you. *Many Thanks*.

Eighth, I cannot forget all my dear friends here in Montreal. Those who really proved to be there when I needed them especially, *Walid Abou Assaly*, *Georges Dagher*, *Siham Farhoud*, Professor *Georges Kanaan* and all members of the *Paroisse Notre Dame de L'Assomption Choir*. They have always motivated me and believed in my capabilities. I am highly grateful for their kind help and support. To all of you, *So Many Thanks*.

Last but not least, my most tender thanks go to those people who are the closest to my heart: my father *Joseph Khabbaz* for all his prayers from up above and to who I dedicate all this work, my mother *Nada Khabbaz*, my grand-mothers *Natacha Khabbaz* and *Andree Sarrouf*, the ever amazing brother and best friend *Charbel Abou Jreish* and finally *Abdallah Khoury*. Each and every one of you has played an ever fundamental role in my life. Without each and every one of you, I would have not been able to achieve my ambitions. You always believed in me and supported me on all levels. You have filled my heart with love and always made me feel how proud you were of me. This alone has rendered me steadfast and pushed me to never bend down to difficulty and always do my best at things. All of you constitute the backbone and origin of my happiness. I owe you my every achievement. *I Love You All*.

Maurice J. Khabbaz

Montreal, May 2012.

Contents

List of Figures

List of Acronyms

3G	Third Generation
4G	Fourth Generation
ACK	Acknowledgement
AMC	Adaptive Modulation and Coding
ARQ	Automatic Repeat Request
BBR	Bulk Bundle Release
CLO	Cross-Layer Optimization
CRT	Cognitive Radio Technology
CSMM	City Section Mobility Model
DSA	Dynamic Spectrum Assignment
DODD	Delay-Optimal Data Delivery
DSRC	Dedicated Short Range Communications
FCC	Federal Communications Commission
FMM	Freeway Mobility Model
FTM	Free-flow Traffic Model
GBRS	Greedy Bundle Release Scheme
GN	Global Network
IEEE	Institute of Electrical and Electronics Engineers
ICRCN	Intermittently Connected Roadside Communication Network
ITS	Intelligent Transportation System

LMS	Location and Monitoring Service
LSA	Link Scheduling and Activation
LTE	Long Term Evolution
MAC	Medium Access Control
MANET	Mobile AdHoc Network
MB	Main Buffer
MDP	Markov Decision Process
MMM	Manhattan Mobility Model
MUD	Multi-user Decoding
NACK	Negative Acknowledgement
NTL	National Transportation Library
OFDM	Orthogonal Frequency Division Multiplexing
PDA	Personal Digital Assistant
PBRS	Probabilistic Bundle Release Scheme
PHY	Physical Layer
PRC	Power Rate Control
RCT	Relay-based Cooperative Techniques
RCN	Roadside Communication Network
RITA	Research and Innovative Technology Administration
S2S	SRU-to-SRU
SA	Smart Antenna
SCF	Store-Carry-Forward
SRU	Stationary Roadside Unit
TCP	Transmission Control Protocol
TRC	Transmission Rate Control
V2V	Vehicle-to-Vehicle

V2S	Vehicle-to-SRU
VANET	Vehicular Ad-Hoc Network
VS	Virtual Space
WAVE	Wireless Access in Vehicular Environments
WiMAX	Worldwide Interoperability for Microwave Access

Chapter 1

Introduction

1.1 Overview

A couple of years ago, according to [1], as some government officials enthusiastically spoke about a new telephone system for villages and remote rural areas in developing nations, villagers questioned the utility and benefits of this new system as, at that time, given the fact that they lived in these quite isolated areas, they really knew nobody who owned a telephone. Yet, irrespective of this delicate observation, the telephone system was conscientiously set up as part of the government's commission to interconnect these villages to neighbouring cities and towns. Even though very few villagers sporadically utilized this new telephone system, the other majority of them still engaged in long travels to join their families or obtain some information that habitants of the civilized nations were able to procure in no time over the Internet.

To render a long story short, the primitive telephone service erroneously believed to be the minimal-cost connectivity provisioning solution has lead to the cataclysmic suspension of the of *all-time-anywhere-broadband-connectivity* plan. Indeed, such a compromise is irregularly tragic given the exponentially advancing world of wireless

digital communication and technology which renders the installation costs of an analog telephone system, as opposed to the adoption of wireless broadband, grow far beyond any expectation. Consequently, instead of reneging the primary objective of *broadband-connectivity-to-all*, government agencies as well as the private sectors and research communities were incentivized to engage into establishing the foundation of a progressive and economic-status-driven migration from *e-Government*, [2], to ubiquitous broadband connectivity whose charges are handled by local users. The marriage of wireless technology to the asynchronous type of services constituted the ever embraced kernel that allowed for leapfrogging past the elevated expenses of primitive analog connectivity solutions and launch into the development of a full-fledged digital wireless broadband infrastructure, [1].

Today, wireless communication technology is advancing revolutionarily. Key drivers for this unprecedented evolution include but are not limited to:

1. The maturation of third-generation ($3G$) wireless network services.

2. The development of smart-phones (*e.g.* iPhone, BlackBerry, Galaxy Nexus and so many more) as well as other mobile computing devices (*e.g.* Laptops, PDAs and so forth).

3. The emergence of broad new classes of connected devices (*e.g.* SmartPads).

4. The roll out of $4G$ wireless technologies such as Long Term Evolution (LTE) and WiMAX, [3].

Recently, major wireless operators in the United States (*e.g.* AT&T and VERIZON) have reported massive data traffic growths in their networks which is partly driven part by the usage of smart-phones. According to CISCO, wireless networks in North America carried approximately 17 *petabytes* per month in 2009, [4]. It is also projected that in 2014 these networks will carry around a 40-fold increase. The

reason behind this substantial traffic growth is the increased adoption of Internet-connected mobile computing devices and increased data consumption per device [5]. Furthermore, a surge of machine-based wireless broadband communications is forecasted for the next few coming years, as more smart devices (*e.g.* electric vehicles, body sensors, wireless enabled cameras, smart meters and so forth) will exploit this type of universal wireless connectivity. The aggregate impact of these devices on demand for wireless broadband access could be enormous, [5].

Improving the wireless channel capacity has been the limiting factor for unleashing the broadband capabilities; this has been an ominous task, irrespective of the recently witnessed progress in the techniques used for improving the performance and reliability of wireless communication as well as mitigating the effects of interference, fading, and detrimental propagation conditions, and finally increasing the spectrum efficiency. These techniques include but are not limited to:

1. Adaptive Modulation and Coding (AMC), [6].
2. Multi-user Decoding (MUD), [7].
3. Smart Antenna (SA), [8].
4. Orthogonal Frequency Division Multiplexing (OFDM), [9].
5. Relay-based Cooperative Techniques (RCT), [10].
6. Cognitive Radio Technology (CRT) and Dynamic Spectrum Assignment (DSA) [11].
7. Routing, Power and Transmission Rate Control (PRC/TRC) Techniques, [12].
8. Link Scheduling and Activation (LSA), [13].
9. Cross-Layer Optimization (CLO), [14].

Besides increasing the capacity of future wireless systems, one other objective for a prevalent broadband is to extend the wireless service coverage. One technical solution for achieving this objective has already attracted growing interests and it essentially consists of deploying home base stations, commonly known as Femtocells, [15]. Femtocells operate on licensed bands and are deployed by mobile operators to increase the coverage inside homes and buildings and provide high-speed wireless connectivity. There remain however technical and economic challenges, which could hinder their mass deployments. For instances, interference mitigation between neighbouring Femtocells as well as between Femtocells and Macrocells, opportunistic cooperation in cognitive Femtocell networks, distributed coordination and resource allocation, multi-cell coordination and interference control, providing incentives for users to deploy and open up their Femtocell networks and so forth, all are challenging problems.

In addition to deploying home base stations, currently road base stations or access points, commonly known as stationary roadside units (SRUs), are becoming more and more prevalent, to support the development and implementation of Intelligent Transportation Systems (ITS); currently, this is gaining significant momentum, especially after the Federal Communication Commission (FCC) in the United States has allocated 75 (MHz) of spectrum over the 5.9 (GHz) licensed band for the purpose of integrating radio-based technologies into the nation's vehicular infrastructure, [16]. Also, the Institute of Electrical and Electronics Engineers (IEEE) has recently released the 1609 protocol suite and the 802.11p standard for Wireless Access in Vehicular Environments (WAVE), [17]. ITS radio services include Dedicated Short Range Communications (DSRC) service, which involves vehicle-to-vehicle and vehicle-to-infrastructure communications, Location and Monitoring Service (LMS)

for determining the location and status of mobile radio units and so much more. Vehicular networking will also enable diverse applications associated with traffic management, passenger and road safety (*e.g.* [18, 19]), environment monitoring and road surveillance, Location lookup and hot-spot guidance (*e.g.* [20]), location management (*e.g.* [21]), on the fly Internet access, remote region connectivity (*e.g.* [1, 22]), information sharing and dissemination (*e.g.* [23]), peer-to-peer services and infotainment (*e.g.* [24]) and so forth. These vehicular networks will serve as catalyst for increasing the coverage of broadband and are poised to become the largest and most widely distributed ad hoc networks. Indeed, their auto-integration as part of the catholic Global Network (GN) is being steadily promoted. Nevertheless, a wide variety of challenges need to be resolved before a full-fledged vehicular network can be deployed.

1.2 Problem Statement

As the usage of wireless broadband communications increases, demand for other wireless services, such as point-to-point microwave backhaul and unlicensed networks to enhance the overall broadband access probability, increases. Such wireless backhauls transport large quantities of data to and from cell sites, especially in rural areas. Hence, unleashing the full potential of broadband will require looking beyond efficient techniques for increasing the wireless channel capacity as well as spectrum utilization and allocation in wireless cellular and/or wireless home networks (*i.e.* last mile connectivity); it requires addressing other potential network bottlenecks, namely backhaul connectivity. However, when the spectrum is in shortage, the utilization of microwave links to connect remotely located cell sites becomes difficult and may

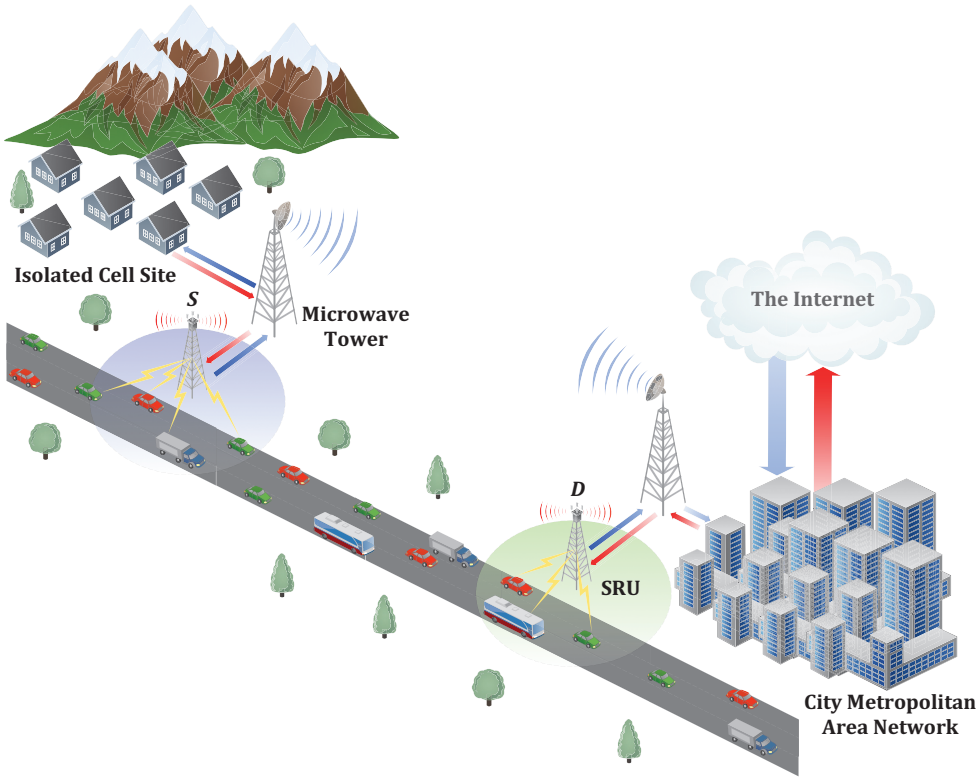

Figure 1.1: Intermittently connected roadside subnetwork serving as a emergency data transport backhaul whenever the microwave link is down.

suffer from bandwidth insufficiency to carry the aggregate traffic. Under such circumstances, vehicular networks have the potency of acting as cooperative content distribution and sharing systems that enable data transfers from one cell site to the other. In particular, as shown in Figure 1.1, one SRU is deployed in the proximity of each cell site. These SRUs will opportunistically exploit mobile vehicles plying between them as physical data carriers from one cell site to another. As a result, the vehicular infrastructure presents itself as a naturally established and effective data emergency transport backhaul that serves the purpose of re-establishing connectivity between the disconnected cell sites at any time the microwave link goes down. Furthermore, it has been widely established that the installation and maintenance of networking infrastructure in rural and sparsely populated areas is significantly costly, [1]. An efficient and cost-nominal solution lies in the deployment of SRUs along roadways

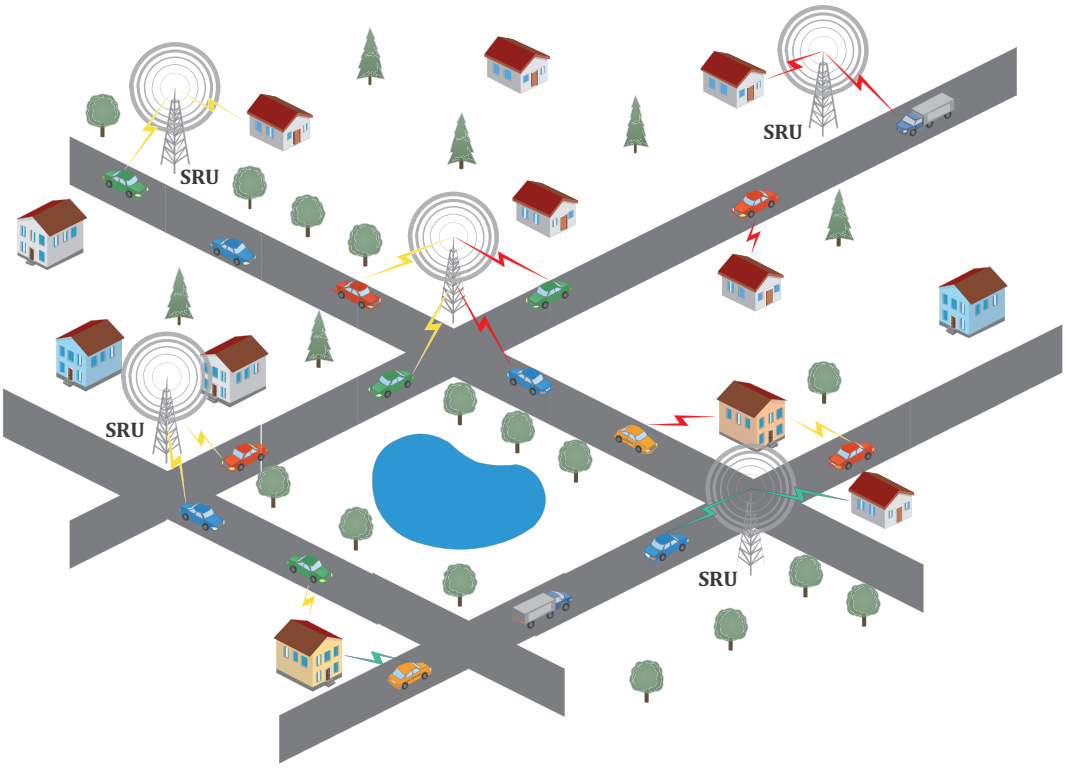

Figure 1.2: SRUs in a rural ICRCN serving as routers or as access points in hot spots.

within these areas as shown in Figure 1.2. In some situations, it is possible that very few of these SRUs, called *gateways*, be privileged by a connection to the Internet. On the exception of these gateways which require minimal networking infrastructure, all other SRUs may be arbitrarily deployed along roadsides with no direct connectivity to each other or to any backbone network. End users deposit data at arbitrary SRUs and, from that point on, it is the job of these SRUs to opportunistically exploit the transport infrastructure as a means for appropriately routing the incoming data messages to their intended destinations. Therefore, in this context, SRUs are characterized by a dual functionality. They may act as either routers or as access points in hot spots, [25, 26]. In either one of the two above-described scenarios the type of inter-SRU communication that takes place is by no means similar to any connectivity established between two wireless nodes operating within a typical Mobile Ad Hoc

Network (MANET). In particular, the functionality as well as the performance of the Roadside Communication Network (RCN) is highly correlated to the behaviour of vehicular traffic. Vehicular traffic, however, is a remarkably random spatiotemporal process that is affected by numerous microscopic factors such as weather, road geometry, commuter skills and habits and the like. For example, in populated areas as well as during rush hours, roadways witness a much greater vehicular density with vehicles navigating at low speeds. This promotes the network's connectivity as the formation of continuous end-to-end paths between communicating SRUs through the vehicles becomes more likely feasible. Under such conditions, the existing MANET protocols can be used for routing and forwarding data between two communicating SRUs. In contrast, in rural areas as well as during non-rush hours and night times, the vehicular density over a particular roadway swings between medium to low and vehicles tend to navigate at high speeds. In Traffic Flow Theory, this type of traffic is known as the Free-flow vehicular traffic, [27, 28]. Under Free-flow traffic conditions, the contact between two arbitrary vehicles, if ever established, is characterized by a very short duration. The contact between a vehicle and an SRU is also short. Consequently, volatile (*i.e.* intermittent) connectivity that is characterized by irregular delays becomes a major obstacle that stands in the way of the utilization of typical MANET communication protocols.

A recently published survey, [29], indicates that dense vehicular networks, otherwise known as Vehicular Ad-Hoc Networks (VANETs), have received significant attention throughout the past couple of years. However, the majority of the published work on VANETs are founded on top of the continuous end-to-end connectivity assumption. Intermittently Connected Roadside Communication Networks (ICRCNs), however, operate beyond the end-to-end connectivity hypothesis. This particular area remains an open and immature field of research and constitutes the core of this

thesis. More precisely, we consider an intermittently connected roadside communication subnetwork scenario consisting of two SRUs, a source S and a destination D, deployed along a one-dimensional uninterrupted roadway segment experiencing Free-flow vehicular traffic conditions. The distance separating these two SRUs is much larger than their respective coverage range. Hence, they cannot directly communicate. Consequently, in the absence of any kind of networking infrastructure that connects S to D, mobile vehicles equipped with wireless devices and computerized control modules serve as opportunistic *store-carry-forward* (SCF) devices that physically transport data from S to D. S communicates data bundles to D using these vehicles. At this level, it is important to mention that, recently, a lot of work and investigations on inter-vehicular communications are ongoing, [24, 29–36]. Unfortunately, thus far, results highlight a remarkable amount of technical challenges facing this type of communication as well as its inefficiency. Hence, the various studies conducted in this thesis are built upon the assumption that no inter-vehicular communication takes place. Vehicles only communicate with the SRUs. Consequently, the data delivery process consists of two hops, namely: *i*) from S to the carrying vehicle and *ii*) from the carrying vehicle to D. As a result, a data message may experience an irregularly high end-to-end delivery delay. This is especially true since S may wait a certain period of time that ranges from a few seconds to a few minutes before a vehicle arrives and then vehicles may travel the distance from S to D during a period of time that ranges from a few minutes to even a couple of hours. Hence, end-to-end data delivery delay-minimization in this context becomes of particular interest. In this thesis several data relaying schemes are developed for this purpose. The average message end-to-end delivery delay is composed of two factors, namely:

1. *The average message queueing delay*: The average time period during which a message is buffered at the source SRU. This time period is lower bounded by

the time where the message arrives to the source SRU and upper bounded by the time where the SRU releases the message to a vehicle.

2. *The average message transit delay*: The average time period that a message spends in travelling over a vehicle from S to D. This time interval is equivalent to the vehicle's average travel time from S to D.

Queueing models are proposed to represent the behaviour of S as well as to evaluate its performance, particularly in terms of the average queueing delay, under each of the developed schemes. In addition, thorough analysis is performed for the purpose of determining the average message transit delay from S to D. Furthermore, it has been observed from the open literature that the majority of the work addressing issues in vehicular networking was built on top of independently developed vehicular traffic models that are tailored to specifically suite their enclosing studies. These existing models are, indeed, founded on top of restrictive assumptions that drive them away from reality. Knowing that the performance of data relaying schemes in the above-described context is highly dependent on the behaviour of vehicular traffic, a comprehensive overview of traffic behaviour is conducted in light of the rudimentary principles of traffic theory. This overview provided further insight into to the adoption of a simple and accurate Free-flow vehicular traffic model that that was developed in [37]. This model allows for the selection of appropriate vehicle flow and speed distributions in order to parallel the realistic traffic behaviour as observed by traffic theorists and engineers. This newly developed vehicular traffic model may serve as a building block for the developed schemes in this thesis.

1.3 Thesis Contributions

The following are the major contributions of this thesis:

1. The first contribution of this thesis manifests itself in the development of a Probabilistic Bundle[1] Release Scheme (PBRS), [39]. This scheme is to be deployed at SRUs operating in the context of the earlier-described IRCN scenario and has the objective of minimizing the bundle end-to-end delivery delay. In this context, delivery delay minimization is often desirable and emerges as a quite delicate yet rarely and inadequately addressed problem in the open literature where some of the existing solutions are infeasible due to their complexity while others are based on unrealistic implicit assumptions (*e.g.* complete network information availability). As opposed to these existing solutions, PBRS is a simple scheme that is designed around minimal network information knowledge. It relies on a novel and original probabilistic parameter P_{br} called the *probability of bundle release*. P_{br} indicates to the source SRU which among the arriving vehicles are those that achieve relatively faster bundle transits. Consequently, the source releases bundles, one at a time, only to those vehicles. On average, this scheme ensures the minimization of the bundle transit delay. For the purpose of evaluating the performance of PBRS, another benchmark scheme, called the Greedy Bundle Release Scheme (GBRS) is developed. Under GBRS, the source SRU greedily released a bundle to every arriving vehicle irrespective of its speed. Two queueing models are developed to respectively characterize the source SRU under both schemes.

2. Enlightened by rudimentary principles borrowed from vehicular traffic theory [27, 28], the second contribution of this thesis appears in the layout of a comprehensive overview of the Free-flow vehicular traffic behaviour. Precisely, this overview helps in identifying the macroscopic vehicular traffic features as

[1]Data and control signals are combined in a single atomic entity, called bundle, that is transmitted across an intermittently connected network. It is simply a message, [38]

described by traffic theorists and in characterizing the random, density dependent behaviour of traffic flow, vehicle speeds and travel times using appropriate and highly accurate probability distributions. The acquired knowledge following this vehicular traffic overview has lead to the meticulous selection and adoption of an existing queueing-theory-inspired traffic model developed in [37]. Throughout this thesis, this model is referred to as the Free-flow Traffic Model (FTM). It is found that this model accurately captures the dynamics of a roadway experiencing Free-flow vehicular traffic. Particularly, since, under such traffic conditions, the probability that a given roadway segment attains full capacity[2] is zero, the road segment may, as done in [37], be modelled as an infinite-server queueing system and each vehicle navigating over that segment as a job occupying one of the available servers for a finite amount of time. This amount of time is equivalent to the vehicle's residence time (*i.e.* the amount of time this vehicle will take to travel the entire segment's length) and depends on the vehicle's speed and the length of the segment. Nonetheless, the computation of the mean vehicle's residence time using the vehicle speed distribution utilized in [37] is a complex task. This is especially true since this distribution leads to an integral expression that has no closed-form solution. To work around this problem, the authors of [37] have resorted to numerical evaluation. In contrast, in this thesis, we propose to approximate the vehicle residence time distribution by a two-phase Coxian distribution. We show that the proposed approximation leads to highly accurate results, let along that it provides a simple closed-form expression for the vehicle residence time distribution as well as its mean. It is important to note that one of the major performance measures of FTM is the number of vehicles residing within the considered road

[2]A segment of a road has a well determined length. Consequently, only a finite number of vehicles may simultaneously navigate within that segment. This number is referred to as the capacity of the road segment.

segment which is equivalent to the number of busy servers. This metric was characterized in [37] by a probability distribution that is highly dependent on the average vehicle residence time. Hence, using our approximated version of the average vehicle residence time we show that the approximated steady-state distribution of the number of busy servers is also highly accurate.

3. The advancements in wireless technology have allowed for data transmission rates in the order of tens of *Mbps* resulting in a negligible bundle transmission time when compared to a vehicle's *dwell time* (*i.e.* the amount of time a vehicle resides in the range of the source). Consequently, the opportunistic release of only a single bundle (as PBRS does) yields a waste of precious amounts of residual vehicle dwell times during which the source remains idle while buffered bundles rapidly accumulate queueing delays. Alternatively, releasing as many bundles as possible during the entire vehicle dwell time seems to be a promising and much more efficient approach. Therefore, the third thesis contribution consists of proposing a variation of PBRS and GBRS with Bulk Bundle Release (BBR), [40]. The size of a bulk is a random variable that highly depends on the number of buffered bundles at the source and the bundle admission capabilities of arriving vehicles. PBRS-BBR inherits from its non-BBR ancestor the efficiency of releasing bulks to vehicles that contribute the most to the minimization of the mean bundle transit delay. GBRS-BBR, however, unwisely releases bulks to every arriving vehicle. The general potency of the BBR mechanism in boosting the performance of IRCN data relaying strategies, the delay performance of PBRS-BBR and GBRS-BBR as well as their realistic aspect are underlined using a detailed analytical study that exploits the probability distributions of traffic flow and vehicle speeds drawn from the above-established vehicular traffic model.

4. The fourth and last contribution of this thesis lies in the development of a revolutionary and complete knowledge *unaware* Delay-Optimal Data Delivery (DODD) scheme, [41]. The primary objective of DODD is to achieve delay-minimal bundle delivery from the source SRU to the destination SRU. The core of DODD is structured on top of the famous principle of packet retransmission mechanisms used in typical data communication networks for the purpose of recovering from packet losses or transmission errors. In contrast, DODD leverages such a mechanism together with the concept of *Virtual Space* (refer to [42]) for the purpose of enabling the source SRU to perform necessary retransmissions of bundle copies to faster arriving vehicles. These vehicles will, in turn, secure earlier delivery of the retransmitted copies to the destination SRU. A queueing model that characterizes the operation of the source SRU under DODD is presented and followed by extensive mathematical analysis for the purpose of evaluating the achieved end-to-end delivery delay thereafter.

1.4 Thesis Outline

The remaining of this thesis is organized as follows. Chapter 2 presents the background and literature survey on existing related work to the investigated problems throughout this thesis. Chapter 3 introduces the bundle release probability and presents the probabilistic and greedy bundle release schemes PBRS and GBRS. In Chapter 4, a comprehensive study is conducted on the Free-flow vehicular traffic behaviour followed by the presentation of a Simple Free-flow Traffic Model. Using this model as a building block, Chapter 5 presents the Bulk-Bundle-Release-enabled (BBR) versions of PBRS and GBRS. Building on the problem understanding and knowledge acquired throughout the development of PBRS, GBRS and their BBR-enabled versions, a Delay-Optimal Data Delivery (DODD) scheme is presented in

Chapter 6. Finally, Chapter 7 concludes the thesis and presents a collection of open issues for future consideration.

Chapter 2

Background and Related Work

This chapter presents the background as well as the literature survey on major work related to the investigated topics throughout this thesis.

2.1 Vehicular Networking and Communications

As already described in Chapter 1, the networking scenario under the microscope focuses on the establishment of connectivity between two SRUs, either one or both of which being completely isolated . This particular type of data communication, even though relying on the transport infrastructure, has, thus far, received very little attention. In fact, the majority of the published work on vehicular networking revolves around the inter-vehicular as well as the vehicle-to-SRU type of communication both in the downlink and uplink direction. A brief overview of a prime selection of these studies in summarized as follows.

2.1.1 Inter-Vehicular Communication

A recent survey, [29], revealed that this type of communication remains stringently limited and often impossible due to the high speeds of crossing vehicles that result

in very short contact durations. A contemporaneous study [34] based on real-world experimentations concludes that the contact durations between vehicles crossing at 20, 40 and 60 *kilometers per hour* $\left(\frac{Km}{hr}\right)$ are respectively 40, 15 and 11 *seconds*. In particular, in four out of ten experiments, whenever crossing vehicles are navigating at 60 $\left(\frac{Km}{hr}\right)$ the maximum goodput achieved by TCP is 80 *kilobytes*. In the other six experiments, no data transfer was feasible at all. UDP exhibited a better performance under the same conditions with about 2 *megabytes* of transferred data. The authors of [34] also indicate that under speeds higher than 60 $\left(\frac{Km}{hr}\right)$, TCP completely fails while UDP's performance significantly degrades. In addition, whenever vehicle-to-vehicle (V2V) communication is used, when possible, to form unicast end-to-end paths between two communicating nodes, it was proven in [43] that 91% of these paths had a lifetime that is no longer than 50 seconds. Moreover, significant data losses occurred around the third and fourth hop due to path disruption. This uncovers the inefficiency of the typical Internet protocol suite when used for inter-vehicular communication and especially for transferring large amounts of data over multi-hop paths. To remedy this problem, the IEEE has recently developed the 1609 family of standards for Wireless Access in Vehicular Environment (WAVE), [44]. In particular, the IEEE 1609.3 defines network and transport layer services including addressing and routing. The 1609 family was complemented by the recent release of the IEEE 802.11p standard as an extension to the typical 802.11 known as WiFi, [17]. The 802.11p encloses several Medium Access Control (MAC) and Physical Layer (PHY) refinements to support wireless access in vehicular environments. Nevertheless, according to [44], the 1609 family of standards is still under trial and not yet finalized. Also, following a recent post from the Research and Innovative Technology Administration (RITA) of the National Transportation Library (NTL), the 1609 protocol suite, thus far, suffers from several shortcomings, these being caused by the highly

dynamic nature of the radio mobility and repetitive link disruptions, [45]. As such, it still cannot be relied on to expedite large data transfers in the context of the earlier considered networking scenario in Chapter 1. For this reason, throughout this thesis, inter-vehicular communication is disabled.

2.1.2 Vehicle-To-SRU Communication

In [46], the authors provide more insight into drive-through Internet access using Vehicle-To-SRU (V2S) communication. The authors of [47] investigate the usability of WiMAX as an alternative to WiFi for V2S communication. Initial real-world measurements show that, even though WiMAX offers a longer communication range than WiFi, its latency can be significantly larger than that of WiFi for distances that are less than 100 *meters*. Also, they indicate that the setting of frame size has a strong impact on the performance of WiMAX. Following their extension of the IEEE 802.11*p* standard in [48], the authors in [49] propose a communication system for safety-critical V2S communication with the objective of efficiently distributing resources between safety-critical and non-safety-critical data. The work of [50] revolves around a study of the access and connectivity probabilities between vehicles and SRUs. A trade-off is revealed between key system parameters such as inter-SRU distance, vehicular density, SRU and vehicle transmission ranges. The authors study the collective impact of these parameters on the access and connectivity probabilities under different channel modes with the objective of providing more insight for improving network planning, SRU deployment and resource provisioning. In [51], multi-hop packet delivery delay is studied in the context of a low density vehicular network. There, the authors' primary objective was to come up with an optimal SRU placement strategy that stochastically limits the worst case data delivery delay to a given bound.

2.1.3 Inter-SRU Communication

The exploitation of the mobile vehicular infrastructure to achieve this type of communication is mostly applicable in developing nations as well as in rural and mountainous areas where the setup of networking infrastructure is significantly costly. Furthermore, as mentioned earlier, the vehicular infrastructure provides unparalleled opportunistic connectivity solution to offload data traffic and relieve backbone wireless networks from congestions. Interestingly, whenever a microwave link such as the one depicted in Figure 1.1 fails, vehicular networks provide a precious backup channel to work around this failure until it is fixed and the link restored. Of course this is doable at the cost of some irregular delays. However, delayed connectivity is certainly much better than no connectivity at all. Very little work has been done in this area especially under conditions of low-to-medium vehicular traffic. The authors of [52] focus on the design of the SRU-to-vehicle data transfer mechanisms using typical WiFi. In addition, they investigate the development of data delivery schemes that exploit the vehicular infrastructure to achieve reliable S2S data delivery. They indicate that rateless coding schemes are efficient for transferring small-to-moderate size files, while hybrid ARQ/data replication schemes are suitable for larger file transfers. In [53], the authors investigate the feasibility of data relaying through vehicles as a minimal-cost strategy that provides inter-SRU virtual data paths. They develop a protocol suite for this purpose and reveal that an effective throughput of 4.5 *Mbps* is achievable with minimal overhead for a peak data rate of 11 *Mbps*. In addition, they show that in worst cases where only a fraction that is as low as 5% of the vehicles are communication-enabled, the obtained throughput is approximately 2 *Mbps*. In [25], the authors investigate a joint scheduling/delay optimization problem in a similar context. However, there, delay-optimality was achieved under the assumption of complete *a priori* knowledge of vehicle parameters (*i.e.* arrival time and speed).

In reality, a vehicle's parameters are unknown until this vehicle enters the coverage range of S. In addition to the above summarized work, real-life projects implementing inter-SRU communication include KioskNet [54], DakNet [1] and DieselNet [22]. All of these projects aim at provisioning remote villages and underdeveloped rural communities with asynchronous messaging services. They primarily exploit buses plying between isolated regions as data mules carrying information messages from one village to another. Ultimately, these buses may cross a wireless Internet gateway and forward all of the messages they carry on to the Internet or vice versa.

2.2 Vehicular Traffic Models

The research community has thus far witnessed the publication of various seminal studies incorporating traffic models that attempt to emulate realistic vehicular traffic behaviour. A distinguished selection of these traffic models is surveyed in this section.

Stochastic Traffic Models

These models are simplistic and do not account for any of the fundamental principles of vehicular traffic theory. They describe the random mobility of vehicles using graphs that represent roadway topologies. The movement of vehicles is random in the sense that either individual or a group of vehicles navigate at random speeds over any arbitrary one of the paths represented by the graph. The interactive behaviour among vehicles as well as the correlation between the vehicular density, vehicles' speeds and the overall traffic flow rate is often neglected or over-simplified. The performance of these models is traditionally contrasted to fully random mobility models that impose no constraints on the nodes' mobility (*e.g.* Random Walk [55], Random Waypoint [56]). Most stochastic models deviate from reality due to their highly restrictive assumptions.

Examples of stochastic traffic models include the City Section Mobility Model (CSMM) introduced in [57]. Under CSMM all edges of the roadway topology graph are considered bi-directional and one-dimensional roads. All the edges intersect and form a grid. Vehicles select at random one of the intersections as their travel destination. They move towards this destination at constant speed. Motions are either vertical or horizontal. In addition, the model distinguishes between two speed levels respectively a high and a low speed.

In [58], the authors investigate the effect of different mobility models on a selection of vehicular networking performance metrics. For this purpose they adopt a Freeway Mobility Model (FMM) and a Manhattan Mobility Model (MMM). Under FMM, freeways are considered to be multi-lane and bi-directional. Furthermore, the vehicular mobility is subject to a set of constraints, namely: *a*) a vehicle is not allowed to switch lanes, *b*) the speeds of vehicles are assumed to be uniformly distributed over a specific range, and *c*) vehicles must be spaced out by a minimum safety distance. Finally, the authors conduct their study under the assumption that no more than one vehicle exists on the considered roadway segment.

Traffic Stream Models

Such models interpret vehicular mobility as a hydrodynamic spatiotemporal phenomenon. They fall under the category of macroscopic models. This is especially true since they regard vehicular traffic as a flow and relate the three fundamental macroscopic parameters, namely: *i*) the vehicular density, *ii*) the vehicles' speed and *iii*) the traffic flow rate. Traffic stream models do not independently consider the per vehicle behaviour. Instead, they describe the collective behaviour of large vehicles streams. This renders them of particular utility for high-level analytical studies of traffic behaviour as part of the design of data delivery schemes for vehicular networks.

Nevertheless, the existing macroscopic models in the open literature are based on different restrictive and case specific assumptions. Hence, comparing the performance of designed data delivery strategies built on top of these models becomes not meaningful. The networking research community lacks a universal macroscopic model that is simple, realistically accounts for the fundamental principles of vehicular traffic theory and hence constitute the primary building block in the design of vehicular networking data delivery schemes.

The simplest model of this kind was proposed in [59] where the authors assume that the velocity is a function of the density. This model is particularly capable of modelling kinematic waves and has been used over the past couple of years by researchers in the field of vehicular networking.

The work of [51] addresses the joint connectivity and delay-control problem in the context of a highly restrictive macroscopic vehicular mobility model where vehicles navigate at only two speed levels respectively high speed V_H and low speed V_L. Precisely, the authors assume that a vehicle may assume a speed level V_H (V_L) for an exponentially distributed amount of time before switching to V_L (V_H) independently of the traffic flow and density the values of which seemed to be chosen arbitrarily.

In [60], the authors exploit inter-vehicular communication to establish continuous end-to-end connectivity. However, throughout their study, the authors propose to approximate the macroscopic vehicular traffic dynamics using the combination of: *a*) a fluid model, *b*) a stochastic model and *c*) a density-dependent velocity profile. Even though their proposed approach is remarkably accurate, it is however highly complex.

The authors of [25] adopt the Markov Decision Process (MDP) approach in their design of a data delivery scheme that has the objective of minimizing the transit delay. In addition to the remarkable complexity of their MDP framework, the authors

neglect the correlation between the vehicular flow and speed. Moreover, they assume that vehicle speeds and inter-arrival times are drawn from known but unspecified probability distributions. These assumptions render their work highly theoretical with limited practicality.

Car Following Models

Such models describe the individual behaviour of each vehicle relative to a vehicle ahead. Car following models (*e.g.* [61]) fall under the category of microscopic models which are the most commonly employed to analytically delineate vehicular traffic dynamics. In the majority of car following models, a vehicle's speed and/or acceleration is expressed as a function of factors such as the distance to a front vehicle and the actual speeds of both vehicles. As such, these models implicitly account for the finite driver's reaction time.

Car following models are very flexible. They may account for a large number of parameters that pertain, for example to vehicle technicalities, commuters' skills and habits and weather constraints resulting in a remarkable increase of their degree of accuracy as well as their level of realism. Furthermore, car following models incorporate lane changing routines that allow for the regulation of vehicles' mobility in between lanes. Consequently, these models can easily describe the vehicular traffic behaviour over individual multi-lane roadways. Car following models may be also used to simulate traffic dynamics on independent roadways of an urban scenario. However, in simulations, the interactions between traffic flows at road junctions must be handled with care. In other words, intersections crossing rules in the presence of stop/priority signs and traffic lights have to be defined within the simulation framework. Defining such rules within analytical frameworks is highly complex and often infeasible. This is especially true since the joint complex description of the

acceleration of different vehicles, lane changing and intersection management result in mathematically intractable problems [62].

Compared to macroscopic models, microscopic ones in general and car following models in particular are characterized by a high level of precision. However, they are highly computationally expensive especially whenever the number of simulated vehicles becomes large. It is observed that, in practice, car following models are avoided when large scale simulations are conducted. Instead, discrete time models similar to the one adopted in this manuscript are employed. Detailed discussions and comparisons on the implementation of different car following models may be found in [63–65].

2.3 Data Retransmission Mechanism

All data communication systems are augmented with special mechanisms to recover from data transmission errors or losses. Typically, upon the reception of a packet P, the receiving node R replies to the sending node S through the transmission of a positive (negative) acknowledgment ACK (NACK) indicating that P is error-free (erroneous). Meanwhile, P_C, a copy of P, is buffered at S with a predefined expiry timer. If S receives an ACK, P_C is deleted. The reception of a NACK or non-reception of an ACK/NACK before the timer's expiry triggers the retransmission of the packet. Such recovery mechanisms have been widely studied in the open literature. A selection of major work developed in this field is summarized as follows. The work of [42] presented the queueing analysis of two Automatic Repeat Request (ARQ) protocols for a slotted concentrator network node synchronously transmitting packetized data. In [66], a similar protocol was examined in the context of computer-to-computer communication via a satellite link. In [67], the authors studied the performance of several satellite communication protocols. The authors of [68] developed a model

which describes the behaviour of statistical multiplexors using the Stop-and-Wait and the Continuous Error Detection retransmission protocols. In [69], the author investigates the possibility of tailoring an ARQ protocol for message transmission environments characterized by high error rates and irregular propagation delays.

Chapter 3

A Probabilistic Data Relaying Strategy for Intermittently Connected Roadside Communication Networks

As opposed to the majority of the earlier summarized work and particularly [25] that assumes complete knowledge of network information, throughout this chapter we propose to get away from such an assumption by introducing a novel probabilistic data relaying strategy for intermittently connected roadside communication network scenarios similar to the ones described in chapter 1 and illustrated in Figures 1.1 and 1.2. In particular, we develop a Probabilistic Bundle Release Scheme (PBRS) that has the objective of minimizing the average bundle transit delay and hence the average end-to-end bundle delivery delay. At the core of PBRS lies an original probabilistic parameter called the *bundle release probability*. This parameter indicates to the source SRU which among the arriving vehicles are those that achieve

relatively faster bundle transits. Consequently, similar to the typical Internet packet-like forwarding, the source releases bundles, one at a time, only to those vehicles. Furthermore, another scheme called the Greedy Bundle Release Scheme (GBRS) is developed. Under GBRS, the source SRU releases a bundle to every arriving vehicle. The performance of this scheme will serve as a benchmark when evaluating that of its probabilistic counterpart. Simplicity and unawareness of network information are the two features that distinguish GBRS and PBRS from other existing schemes. As such, the primary contributions of this chapter lie in: *a*) the proposal of a new probabilistic data relaying concept and *b*) the setup of a whole new mathematical framework through which the essence of connectivity intermittence in roadside communication networks is captured and the performances of the proposed schemes are analyzed.

3.1 The Bundle Release Probability

In the ICRCN scenario described in Chapter 1, communication is to be established between the source SRU S and destination SRU D. In the absence of all sorts of networking infrastructures and backbone network connectivities, vehicles restricted to navigable roadways entering the range of S are opportunistically exploited to transport bundles to D. Intuitively, bundles may be greedily released to every arriving vehicle. This is referred to as the Greedy Bundle Relaying Scheme (GBRS). In contrast, a Probabilistic Bundle Relaying Scheme (PBRS) is proposed under which S releases bundles only to the relatively faster vehicles in order to ensure a delay-minimal bundle transit to D. At the heart of PBRS is the bundle release probability $P_{br,i}$, a novel decision parameter expressed as a function of the mean vehicle inter-arrival time the speed V_i of a vehicle i present in the range S and the source-destination distance d_{SD}. This parameter gives S insight into the suitability of vehicle i to carry its bundles

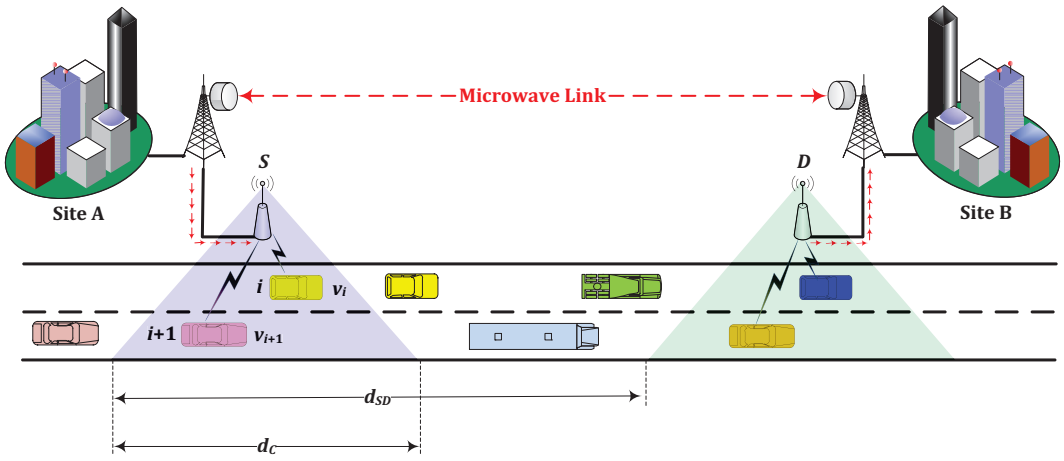

Figure 3.1: Intermittently Connected Roadside Communication Network Scenario.

to D. More specifically, $P_{br,i}$ estimates the level of contribution of an arriving vehicle to the minimization of the overall average bundle transit delay. In this section, we derive a closed form expression for $P_{br,i}$.

3.1.1 Introduction of Concept:

As shown in Figure 3.1, the source S has a coverage range that spans a distance of d_C (meters). S and D are separated by distance $d_{SD} >> d_C$. Vehicles with distinct speeds enter the range of S while navigating towards D. The event of a vehicle entering the range of S is called a vehicle arrival. S becomes aware of the speed, v_i of the i^{th} vehicle only at the instant t_i of arrival of this latter. Hence, with a probability $P_{br,i}$, S releases a *single* bundle M that occupies the topmost position of its queue to the i^{th} vehicle. With a probability $1 - P_{br,i}$ it retains M for a likely better subsequent release opportunity. If M is released to the i^{th} vehicle, it will be successfully delivered at the instant $d_i = t_i + \frac{d_{SD}}{v_i}$. Otherwise, if it is released to the $(i+1)^{th}$ vehicle, it will be successfully delivered at the instant $d_{i+1} = t_{i+1} + \frac{d_{SD}}{v_{i+1}}$. Let $I_{i+1} = t_{i+1} - t_i$ denote the $(i+1)^{th}$ vehicle inter-arrival time. It follows that a better

subsequent release opportunity occurs whenever:

$$d_{i+1} < d_i \Rightarrow I_{i+1} + \frac{d_{SD}}{v_{i+1}} < \frac{d_{SD}}{v_i} \tag{3.1}$$

Condition (3.1) states that not only does the $(i+1)^{th}$ vehicle have to arrive to S before the i^{th} one has reached D, but it also has to reach D before the i^{th} one does. Note that d_{i+1} has to be strictly less than d_i. Had there been equality, then a bundle would have been forced to wait longer in the queue with no benefits. As such, condition (3.1) is the only necessary and sufficient condition based on which a bundle is retained for a *possible* release whenever the next release opportunity arises. In condition (3.1), I_{i+1} and v_{i+1} are the only unknowns.

3.1.2 Basic Assumptions:

The below classical assumptions are borrowed from [25]:

- $A1$: Vehicle inter-arrival times are exponentially distributed with a probability density function $f_I(t) = \mu_v e^{-\mu_v t}$, $t \geq 0$.
- $A2$: Bundle inter-arrival times are exponentially distributed with a probability density function $f_B(t) = \lambda e^{-\lambda t}$, $t \geq 0$.
- $A3$: Bundle transmissions are instantaneous.
- $A4$: Vehicle speeds are uniformly distributed over $[V_{min}; V_{max}]$ with a probability density function $f_V(v) = \frac{1}{V_{max} - V_{min}}$.
- $A5$: The source node has an infinite queue size.
- $A6$: A vehicle's speed remains constant during its entire navigation period on the road.

- *A*7: Release decisions are performed independently for each bundle from one opportunity to another.

3.1.3 The Conditional Bundle Release Probability:

In view of the above reasoning and assumptions, the probability of retaining a bundle given that the speed of the current vehicle is v_i such that $v \leq v_i < v + dv$ can be expressed as:

$$Pr\left[d_{i+1} < d_i \middle| v \leq v_i < v + dv\right] = Pr\left[I_{i+1} + \frac{d_{SD}}{v_{i+1}} < \frac{d_{SD}}{v_i} \middle| v \leq v_i < v + dv\right] \quad (3.2)$$

Let R be the event that a bundle is released. The conditional bundle release probability $P_{br,i}$ is defined as the probability of occurrence of R conditioned by the current vehicle's speed being v_i such that $v \leq v_i < v + dv$. It is mathematically expressed as:

$$P_{br,i} = Pr\left[R \middle| v \leq v_i < v + dv\right] = 1 - Pr\left[I_{i+1} + \frac{d_{SD}}{v_{i+1}} < \frac{d_{SD}}{v_i} \middle| v \leq v_i < v + dv\right] \quad (3.3)$$

Define the two random variables $T_d = \frac{d_{SD}}{v_{i+1}}$ and $\Delta = I_{i+1} + T_d$. As such, equation (4.2) can be rewritten as:

$$\begin{aligned} P_{br,i} &= 1 - Pr\left[I_{i+1} + T_d < \frac{d_{SD}}{v_i} \middle| v \leq v_i < v + dv\right] \\ &= 1 - Pr\left[\Delta < \frac{d_{SD}}{v_i} \middle| v \leq v_i < v + dv\right] \end{aligned} \quad (3.4)$$

While $f_{I_{i+1}}(t) = f_I(t)$ given in assumption (3), let $f_{T_d}(t)$ denote the probability density function of T_d. Following the above assumption (4), it is easy to show that $f_{T_d}(t)$ is given by:

$$f_{T_d}(t) = \frac{d_{SD}}{(V_{max} - V_{min})t^2}, \text{ for } \frac{d_{SD}}{V_{max}} \leq t \leq \frac{d_{SD}}{V_{min}} \quad (3.5)$$

Let $f_{\Delta}(\delta)$ denote the probability density function of Δ. It is given by the convolution of $f_{I_{i+1}}(t)$ and $f_{T_d}(t)$. A closed-form expression of $f_{\Delta}(\delta)$ is derived next.

1) Derivation of $f_{\Delta}(\delta)$:

Notice that whenever $\delta \leq \frac{d_{SD}}{V_{max}}$, the product of the two probability density function is zero resulting in $f_{\Delta}(\delta) = 0$. There exists two other cases in which $f_{\Delta}(\delta)$ is non-zero, namely: (i) $\delta \in \left[\frac{d_{SD}}{V_{max}}; \frac{d_{SD}}{V_{min}}\right]$ and (ii) $\delta \in \left[\frac{d_{SD}}{V_{min}}; +\infty\right]$. The expression of $f_{\Delta}(\delta)$ will be derived separately for each of the two cases.

- ***Case 1:*** $\delta \in \left[\frac{d_{SD}}{V_{max}}; \frac{d_{SD}}{V_{min}}\right]$

$$f_{\Delta}(\delta) = \int_{\frac{d_{SD}}{V_{max}}}^{\delta} \frac{d_{SD}\mu_v e^{-\mu_v(\delta - t)}}{(V_{max} - V_{min})t^2} dt = \frac{d_{SD}\mu_v e^{-\mu_v \delta}}{V_{max} - V_{min}} \int_{\frac{d_{SD}}{V_{max}}}^{\delta} \frac{e^{\mu_v t}}{t^2} dt \tag{3.6}$$

We define $\psi(\delta) = \int_{\frac{d_{SD}}{V_{max}}}^{\delta} \frac{e^{\mu_v t}}{t^2} dt$. It can be easily shown from [70] that:

$$\psi(\delta) = \frac{V_{max} e^{\mu_v \frac{d_{SD}}{V_{max}}}}{d_{SD}} - \frac{e^{\mu_v \delta}}{\delta} + \mu_v \int_{\frac{d_{SD}}{V_{max}}}^{\delta} \frac{e^{\mu_v t}}{t} dt \tag{3.7}$$

Note that a special function known as the *Exponential Integral Function* is defined in [70] as:

$$Ei(x) = \int_{-\infty}^{x} \frac{e^y}{y} dy = \int_{-\infty}^{\frac{x}{\mu}} \frac{e^{\mu_v t}}{t} dt \tag{3.8}$$

Consequently, the integral term in (3.7) is re-written as:

$$\int_{\frac{d_{SD}}{V_{max}}}^{\delta} \frac{e^{\mu_v t}}{t} dt = \int_{-\infty}^{\delta} \frac{e^{\mu_v t}}{t} dt - \int_{-\infty}^{\frac{d_{SD}}{V_{max}}} \frac{e^{\mu_v t}}{t} dt = Ei(\mu_v \delta) - Ei\left(\mu_v \frac{d_{SD}}{V_{max}}\right) \tag{3.9}$$

Using (3.9), equation (3.7) is re-written as:

$$\psi(\delta) = \frac{V_{max} e^{\mu_v \frac{d_{SD}}{V_{max}}}}{d_{SD}} - \frac{e^{\mu_v \delta}}{\delta} + \mu_v \left[Ei(\mu_v \delta) - Ei\left(\mu_v \frac{d_{SD}}{V_{max}}\right)\right] \tag{3.10}$$

It follows that the p.d.f of Δ in (3.6) is:

$$f_\Delta(\delta) = \frac{\mu_v d_{SD} \cdot \psi(\delta) \cdot e^{-\mu_v \delta}}{V_{max} - V_{min}} \text{ , for } \delta \in \left[\frac{d_{SD}}{V_{max}}; \frac{d_{SD}}{V_{min}}\right] \tag{3.11}$$

- ***Case 2:*** $\delta \in \left[\frac{d_{SD}}{V_{min}}; +\infty\right]$

In this case, the upper bound of the integration domain in (3.6) becomes $\frac{d_{SD}}{V_{min}}$. Hence:

$$f_\Delta(\delta) = \frac{d_{SD} \mu_v e^{-\mu_v \delta}}{V_{max} - V_{min}} \int_{\frac{d_{SD}}{V_{max}}}^{\frac{d_{SD}}{V_{min}}} \frac{e^{\mu_v t}}{t^2} dt \tag{3.12}$$

Notice that $\int_{\frac{d_{SD}}{V_{max}}}^{\frac{d_{SD}}{V_{min}}} \frac{e^{\mu_v t}}{t^2} dt = \psi\left(\frac{d_{SD}}{V_{min}}\right)$ is a constant term. Thus, using (3.10) we have:

$$f_\Delta(\delta) = \frac{\mu_v d_{SD} \cdot \psi\left(\frac{d_{SD}}{V_{min}}\right) \cdot e^{-\mu_v \delta}}{V_{max} - V_{min}} \text{ , for } \delta \in \left[\frac{d_{SD}}{V_{min}}; +\infty\right] \tag{3.13}$$

Finally, the derived expressions in cases 1 and 2 are grouped together:

$$f_\Delta(\delta) = \begin{cases} \frac{\mu_v d_{SD} \cdot \psi(\delta) \cdot e^{-\mu_v \delta}}{V_{max} - V_{min}} & \text{, for } \delta \in \left[\frac{d_{SD}}{V_{max}}; \frac{d_{SD}}{V_{min}}\right] \\ \frac{\mu_v d_{SD} \cdot \psi\left(\frac{d_{SD}}{V_{min}}\right) \cdot e^{-\mu_v \delta}}{V_{max} - V_{min}} & \text{, for } \delta \in \left[\frac{d_{SD}}{V_{min}}; +\infty\right] \\ 0 & \text{, Otherwise} \end{cases} \tag{3.14}$$

Let $F_\Delta(\tau)$ denote the cumulative distribution function of Δ. It is derived next.

2) Derivation of $F_\Delta(\tau)$:

Note that Δ is a truncated continuous random variable in the range $\left[\frac{d_{SD}}{V_{max}}; +\infty\right]$. As such, when deriving its truncated cumulative distribution function, two cases must also be distinguished.

- ***Case 1:*** $\tau \in \left[\frac{d_{SD}}{V_{max}}; \frac{d_{SD}}{V_{min}}\right]$

$$F_{\Delta}(\tau) = Pr\left[\Delta < \tau \middle| \frac{d_{SD}}{V_{max}} \leq \tau \leq \frac{d_{SD}}{V_{min}}\right] = \frac{\displaystyle\int_{\frac{d_{SD}}{V_{max}}}^{\tau} \frac{\mu_v d_{SD} \cdot \psi(\delta) \cdot e^{-\mu_v \delta}}{V_{max} - V_{min}} d\delta}{\displaystyle\int_{\frac{d_{SD}}{V_{max}}}^{\frac{d_{SD}}{V_{min}}} \frac{\mu_v d_{SD} \cdot \psi(\delta) \cdot e^{-\mu_v \delta}}{V_{max} - V_{min}} d\delta}$$

$$= \frac{\displaystyle\int_{\frac{d_{SD}}{V_{max}}}^{\tau} \psi(\delta) \cdot e^{-\mu_v \delta} d\delta}{\displaystyle\int_{\frac{d_{SD}}{V_{max}}}^{\frac{d_{SD}}{V_{min}}} \psi(\delta) \cdot e^{-\mu_v \delta} d\delta} \tag{3.15}$$

Define $\varphi(\tau) = \displaystyle\int_{\frac{d_{SD}}{V_{max}}}^{\tau} \psi(\delta) e^{-\mu_v \delta} d\delta$. Notice that the denominator of (3.15) is a normalization constant equal to $\varphi(\frac{d_{SD}}{V_{min}})$. Using (3.10), $\varphi(\tau)$ is re-written as:

$$\varphi(\tau) = \int_{\frac{d_{SD}}{V_{max}}}^{\tau} \left[\frac{V_{max} e^{\mu_v \frac{d_{SD}}{V_{max}}}}{d_{SD}} - \frac{e^{\mu_v \delta}}{\delta} + \mu_v \left(Ei(\mu_v \delta) - Ei\left(\mu_v \frac{d_{SD}}{V_{max}}\right)\right)\right] e^{-\mu_v \delta} d\delta \tag{3.16}$$

Using simple integral decomposition, it can be easily shown that:

$$\varphi(\tau) = \left[Ei\left(\mu_v \frac{d_{SD}}{V_{max}}\right) - \frac{V_{max} e^{\mu_v \frac{d_{SD}}{V_{max}}}}{d_{SD}}\right]\left(e^{-\mu_v \tau} - e^{-\mu_v \frac{d_{SD}}{V_{max}}}\right) - \ln\left(\frac{\tau V_{max}}{d_{SD}}\right) + \mu_v \int_{\frac{d_{SD}}{V_{max}}}^{\tau} Ei(\mu_v \delta) \cdot e^{-\mu_v \delta} d\delta \tag{3.17}$$

Define $h(\tau) = \int_{\frac{d_{SD}}{V_{max}}}^{\tau} Ei(\mu_v \delta) \cdot e^{-\mu_v \delta} d\delta$. Integrating $h(\tau)$ by parts with $u = Ei(\mu_v \delta)$ and $dv = e^{-\mu_v \delta}$ results in having:

$$h(\tau) = Ei\left(\mu_v \frac{d_{SD}}{V_{max}}\right) \frac{e^{-\mu_v \frac{d_{SD}}{V_{max}}}}{\mu_v} - Ei(\mu_v \tau) \frac{e^{-\mu_v \tau}}{\mu_v} + \int_{\frac{d_{SD}}{V_{max}}}^{\tau} \frac{e^{-\mu_v \delta}}{\mu_v} \frac{d[Ei(\mu_v \delta)]}{d\delta} d\delta \quad (3.18)$$

It is stated in [70] that:

$$Ei(x) = \ln(x) + \sum_{k=1}^{\infty} \frac{x^k}{k \cdot k!} \quad (3.19)$$

Through straight forward differentiation of the right-hand-side of equation (3.19) with respect to δ we obtain:

$$\frac{d}{d\delta} Ei(\mu_v \delta) = \frac{\mu_v}{\mu_v \delta} + \sum_{k=1}^{\infty} \frac{k \mu_v (\mu_v \delta)^{k-1}}{k \cdot k!} = \frac{1}{\delta} + \frac{1}{\delta} \sum_{k=1}^{\infty} \frac{(\mu_v \delta)^k}{k!} = \frac{1}{\delta} + \frac{1}{\delta}(e^{\mu_v \delta} - 1) = \frac{e^{\mu_v \delta}}{\delta} \quad (3.20)$$

Incorporating the result of (3.20) into (3.18) leads to:

$$h(\tau) = Ei\left(\mu_v \frac{d_{SD}}{V_{max}}\right) \frac{e^{-\mu_v \frac{d_{SD}}{V_{max}}}}{\mu_v} - Ei(\mu_v \tau) \frac{e^{-\mu_v \tau}}{\mu_v} + \frac{1}{\mu_v} \ln\left(\frac{\tau V_{max}}{d_{SD}}\right) \quad (3.21)$$

At this point, combining (3.21) with (3.17) gives:

$$\varphi(\tau) = \left[Ei\left(\mu_v \frac{d_{SD}}{V_{max}}\right) - \frac{V_{max} e^{\mu_v \frac{d_{SD}}{V_{max}}}}{d_{SD}} - Ei(\mu_v \tau)\right] e^{-\mu_v \tau} + \frac{V_{max}}{\mu_v d_{SD}} \quad (3.22)$$

Finally it can be written:

$$F_{\Delta}(\tau) = \frac{\varphi(\tau)}{\varphi\left(\frac{d_{SD}}{V_{min}}\right)} \text{ , for } \tau \in \left[\frac{d_{SD}}{V_{max}}; \frac{d_{SD}}{V_{min}}\right] \quad (3.23)$$

- ***Case 2:*** $\tau \in \left[\frac{d_{SD}}{V_{min}}; +\infty\right]$

$$F_{\Delta}(\tau) = Pr\left[\Delta < \tau \middle| \tau > \frac{d_{SD}}{V_{min}}\right] = \frac{\int_{\frac{d_{SD}}{V_{max}}}^{\frac{d_{SD}}{V_{min}}} \psi(\delta) \cdot e^{-\mu_v \delta} d\delta + \psi(\frac{d_{SD}}{V_{min}}) \int_{\frac{d_{SD}}{V_{max}}}^{\tau} e^{-\mu_v \delta} d\delta}{\int_{\frac{d_{SD}}{V_{max}}}^{\frac{d_{SD}}{V_{min}}} \psi(\delta) \cdot e^{-\mu_v \delta} d\delta + \psi(\frac{d_{SD}}{V_{min}}) \int_{\frac{d_{SD}}{V_{max}}}^{\infty} e^{-\mu_v \delta} d\delta} \tag{3.24}$$

Using (3.17) and (3.22) combined with simple integration techniques, it can be easily shown that:

$$F_{\Delta}(\tau) = \frac{\varphi(\frac{d_{SD}}{V_{min}}) - \frac{\psi(\frac{d_{SD}}{V_{min}})}{\mu_v}\left(e^{-\mu_v \tau} - e^{-\mu_v \frac{d_{SD}}{V_{max}}}\right)}{\varphi(\frac{d_{SD}}{V_{min}}) + \frac{\psi(\frac{d_{SD}}{V_{min}})}{\mu_v} e^{-\mu_v \frac{d_{SD}}{V_{max}}}} \text{ , for } \tau \in \left[\frac{d_{SD}}{V_{min}}; +\infty\right] \tag{3.25}$$

Grouping (3.23) and (3.25) together:

$$F_{\Delta}(\tau) = \begin{cases} \frac{\varphi(\tau)}{\varphi\left(\frac{d_{SD}}{V_{min}}\right)} & \text{, for } \tau \in \left[\frac{d_{SD}}{V_{max}}; \frac{d_{SD}}{V_{min}}\right] \\ \frac{\varphi(\frac{d_{SD}}{V_{min}}) - \frac{\psi(\frac{d_{SD}}{V_{min}})}{\mu_v}\left(e^{-\mu_v \tau} - e^{-\mu_v \frac{d_{SD}}{V_{max}}}\right)}{\varphi(\frac{d_{SD}}{V_{min}}) + \frac{\psi(\frac{d_{SD}}{V_{min}})}{\mu_v} e^{-\mu_v \frac{d_{SD}}{V_{max}}}} & \text{, for } \tau \geq \frac{d_{SD}}{V_{min}} \end{cases} \tag{3.26}$$

The above analysis is validated by carrying out a series of comparisons between numerical and simulation results. For this purpose, the simulator used in section VI was enabled to track and record the random vehicle inter-arrival times and transit delays. 10^8 samples are taken for each and averaged out over multiple runs of the simulator to ensure high accuracy. Summing those values one-to-one leads to simulated versions of Δ for which the corresponding simulated versions of the density and cumulative distribution functions can be easily obtained. In addition, the theoretical versions of these functions were computed numerically using their respective earlier-derived equations (3.14) and (3.26). Both simulation and theoretical results were plotted concurrently as shown in Figures 3.2(a) and 3.2(b) respectively. With no further dwelling, the figures are tangible proofs of the validity and remarkable

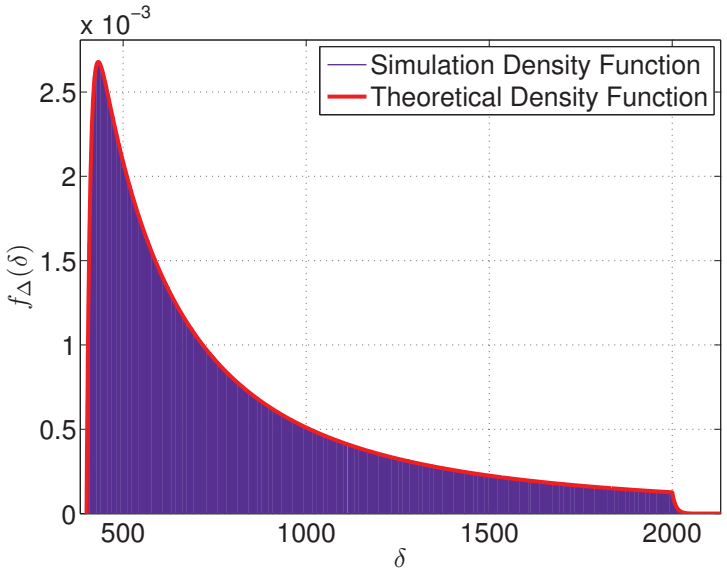

(a) Probability Density Function of Δ.

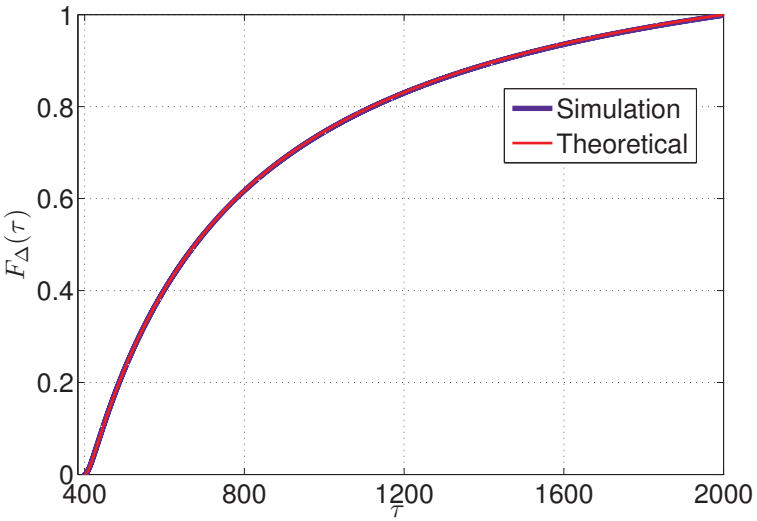

(b) Cumulative Distribution Function of Δ.

Figure 3.2: Simulated VS Theoretical versions of the density and cumulative distribution functions of Δ.

accuracy of our derivations as in both of them, the simulated and theoretical curves completely overlap.

3) Closed-Form Expression of the Conditional Bundle Release Probability:

Building on the above, the bundle release probability given that the current vehicle speed is $V_i = v_i$ given in equation (4.2) can be expressed as:

$$P_{br,i} = 1 - F_{\Delta}\left(\frac{d_{SD}}{v_i}\right) \tag{3.27}$$

It is worth noting that since $v_i \in [V_{min}; V_{max}]$, then $\frac{d_{SD}}{v_i} \in \left[\frac{d_{SD}}{V_{max}}; \frac{d_{SD}}{V_{min}}\right]$. Hence $P_{br,i}$ is given by:

$$\begin{aligned} P_{br,i} &= 1 - \frac{\varphi(\frac{d_{SD}}{v_i})}{\varphi\left(\frac{d_{SD}}{V_{min}}\right)} \\ &= 1 - \frac{\left[Ei\left(\mu_v \frac{d_{SD}}{V_{max}}\right) - \frac{V_{max} e^{\mu_v \frac{d_{SD}}{V_{max}}}}{\mu_v d_{SD}} - Ei(\mu_v \frac{d_{SD}}{v_i})\right] e^{-\mu_v \frac{d_{SD}}{v_i}} + \frac{V_{max}}{\mu_v d_{SD}}}{\left[Ei\left(\mu_v \frac{d_{SD}}{V_{max}}\right) - \frac{V_{max} e^{\mu_v \frac{d_{SD}}{V_{max}}}}{\mu_v d_{SD}} - Ei(\mu_v \frac{d_{SD}}{V_{min}})\right] e^{-\mu_v \frac{d_{SD}}{V_{min}}} + \frac{V_{max}}{\mu_v d_{SD}}} \end{aligned} \tag{3.28}$$

Figure 3(a) illustrates the variations of the conditional bundle release probability given in (3.28) as a function of $\frac{d_{SD}}{v_i}$. Indeed, the area under the curve is exactly equal to 1 which satisfies the fundamental axiom of probability and proves the validity of the derived expression. In addition, notice that as $\frac{d_{SD}}{v_i}$ increases (*i.e.* v_i decreases), $P_{br,i}$ will decrease. This stems from the basic property of the bundle release probability that is designed to indicate to the source node those vehicles with relatively high speeds that are most suitable to transport bundles to the destination during the shortest transit period. Figure 3.3(b) shows the $P_{br,i}$ curves for different values of the

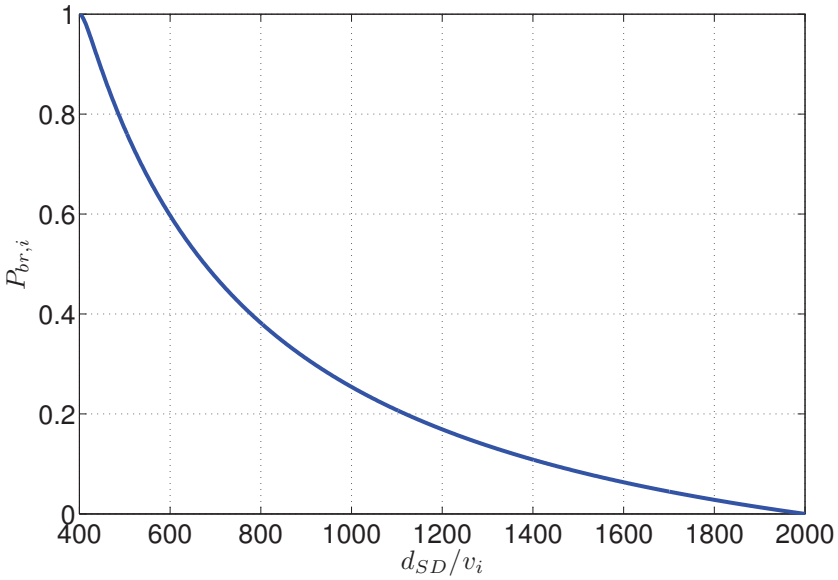

(a) $\mu_v = 0.1$.

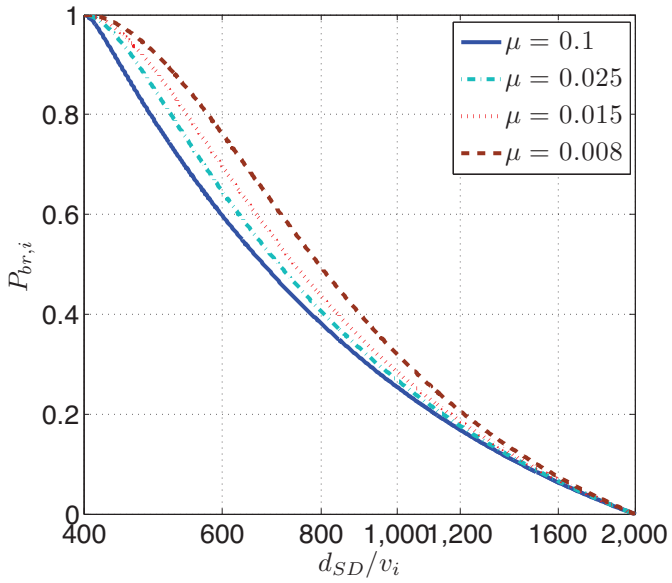

(b) $0.008 \leq \mu_v \leq 0.1$.

Figure 3.3: Conditional Bundle Release Probability.

vehicle inter-arrival rate μ_v. It is quite important to highlight the fact that whenever μ_v decreases vehicle arrivals become more spaced out in time. At the bundle level, this is interpreted as waiting in the source node's buffer for a longer period of time before the occurrence of a suitable release opportunity. As such, the cumulative waiting time of a bundle in the queue becomes longer as the vehicle inter-arrival time increases. Nevertheless, $P_{br,i}$ is an adaptive parameter that will account for this situation and limit this additional waiting time by allowing a portion of slower vehicles to transport bundles from the source to the destination. This explains why, for a fixed $\frac{d_{SD}}{v_i}$, the corresponding $P_{br,i}$ increases as μ_v increases.

4) The Average Bundle Release Probability:

From probability theory, we know that:

$$Pr\left[R, v \leq v_i < v + dv\right] dv = P_{br,i} \cdot f_{V_i}(v) = P_{br,i} \cdot \frac{1}{V_{max} - V_{min}} \tag{3.29}$$

Since R is the event that a bundle is released, it follows from equation (4.3) that the average bundle release probability can be written as:

$$P_{br} = Pr[R] = \int_{V_{min}}^{V_{max}} \frac{1}{V_{max} - V_{min}} P_{br,i} dv_i \tag{3.30}$$

$$
\begin{aligned}
P_{br} &= Pr\left[R\right] = \int_{V_{min}}^{V_{max}} \frac{P_{br,i}}{V_{max}-V_{min}} dv_i = \frac{1}{V_{max}-V_{min}} \int_{V_{min}}^{V_{max}} P_{br,i} dv_i \\
&= \frac{1}{V_{max}-V_{min}} \int_{V_{min}}^{V_{max}} dv_i \\
&- \frac{1}{V_{min}-V_{max}} \times \\
&\quad \int_{V_{min}}^{V_{max}} \left(\frac{\left[Ei\left(\mu_v \frac{d_{SD}}{V_{max}}\right) - \frac{V_{max} e^{\mu_v \frac{d_{SD}}{V_{max}}}}{\mu_v d_{SD}} - Ei\left(\mu_v \frac{d_{SD}}{v_i}\right) \right] e^{-\mu_v \frac{d_{SD}}{v_i}} + \frac{V_{max}}{\mu_v d_{SD}}}{\left[Ei\left(\mu_v \frac{d_{SD}}{V_{max}}\right) - \frac{V_{max} e^{\mu_v \frac{d_{SD}}{V_{max}}}}{\mu_v d_{SD}} - Ei\left(\mu_v \frac{d_{SD}}{V_{min}}\right) \right] e^{-\mu_v \frac{d_{SD}}{V_{min}}} + \frac{V_{max}}{\mu_v d_{SD}}} \right) dv_i \\
&= 1 - \frac{\int_{V_{min}}^{V_{max}} \left(\left[Ei\left(\mu_v \frac{d_{SD}}{V_{max}}\right) - \frac{V_{max} e^{\mu_v \frac{d_{SD}}{V_{max}}}}{\mu_v d_{SD}} - Ei\left(\mu_v \frac{d_{SD}}{v_i}\right) \right] e^{-\mu_v \frac{d_{SD}}{v_i}} + \frac{V_{max}}{\mu_v d_{SD}} \right) dv_i}{(V_{max}-V_{min}) \left(\left[Ei\left(\mu_v \frac{d_{SD}}{V_{max}}\right) - \frac{V_{max} e^{\mu_v \frac{d_{SD}}{V_{max}}}}{\mu_v d_{SD}} - Ei\left(\mu_v \frac{d_{SD}}{V_{min}}\right) \right] e^{-\mu_v \frac{d_{SD}}{V_{min}}} + \frac{V_{max}}{\mu_v d_{SD}} \right)}
\end{aligned}
\tag{3.31}
$$

Define the constant $\xi = \frac{1}{(V_{max}-V_{min}) \left(\left[Ei\left(\mu_v \frac{d_{SD}}{V_{max}}\right) - \frac{V_{max} e^{\mu_v \frac{d_{SD}}{V_{max}}}}{\mu_v d_{SD}} - Ei\left(\mu_v \frac{d_{SD}}{V_{min}}\right) \right] e^{-\mu_v \frac{d_{SD}}{V_{min}}} + \frac{V_{max}}{\mu_v d_{SD}} \right)}$.
It follows that equation (3.31) can be re-written as:

$$
\begin{aligned}
P_{br} &= 1 - \xi \int_{V_{min}}^{V_{max}} \left(\left[Ei\left(\mu_v \frac{d_{SD}}{V_{max}}\right) - \frac{V_{max} e^{\mu_v \frac{d_{SD}}{V_{max}}}}{\mu_v d_{SD}} - Ei\left(\mu_v \frac{d_{SD}}{v_i}\right) \right] e^{-\mu_v \frac{d_{SD}}{v_i}} + \frac{V_{max}}{\mu_v d_{SD}} \right) dv_i \\
&= 1 - \xi \left(\left[Ei\left(\mu_v \frac{d_{SD}}{V_{max}}\right) - \frac{V_{max} e^{\mu_v \frac{d_{SD}}{V_{max}}}}{\mu_v d_{SD}} \right] \int_{V_{min}}^{V_{max}} e^{-\mu_v \frac{d_{SD}}{v_i}} dv_i - \right. \\
&\qquad \left. \int_{V_{min}}^{V_{max}} Ei\left(\mu_v \frac{d_{SD}}{v_i}\right) e^{-\mu_v \frac{d_{SD}}{v_i}} dv_i - \frac{V_{max}}{\mu_v d_{SD}} \int_{V_{min}}^{V_{max}} dv_i \right)
\end{aligned}
\tag{3.32}
$$

Through a simple change of variable, let $\tau_i = \frac{d_{SD}}{v_i}$. In other words $v_i = \frac{d_{SD}}{\tau_i}$. Thus, $dv_i = -\frac{d_{SD}}{\tau_i^2} d\tau_i$. Since $V_{min} \leq v_i \leq V_{max}$, therefore $\frac{d_{SD}}{V_{max}} \leq \tau_i \leq \frac{d_{SD}}{V_{min}}$. As such,

equation (3.32) can be rewritten as:

$$P_{br} = 1 + \xi d_{SD} \left(\left[Ei\left(\mu_v \frac{d_{SD}}{V_{max}}\right) - \frac{V_{max} e^{\mu_v \frac{d_{SD}}{V_{max}}}}{\mu_v d_{SD}} \right] \int_{\frac{d_{SD}}{V_{max}}}^{\frac{d_{SD}}{V_{min}}} \frac{e^{-\mu_v \tau_i}}{\tau_i^2} d\tau_i - \right.$$
$$\left. \int_{\frac{d_{SD}}{V_{max}}}^{\frac{d_{SD}}{V_{max}}} \frac{Ei(\mu_v \tau_i) e^{-\mu_v \frac{d_{SD}}{v_i}}}{\tau_i^2} d\tau_i - \frac{V_{max}}{\mu_v d_{SD}} \int_{\frac{d_{SD}}{V_{max}}}^{\frac{d_{SD}}{V_{min}}} \frac{1}{\tau_i^2} d\tau_i \right)$$
$$= 1 + \xi d_{SD} \left(\left[Ei\left(\mu_v \frac{d_{SD}}{V_{max}}\right) - \frac{V_{max} e^{\mu_v \frac{d_{SD}}{V_{max}}}}{\mu_v d_{SD}} \right] \int_{\frac{d_{SD}}{V_{max}}}^{\frac{d_{SD}}{V_{min}}} \frac{e^{-\mu_v \tau_i}}{\tau_i^2} d\tau_i - \right.$$
$$\left. \int_{\frac{d_{SD}}{V_{max}}}^{\frac{d_{SD}}{V_{max}}} \frac{Ei(\mu_v \tau_i) e^{-\mu_v \frac{d_{SD}}{v_i}}}{\tau_i^2} d\tau_i - \frac{V_{max}(V_{max} - V_{min})}{\mu_v d_{SD}^2} \right) \tag{3.33}$$

On one hand, it can be easily shown from [70] that:

$$\int_{\frac{d_{SD}}{V_{max}}}^{\frac{d_{SD}}{V_{min}}} \frac{e^{-\mu_v \tau_i}}{\tau_i^2} d\tau_i = \frac{V_{max} e^{-\mu_v \frac{d_{SD}}{V_{max}}}}{d_{SD}} - \frac{V_{min} e^{-\mu_v \frac{d_{SD}}{V_{min}}}}{d_{SD}} - \mu_v \left[Ei\left(-\mu_v \frac{d_{SD}}{V_{min}}\right) - Ei\left(-\mu_v \frac{d_{SD}}{V_{max}}\right) \right] \tag{3.34}$$

On the other hand, through simple integration by parts with $u = Ei(\mu_v \tau_i)$ and $dv = \frac{e^{-\mu_v \tau_i}}{\tau_i^2}$ it can be shown that:

$$\int_{\frac{d_{SD}}{V_{max}}}^{\frac{d_{SD}}{V_{max}}} \frac{Ei(\mu_v \tau_i) e^{-\mu_v \tau_i}}{\tau_i^2} d\tau_i = \frac{V_{max} Ei\left(\mu_v \frac{d_{SD}}{V_{max}}\right) e^{-\mu_v \frac{d_{SD}}{V_{max}}}}{d_{SD}} - \frac{V_{min} Ei\left(\mu_v \frac{d_{SD}}{V_{min}}\right) e^{-\mu_v \frac{d_{SD}}{V_{min}}}}{d_{SD}}$$
$$+ \mu_v \left[Ei\left(-\mu_v \frac{d_{SD}}{V_{max}}\right) - Ei\left(-\mu_v \frac{d_{SD}}{V_{min}}\right) \right] + \frac{V_{max} - V_{min}}{d_{SD}}$$
$$+ \mu_v \int_{\frac{d_{SD}}{V_{max}}}^{\frac{d_{SD}}{V_{min}}} \frac{Ei(-\mu_v \tau_i) e^{\mu_v \tau_i}}{\tau_i} d\tau_i \tag{3.35}$$

Again through integration by parts with $u = Ei(-\mu_v \tau_i)$ and $dv = \frac{e^{\mu_v \tau_i}}{\tau_i}$, it can be

shown that:

$$\int_{\frac{d_{SD}}{V_{max}}}^{\frac{d_{SD}}{V_{min}}} \frac{Ei(-\mu_v\tau_i)e^{\mu_v\tau_i}}{\tau_i}d\tau_i = Ei\left(-\mu_v\frac{d_{SD}}{V_{min}}\right)Ei\left(\mu_v\frac{d_{SD}}{V_{min}}\right) - Ei\left(-\mu_v\frac{d_{SD}}{V_{max}}\right)Ei\left(\mu_v\frac{d_{SD}}{V_{max}}\right) - \int_{\frac{d_{SD}}{V_{max}}}^{\frac{d_{SD}}{V_{min}}} \frac{Ei(\mu_v\tau_i)e^{-\mu_v\tau_i}}{\tau_i}d\tau_i \tag{3.36}$$

Now building on the knowledge of (3.19), it can be shown that:

$$\begin{aligned}\int_{\frac{d_{SD}}{V_{max}}}^{\frac{d_{SD}}{V_{min}}} \frac{Ei(\mu_v\tau_i)e^{-\mu_v\tau_i}}{\tau_i}d\tau_i &= \int_{\frac{d_{SD}}{V_{max}}}^{\frac{d_{SD}}{V_{min}}} \left[\ln(\mu_v\tau_i) + \sum_{k=1}^{\infty}\frac{(\mu_v\tau_i)^k}{k\cdot k!}\right]\frac{e^{-\mu_v\tau_i}}{\tau_i}d\tau_i \\ &= \int_{\frac{d_{SD}}{V_{max}}}^{\frac{d_{SD}}{V_{min}}} \ln(\mu_v\tau_i)\frac{e^{-\mu_v\tau_i}}{\tau_i}d\tau_i + \sum_{k=1}^{\infty}\frac{\mu_v^k}{k\cdot k!}\int_{\frac{d_{SD}}{V_{max}}}^{\frac{d_{SD}}{V_{min}}}\tau_i^{k-1}e^{-\mu_v\tau_i}d\tau_i \\ &= \int_{\frac{d_{SD}}{V_{max}}}^{\frac{d_{SD}}{V_{min}}} \ln(\mu_v\tau_i)\frac{e^{-\mu_v\tau_i}}{\tau_i}d\tau_i \\ &\quad + \sum_{k=1}^{\infty}\frac{\mu_v^k}{k\cdot k!}\left[\int_0^{\frac{d_{SD}}{V_{min}}}\tau_i^{k-1}e^{-\mu_v\tau_i}d\tau_i - \int_0^{\frac{d_{SD}}{V_{max}}}\tau_i^{k-1}e^{-\mu_v\tau_i}d\tau_i\right]\end{aligned} \tag{3.37}$$

Consider the *Lower Incomplete Gamma Function* defined in [70] as:

$$\gamma(x,k) = \int_0^x y^{k-1}e^{-y}dy \tag{3.38}$$

Using a simple variable transformation, let $y = \mu_v\tau_i$. Consequently, $dy = \mu_v d\tau_i$. Also, since $0 \leq y \leq x$, therefore $0 \leq \tau_i \leq \frac{x}{\mu_v}$. Thus equation (3.38) is rewritten as:

$$\gamma(x,k) = \mu_v^k\int_0^{\frac{x}{\mu_v}}\tau_i^{k-1}e^{-\mu_v\tau_i}d\tau_i \tag{3.39}$$

It follows that equation (3.37) can be re-written as:

$$\int_{\frac{d_{SD}}{V_{max}}}^{\frac{d_{SD}}{V_{min}}} \frac{Ei(\mu_v\tau_i)e^{-\mu_v\tau_i}}{\tau_i}d\tau_i = \int_{\frac{d_{SD}}{V_{max}}}^{\frac{d_{SD}}{V_{min}}} \ln(\mu_v\tau_i)\frac{e^{-\mu_v\tau_i}}{\tau_i}d\tau_i + \sum_{k=1}^{\infty}\frac{1}{k\cdot k!}\left[\gamma\left(\mu_v\frac{d_{SD}}{V_{min}},k\right)-\gamma\left(\mu_v\frac{d_{SD}}{V_{max}},k\right)\right] \quad (3.40)$$

where $\gamma(x,k) = \int_0^x y^{k-1}e^{-y}dy = \mu^k\int_0^{\frac{x}{\mu}}\tau_i^{k-1}e^{-\mu\tau_i}d\tau_i$ is the *Lower Incomplete Gamma Function* as defined in [70]. Building on the knowledge obtained from [70] and [71], it can be shown that:

$$\begin{aligned}\int_{\frac{d_{SD}}{V_{max}}}^{\frac{d_{SD}}{V_{min}}} \ln(\mu_v\tau_i)\frac{e^{-\mu_v\tau_i}}{\tau_i}d\tau_i = \frac{1}{2}\ln\left(\frac{V_{max}}{V_{min}}\right)\ln\left(\frac{d_{SD}^2}{V_{max}V_{min}}\right) - \\ \frac{d_{SD}}{V_{min}}\left[-F\left(\{1,1,1\};\{2,2,2\};\frac{d_{SD}}{V_{min}}\right)+\right. \\ \left.\frac{V_{min}\ln\left(\frac{d_{SD}}{V_{min}}\right)\left[\ln\left(\frac{d_{SD}}{V_{min}}\right)+\Gamma\left(\frac{d_{SD}}{V_{min}},0\right)+\gamma_E\right]}{d_{SD}}\right]+ \\ \frac{d_{SD}}{V_{max}}\left[-F\left(\{1,1,1\};\{2,2,2\};\frac{d_{SD}}{V_{max}}\right)+\right. \\ \left.\frac{V_{max}\ln\left(\frac{d_{SD}}{V_{max}}\right)\left[\ln\left(\frac{d_{SD}}{V_{max}}\right)+\Gamma\left(\frac{d_{SD}}{V_{max}},0\right)+\gamma_E\right]}{d_{SD}}\right]\end{aligned} \quad (3.41)$$

where:

- $\Gamma(x,k) = \int_x^{\infty} y^{k-1}e^{-y}dy$ is the *Upper Incomplete Gamma Function.*
- $F(\{a_1,...,a_p\};\{b_1,...,b_q\};x) = \sum_{k\geq 0}\frac{(a_1)_k...(a_p)_k}{(b_1)_k...(b_q)_k}\frac{x^k}{k!}$ is the known *Hypergeometric Function* with $(a_n)_k = \frac{(a+k-1)!}{(a-1)!}$ and $(b_m)_k = \frac{(b+k-1)!}{(b-1)!}$ for $1 \leq n \leq p$ and $1 \leq m \leq q$ respectively, are known as *Pochammer symbols.*

- $\gamma_E = \lim_{n\to\infty}\left(\sum_{k=1}^{n}\frac{1}{k} - \ln(n)\right) = 0.577215664901532...$ is the *Euler-Mascheroni Constant*.

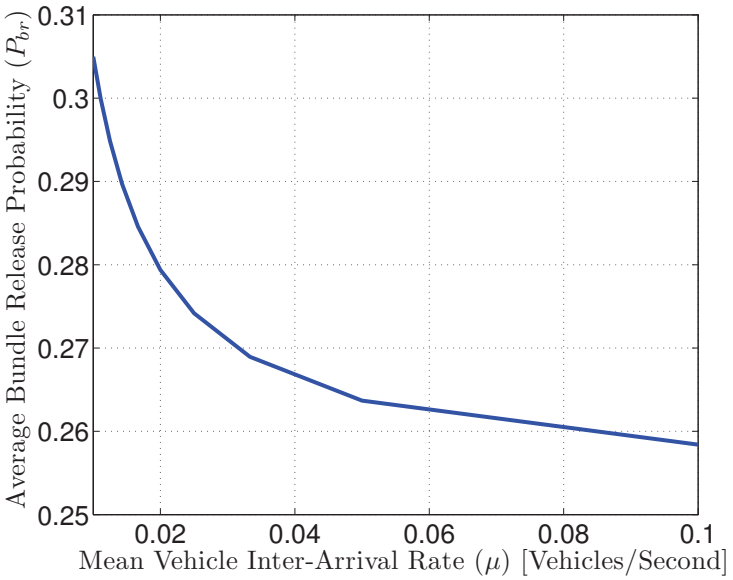

Figure 3.4: Average bundle release probability.

Finally, an expression of the unconditional bundle release probability P_{br} can be obtained by plugging the results obtained from equations (3.34) through (3.41) into equation (3.33).

Consistently with Figure 3.3(b), Figure 3.4 shows that as the vehicle inter-arrival rate μ_v increases the bundle release probability, on average, will decrease. This behavior is a direct result from vehicle arrivals being closer in time to each other and thus causing the arrival of a relatively fast vehicle to become more probable. In fact, the shorter the vehicle inter-arrival time is, the faster a high speed vehicle is expected to arrive. Hence, upon the release of a front bundle to an arriving high speed vehicle, the additional time this bundle has spent waiting at the front of the queue is expected to be very small. It is at the expense of this little extra queueing delay that

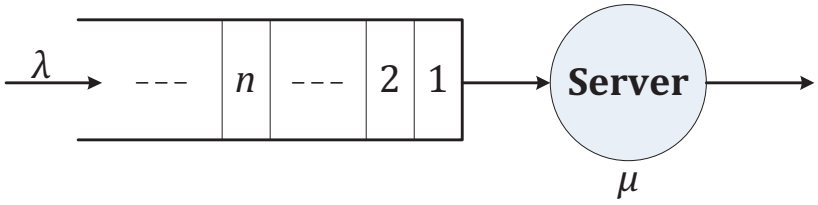

Figure 3.5: An illustration of a source SRU queueing system under GBRS.

P_{br} further restricts the bundle releases to only those relatively fast vehicles hoping that the achieved improvement in their transit periods from source to destination will be able to compensate.

3.2 Modeling And Analysis Of Source SRU Queues

In this section, two analytical queueing models are set up to represent source SRU queues under both the Greedy Bundle Release Scheme (GBRS) and the Probabilistic Bundle Release Scheme (PBRS). Mathematical expressions describing the characteristics of these models are derived. The derivation of the expression that quantifies the *bundle service time* requires particular attention.

Definiton: *The bundle service time denoted by T_s, is the time period that elapses from the instant an arbitrary bundle reaches the top of the SRU queue until the instant it is released to an arriving vehicle.*

3.2.1 GBRS Model Definition and Resolution:

Recall that, under GBRS, a source SRU releases a bundle to every arriving vehicle. As soon as a bundle B_{n-1} is released, bundle B_n will immediately occupy the front of the queue and wait for the next vehicle to arrive. Therefore T_s, in this case, is equivalent to the vehicle inter-arrival time. That is, $T_s = I$ and hence is similarly

exponentially distributed with mean $\frac{1}{\mu_v}$. Figure 3.5 illustrates a source SRU queue under GBRS. Furthermore, given assumption $(A2)$, a source SRU queue under GBRS can be modelled as an $M/M/1$ queueing system. According to [72], the different performance measures relating to such a queueing system are given as follows:

- The probability density function of the number of bundles in the system[1] is given by $P_n = (1-\rho)\rho^n$, for $n \geq 0$ with $\rho = \frac{\lambda}{\mu_v}$.
- The total waiting time in the system (*i.e.* queueing and service) has a probability density function $(\mu_v - \lambda)e^{-(\mu_v-\lambda)t}$, for $t \geq 0$.
- The mean number of bundles in the system is $\overline{N_S} = \frac{\rho}{1-\rho}$.
- The mean number of bundles in the queue is $\overline{N_Q} = \frac{\rho^2}{1-\rho}$.
- The mean system delay is $\overline{W_S} = \frac{1}{\mu_v-\lambda}(sec)$.
- The mean waiting time in the queue is $\overline{W_Q} = \frac{\rho}{\mu_v-\lambda}(sec)$.
- The mean bundle service time is $\overline{T_s} = \frac{1}{\mu_v}(sec)$.

3.2.2 PBRS Model Definition and Resolution:

Under PBRS, upon the occurrence of a release opportunity, the source SRU S relies on the bundle release probability P_{br} to release a bundle to the vehicle that mostly contributes to the minimization of the mean bundle transit delay. Inspired by this observation, the overall service process of an arbitrary bundle M_n can be viewed as subdivided into a random number $K = k$ $(k = 1, 2...)$ of service stages, [73]. While in the j^{th} stage $(j = 1, 2...k)$, bundle M_n is said to receive partial service that is

[1]Typically, a queueing system is composed of a queue and a server. A job completing service will leave the server and depart from the system. As such, the job at the frontmost position of the queue will advance to the server. In the proposed model above, the front most position of the queue (*i.e.* position $n = 1$) is considered to be the server. Subsequent positions $(n = 2, 3, ...)$ belong to the queue.

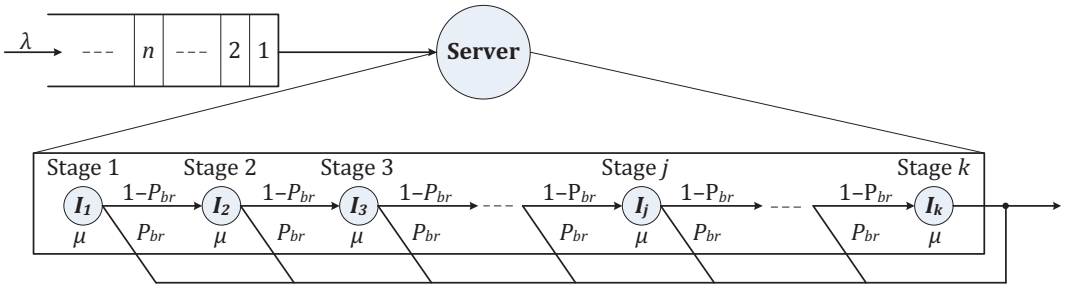

Figure 3.6: Bundle service time composed of several waiting stages.

equivalent to waiting a random amount of time I_j until the next vehicle arrives. The instant when a new vehicle arrives indicates the end of a stage. The instant when S releases M_n to a vehicle passing by, indicates the completion of M_n's service. After M_n is released, the bundle which is queued behind it (*i.e.* M_{n+1}), advances to the queue's front. In view of this, it becomes clear that a bundle advancing to the top of the queue always passes through the first service stage as it has to wait for the next arriving vehicle. It is important to note in this regard that bundles are assumed to be serviced according to the First-In-First-Out (FIFO) principle. After completing service at the j^{th} stage, the bundle is either released by the source with a probability P_{br} if the present opportunity is deemed adequate, or proceeds to stage $j+1$ with a probability $1-P_{br}$. In the latter case, the bundle advances with the hope to find a better release opportunity in the subsequent stages. Following the concept explained above and illustrated in Figure 3.6, a front bundle is said to receive a general type of service (*i.e.* the total service time of a front bundle follows a general distribution). Nevertheless, it can be easily proved that, under PBRS, the total service time T_s, experienced by a bundle occupying the front position of a source SRU queue is exponentially distributed with parameter $\mu_v P_{br}$. For instance, it is clear from Figure 3.6 that a front bundle's total service time T_s is equal to the sum of a number of I_j random variables ($j = 1, 2...$). For example, $T_s = I_1$ with a probability P_{br}; $T_s = I_1 + I_2$ with a probability $P_{br}(1-P_{br})$ and so on. As a result,

the probability that a bundle's total service time T_s is composed of k service stages is given by:

$$f_K(k) = Pr[K = k] = P_{br}(1 - P_{br})^{k-1} \tag{3.42}$$

Each I_j represents a vehicle inter-arrival time. Given that vehicle arrivals are independent, it follows that all I_j are independent and identically exponentially distributed with a density function $f_j(t) = f_I(t)$. In addition, given that the total service process of an arbitrary bundle is composed of $K = k$ stages, the probability that its total service time is equal to the sum of the k individual random partial service times spent at each stage can therefore be expressed as follows:

$$Pr\left[T_s = t = \sum_{j=1}^{k} I_j \middle| K = k\right] = f_1 * ... * f_k(t) \tag{3.43}$$

Consequently, we can express the probability density function of T_s as:

$$\begin{aligned} f_{T_s}(t) &= \sum_{k=1}^{\infty} Pr\left[T_s = t = \sum_{j=1}^{k} I_j \middle| K = k\right] \cdot Pr\left[K = k\right] \\ &= \sum_{k=1}^{\infty} \left[f_1 * ... * f_k(t)\right] \cdot P_{br}\left(1 - P_{br}\right)^{k-1} \end{aligned} \tag{3.44}$$

The Laplace Transform of $f_{T_s}(t)$ can be written as follows:

$$\begin{aligned} F^*_{T_s}(s) &= \sum_{k=1}^{\infty} \left[\frac{\mu_v}{s + \mu_v}\right]^k \cdot P_{br}\left(1 - P_{br}\right)^{k-1} = \frac{P_{br}}{1 - P_{br}} \sum_{k=1}^{\infty} \left[\frac{\mu_v(1 - P_{br})}{s + \mu_v}\right]^k \\ &= \frac{P_{br}}{1 - P_{br}} \left(\sum_{k=0}^{\infty} \left[\frac{\mu_v(1 - P_{br})}{s + \mu_v}\right]^k - 1\right) = \frac{P_{br}}{1 - P_{br}} \left(\frac{1}{1 - \frac{\mu_v(1-P_{br})}{s+\mu_v}} - 1\right) \\ &= \frac{\mu_v P_{br}}{s + \mu_v P_{br}} \end{aligned} \tag{3.45}$$

Finally, by inverting the Laplace Transform of equation (4.9), we get:

$$f_{T_s}(t) = \mu_v P_{br} e^{-\mu_v P_{br} t}, \text{ for } t \geq 0 \tag{3.46}$$

It is clear from equation (3.46) that the bundle service time is exponentially distributed with parameter $\mu_v P_{br}$. At this point, given that bundle inter-arrival time is also exponentially distributed with parameter λ, a stationary roadside unit (SRU) can thus be modelled as an $M/M/1$ queue that has the following characteristics:

- The effective bundle departure rate is $\mu_e = \mu_v P_{br}$.
- The probability density function of the number of bundles in the system is given by $P_n = (1-\rho)\rho^n$, for $n \geq 0$, with $\rho = \frac{\lambda}{\mu_e}$.
- The total waiting time in the system (*i.e.* queuing and service) has a p.d.f $(\mu_e - \lambda)e^{-(\mu_e - \lambda)t}$, for $t \geq 0$.
- The mean number of bundles in the system is $\overline{N_S} = \frac{\rho}{1-\rho}$.
- The mean number of bundles in the queue is $\overline{N_Q} = \frac{\rho^2}{1-\rho}$.
- The mean system delay is $\overline{W_S} = \frac{1}{\mu_e - \lambda}(sec)$.
- The mean waiting time in the queue is $\overline{W_Q} = \frac{\rho}{\mu_e - \lambda}(sec)$.
- The mean bundle service time is $\overline{T_s} = \frac{1}{\mu_e}(sec)$.

3.3 Transit Delay Analysis:

In this section we derive theoretical expressions for the average transit delay under both the Greedy Bundle Relaying Scheme (GBRS) and the Probabilistic Bundle Relaying Scheme (PBRS).

3.3.1 Average Transit Delay under GBRS:

Under GBRS, when the i^{th} vehicle having a constant speed v_i passes by the source, a bundle M is released to this vehicle. The transit delay experienced by M is defined to be the amount of time that takes the vehicle carrying M to travel the distance d_{SD} separating the source SRU from the destination SRU and deliver M. Obviously, this transit delay can be expressed as follows: $T_d = \frac{d_{SD}}{v_i}$. Note that the probability density function of T_d is given by equation (3.5). Hence, the average transit delay $\overline{T_{d,GBRS}}$ under GBRS can be written as:

$$\overline{T_{d,GBRS}} = E[T_d] = \int_{\frac{d_{SD}}{V_{max}}}^{\frac{d_{SD}}{V_{min}}} \frac{t \cdot d_{SD}}{(V_{max} - V_{min})t^2} dt = \frac{d_{SD}}{(V_{max} - V_{min}} \ln\left(\frac{V_{max}}{V_{min}}\right) \quad (3.47)$$

3.3.2 Average Transit Delay under PBRS:

Under PBRS, without loss of generality, assume that the service time of an arbitrary bundle M is composed of k stages. That is, k vehicles passed by the source with respective velocities $v_1, v_2, v_3, ..., v_k$. M was finally released to the k^{th} vehicle. Let v_k be a random variable that represents the speed of the vehicle to which a bundle has been released. We denote by R the event that a bundle is released to a vehicle passing by. The transit delay of a bundle B released to a vehicle having a speed v_k is $T_k = \frac{d_{SD}}{v_k}$. Let $\overline{T_{d,PBRS}} = E[T_k]$ denote the average transit delay under PBRS. The probability that a vehicle's speed is v_k such that $v \leq v_k < v + dv$ and given that a bundle was released to this vehicle is given by:

$$Pr\left[v \leq v_k < v + dv \middle| R\right] = \frac{Pr[v \leq v_k < v + dv, R]}{Pr[R]} \quad (3.48)$$

Using *Baye's Theorem* (refer to [74]), we can rewrite equation (4.12) as:

$$\begin{aligned} Pr\left[v \leq v_k < v + dv \middle| R\right] &= \frac{Pr\left[R \middle| v \leq v_k < v + dv\right] \cdot f_V(v)}{P_{br}} \\ &= \frac{P_{br,k} \cdot f_V(v_k)}{\int_{V_{min}}^{V_{max}} P_{br,k} \cdot f_V(v_k) dv_k} = \frac{P_{br,k} \cdot \frac{1}{V_{max} - V_{min}}}{\int_{V_{min}}^{V_{max}} P_{br,k} \cdot \frac{1}{V_{max} - V_{min}} dv_k} \\ &= \frac{P_{br,k}}{\int_{V_{min}}^{V_{max}} P_{br,k} dv_k} \end{aligned} \tag{3.49}$$

Let $C = \frac{1}{\int_{V_{min}}^{V_{max}} P_{br,k} dv_k}$. As a result, we get:

$$Pr\left[v \leq v_k < v + dv \middle| R\right] = C \cdot P_{br,k} = f_{v_k}(v), \text{ for } v_k \in [V_{min}; V_{max}] \tag{3.50}$$

It is important to highlight that equation (3.50) describes the density function of the speed V_k of a vehicle carrying a bundle, denoted by $f_{v_k}(v)$. Let $F_{v_k}(v)$ and $F_{T_k}(t)$ respectively denote the cumulative distribution function of the transporting vehicle speed v_k and the transit delay achieved under PBRS T_k. Using random variable transformation, we get:

$$F_{T_k}(t) = Pr[T_k \leq t] = Pr\left[\frac{d_{SD}}{v_k} \leq t\right] = 1 - Pr\left[v_k \leq \frac{d_{SD}}{t}\right] = 1 - F_{v_k}\left(\frac{d_{SD}}{t}\right) \tag{3.51}$$

Differentiating both sides of equation (3.51), we obtain:

$$\frac{dF_{T_k}(t)}{dt} = \frac{d\left[1 - F_{v_k}\left(\frac{d_{SD}}{t}\right)\right]}{dt} = -\frac{dF_{v_k}\left(\frac{d_{SD}}{t}\right)}{dt} \tag{3.52}$$

By the Chain Rule, equation (3.52) becomes:

$$f_{T_k}(t) = \frac{d_{SD}}{t^2} f_{V_k}\left(\frac{d_{SD}}{t}\right)$$
$$= \frac{C \cdot d_{SD}}{t^2}\left(1 - \frac{\left[Ei\left(\mu_v \frac{d_{SD}}{V_{max}}\right) - \frac{V_{max} e^{\mu_v \frac{d_{SD}}{V_{max}}}}{\mu_v d_{SD}} - Ei(\mu_v t)\right] e^{-\mu_v t} + \frac{V_{max}}{\mu_v d_{SD}}}{\left[Ei\left(\mu_v \frac{d_{SD}}{V_{max}}\right) - \frac{V_{max} e^{\mu_v \frac{d_{SD}}{V_{max}}}}{\mu_v d_{SD}} - Ei\left(\mu_v \frac{d_{SD}}{V_{min}}\right)\right] e^{-\mu_v \frac{d_{SD}}{V_{min}}} + \frac{V_{max}}{\mu_v d_{SD}}}\right)$$
$$, \text{ for } t \in \left[\frac{d_{SD}}{V_{max}}; \frac{d_{SD}}{V_{min}}\right] \tag{3.53}$$

Therefore, the average transit delay under PBRS is given by:

$$\overline{T_{d,PBRS}} = E[T_k] = \int_{\frac{d_{SD}}{V_{max}}}^{\frac{d_{SD}}{V_{min}}} t \cdot f_{T_k}(t) dt$$
$$= C \cdot d_{SD} \times$$
$$\int_{\frac{d_{SD}}{V_{max}}}^{\frac{d_{SD}}{V_{min}}} \left(\frac{1}{t} - \frac{\left[Ei\left(\mu_v \frac{d_{SD}}{V_{max}}\right) - \frac{V_{max} e^{\mu_v \frac{d_{SD}}{V_{max}}}}{\mu_v d_{SD}} - Ei(\mu_v t)\right] e^{-\mu_v t} + \frac{V_{max}}{\mu_v d_{SD}}}{t \cdot \left(\left[Ei\left(\mu_v \frac{d_{SD}}{V_{max}}\right) - \frac{V_{max} e^{\mu_v \frac{d_{SD}}{V_{max}}}}{\mu_v d_{SD}} - Ei\left(\mu_v \frac{d_{SD}}{V_{min}}\right)\right] e^{-\mu_v \frac{d_{SD}}{V_{min}}} + \frac{V_{max}}{\mu_v d_{SD}}\right)}\right) dt \tag{3.54}$$

Denote by:

- $\xi = \left[Ei\left(\mu_v \frac{d_{SD}}{V_{max}}\right) - \frac{V_{max} e^{\mu_v \frac{d_{SD}}{V_{max}}}}{\mu_v d_{SD}} - Ei\left(\mu_v \frac{d_{SD}}{V_{min}}\right)\right] e^{-\mu_v \frac{d_{SD}}{V_{min}}} + \frac{V_{max}}{\mu_v d_{SD}}$.
- $\zeta = Ei\left(\mu_v \frac{d_{SD}}{V_{max}}\right) - \frac{V_{max} e^{\mu_v \frac{d_{SD}}{V_{max}}}}{\mu_v d_{SD}}$.

Consequently, equation (3.54) can be re-written as:

$$\begin{aligned}\overline{T_{d,PBRS}} &= C \cdot d_{SD}\left[\int_{\frac{d_{SD}}{V_{max}}}^{\frac{d_{SD}}{V_{min}}} \frac{dt}{t} - \int_{\frac{d_{SD}}{V_{max}}}^{\frac{d_{SD}}{V_{min}}} \frac{\left[\zeta - Ei(\mu_v t)\right] e^{-\mu_v t} + \frac{V_{max}}{\mu_v d_{SD}}}{t \cdot \xi} dt\right] \\ &= C \cdot d_{SD}\left[\ln\left(\frac{V_{max}}{V_{min}}\right) - \frac{\zeta}{\xi}\int_{\frac{d_{SD}}{V_{max}}}^{\frac{d_{SD}}{V_{min}}} \frac{e^{-\mu_v t}}{t} dt + \frac{1}{\xi}\int_{\frac{d_{SD}}{V_{max}}}^{\frac{d_{SD}}{V_{min}}} \frac{Ei(\mu_v t)e^{-\mu_v t}}{t} dt \right. \\ &\qquad \left. - \frac{V_{max}}{\xi \mu_v d_{SD}}\int_{\frac{d_{SD}}{V_{max}}}^{\frac{d_{SD}}{V_{min}}} \frac{dt}{t}\right] \\ &= C \cdot d_{SD}\left[\left(1 - \frac{V_{max}}{\xi \mu_v d_{SD}}\right)\ln\left(\frac{V_{max}}{V_{min}}\right) - \frac{\zeta}{\xi}\int_{\frac{d_{SD}}{V_{max}}}^{\frac{d_{SD}}{V_{min}}} \frac{e^{-\mu_v t}}{t} dt \right. \\ &\qquad \left. + \frac{1}{\xi}\int_{\frac{d_{SD}}{V_{max}}}^{\frac{d_{SD}}{V_{min}}} \frac{Ei(\mu_v t)e^{-\mu_v t}}{t} dt\right]\end{aligned} \tag{3.55}$$

From [70] it can be shown that:

$$\int_{\frac{d_{SD}}{V_{max}}}^{\frac{d_{SD}}{V_{min}}} \frac{e^{-\mu_v t}}{t} dt = Ei\left(-\mu_v \frac{d_{SD}}{V_{min}}\right) - Ei\left(-\mu_v \frac{d_{SD}}{V_{max}}\right) \tag{3.56}$$

It follows that equation (3.55) can be re-written as:

$$\begin{aligned}\overline{T_{d,PBRS}} = C \cdot d_{SD}\Bigg[&\left(1 - \frac{V_{max}}{\xi \mu_v d_{SD}}\right)\ln\left(\frac{V_{max}}{V_{min}}\right) - \frac{\zeta}{\xi}\left[Ei\left(-\mu_v \frac{d_{SD}}{V_{min}}\right) - Ei\left(-\mu_v \frac{d_{SD}}{V_{max}}\right)\right] \\ &+ \frac{1}{\xi}\int_{\frac{d_{SD}}{V_{max}}}^{\frac{d_{SD}}{V_{min}}} \frac{Ei(\mu_v t)e^{-\mu_v t}}{t} dt\Bigg]\end{aligned} \tag{3.57}$$

The term $\int_{\frac{d_{SD}}{V_{max}}}^{\frac{d_{SD}}{V_{min}}} \frac{Ei(\mu_v t)e^{-\mu_v t}}{t} dt$ may be computed using exactly the same integration technique as in equation (3.40).

3.4 Simulation Results and Numerical Analysis

A discrete event simulation framework is developed for the purpose of examining the performance of PBRS and GBRS in the context of the sample ICRCN shown in Figure 3.1.

3.4.1 Model Validation and Simulation Accuracy:

Figure 3.7 presents a theoretical evaluation of the performance of both PBRS and GBRS in terms of the following metrics: *a*) the mean number of bundle service stages, *b*) the mean bundle service time and *c*) the mean bundle transit delay. The theoretical curves of these metrics are concurrently plotted with their simulated counterparts as a function of the mean vehicle inter-arrival time. 10^7 bundles were considered per simulation run. Furthermore, all of the metrics were averaged out over multiple runs of the simulator to ensure that a 95% confidence interval is realized. Following the guidelines presented in [25], the following parameter values were taken:

- The mean vehicle inter-arrival time, $\overline{I}$ varies between 10 and 120 (secs).
- The mean bundle inter-arrival time $\overline{B} = 4$ (secs).
- Vehicle speeds vary between $V_{min} = 10$ and $V_{max} = 50$ (m/sec).
- The source-destination distance $d_{SD} = 20000$ (m).

Clearly, Figures 3.7(a) through 3.7(c) are tangible proofs of the validity and remarkable accuracy of the earlier presented queuing models and transit delay analysis. This is especially true since the curves in all of the three plots perfectly overlap with each other.

On a different note, Figure 7(a) shows the mean number of service stages experienced by a front bundle versus the vehicle inter-arrival time. Recall that under

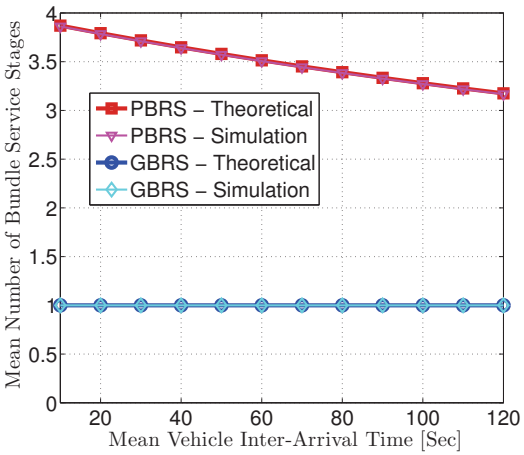

(a) Mean Number of Service Stages.

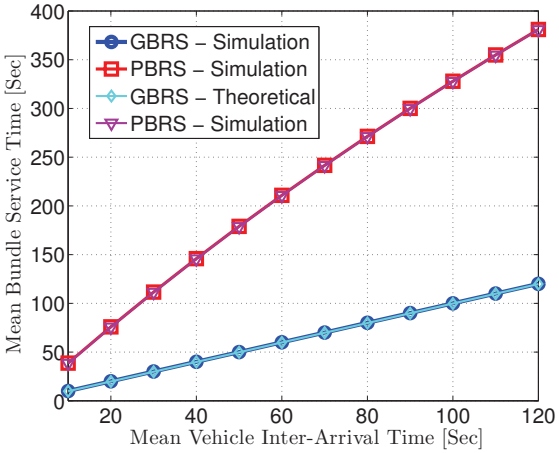

(b) Mean Bundle Service Time (sec).

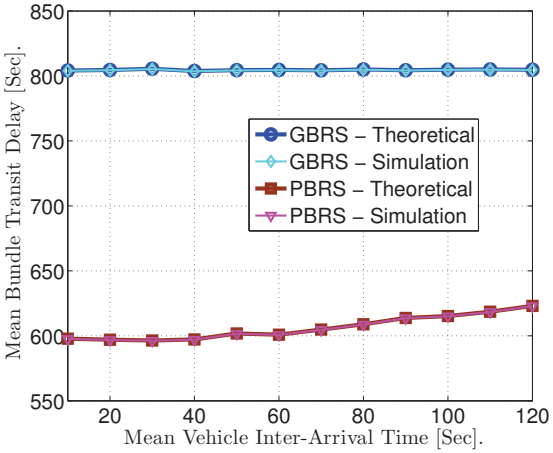

(c) Mean Bundle Transit Delay (sec).

Figure 3.7: Theoretical and simulated performance evaluation of PBRS and GBRS.

GBRS, bundles are greedily cleared out. Therefore, a bundle that has just advanced to the front position of the queue will only have to wait for the immediate arrival of the next vehicle to which it will be released. As such, under GBRS, a front bundle undergoes a single service stage irrespective of the time spacing between vehicle arrivals. In contrast, under PBRS, the source releases bundles only to relatively high speed vehicles in order to ensure that their transit delays are minimized. For this purpose, the bundle release probability P_{br} indicates to the source which of the arriving vehicles are relatively faster than others and more suitable to transport bundles to the destination. As such, the source with a front bundle ready to be released may witness several vehicle arrivals before it finally releases that bundle to a vehicle that P_{br} recommends. To this end, on one hand, the shorter the vehicle inter-arrival time is, the more likely the occurrence of a close high speed vehicle arrival becomes. As a result, P_{br} forces the source to retain its front bundle until a vehicle that is fast enough arrives. Hence, a front bundle may experience an extended waiting time at the front of the source's queue. However, this time extension is expected to be very limited and easily compensated for by the achieved transit delay thereafter. On the other hand, once vehicle arrivals become more spaced in time, the extended waiting period of a front bundle will rapidly grow. To limit this growth, P_{br} adaptively reduces the number of waiting stages a front bundle goes through and allow the source to release it to slower vehicles.

Now recall from our earlier theoretical analysis that the mean bundle service time is inversely proportional to the mean vehicle inter-arrival time and directly proportional to the mean number of bundle service stages. This fact is confirmed in Figure 3.7(b). On one hand, under GBRS, the front bundle always experiences a single service stage. As a result, the mean bundle service time directly follows the mean vehicle inter-arrival time. On the other hand, under PBRS, a front bundle

experiences a service time that is approximately three to four times that under GBRS. In fact, the mean vehicle inter-arrival time and the mean number of bundle service stages are analogous to two opposing forces where if one decreases, the other attempts to counter its effect by increasing. However, the mean vehicle inter-arrival time increases much faster than the mean number of service stages decreases. This directly explains the growing gap between the achieved service times under GBRS and PBRS.

Finally, in terms of transit delay, Figure 7(c) shows that PBRS remarkably outperforms GBRS. This is due to the fact that, under GBRS, the source node does not differentiate between slow and fast vehicles and greedily releases bundles to every arriving vehicle. Under PBRS however, bundles are only released to relatively high speed vehicles. Therefore, on average, the transit delay under PBRS is much lower than that experienced under its greedy counterpart.

3.4.2 Delay Performance Analysis of PBRS and GRBS Under Heavy Offered Data Load:

This subsection is devoted to contrasting the overall performance of the probabilistic scheme with that achieved by greedy forwarding. The adopted metric for performance evaluation is the mean bundle end-to-end delivery delay. Observe that the bundle end-to-end delivery delay is composed of (i) the bundle queueing delay[2], and (ii) the bundle transit delay.

Contrary to our expectations in section (3.4.1), we observed throughout our study that the vehicle inter-arrival time has a major impact on the source node's stability status. This is especially true since typical Internet packet-like forwarding is adopted where only a single bundle is released at a time. Figure 8(a) confirms this fact where

[2]In the context of our study, the bundle service time is nothing but the time period a bundle waits at the front position of the source node's queue. As such, the overall bundle queueing delay is nothing but the sum of the bundle service time and the time period a bundle has waited in all the subsequent queue positions it passed through since the instant of its arrival.

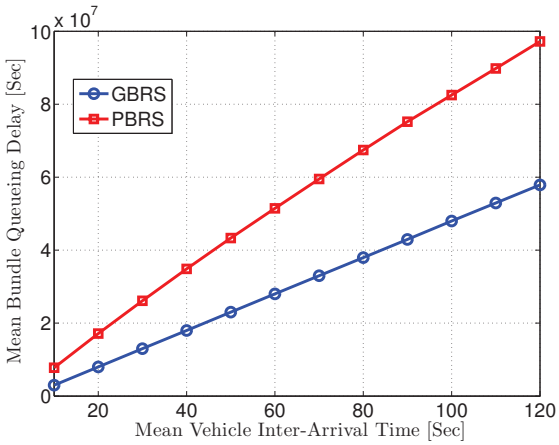

(a) Mean Queueing Delay (sec).

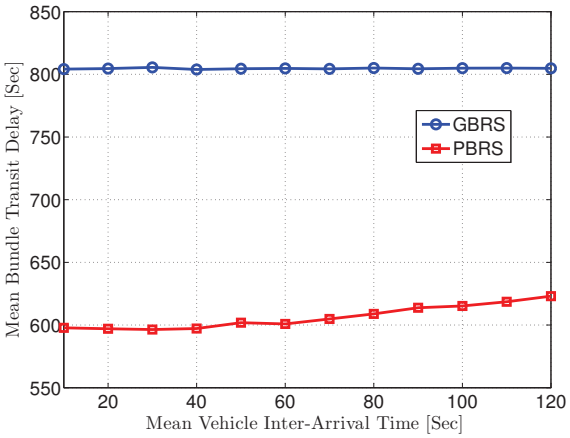

(b) Mean Transit Delay (sec).

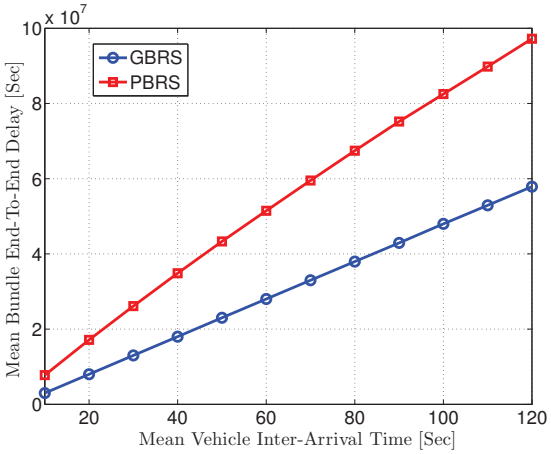

(c) Mean End-To-End Delay (sec).

Figure 3.8: Delay Performance of PBRS versus GBRS.

under both the probabilistic scheme and its greedy counterpart, the experienced queueing delay on average is of the order of 10^7. Indeed this is reasonable since, in our simulations, the considered offered load to the source is relatively high with a bundle inter-arrival time of 4 seconds while the minimum vehicle inter-arrival time is 10 seconds. That is, as far as GBRS is concerned, bundles arrive to the source at a much higher rate than the one at which the source is able to clear them out. Hence, it will not take long before the queue becomes unstable[3] in which case bundles will accumulate and experience uncontrollably growing queueing delays. Under PBRS, the case is even worse since, following P_{br}'s recommendation, bundles are forced to stay in the queue for longer times. In addition, the more vehicle arrivals become spaced out in time, the more unstable the queue will be and the larger the queueing delays grow. Although PBRS results in a significant improvement in terms of the achieved mean bundle transit delay as shown in Figure 8(b), this improvement which is in the order of hundreds of seconds becomes unable to compensate for these excessive queueing delays. In light of this, the resulting end-to-end delivery delay becomes exorbitant as it is primarily governed by the queueing delay as shown in Figure 8(c). It follows that, under such circumstances, both GBRS and PBRS are inefficient. Nonetheless, we observed that allowing both schemes to release a bulk of bundles, each time an opportunity presents itself, will greatly improve the performance of both of them. However, this simple yet very effective option will allow PBRS to remarkably outperform GBRS in terms of average end-to-end delivery delay and hence become of exceptional utility. This point is investigated further in the following section.

[3]According to [72], a queueing system is said to be stable when its load, defined as the ratio of the customer arrival rate over the customer departure rate, $\rho = \frac{\lambda}{\mu_v} < 1$. The system becomes unstable when $\rho \geq 1$. In this chapter the queueing system is the source SRU queue, customers are bundles. The rate of bundle departures is governed by the rate of vehicle arrivals.

3.4.3 Delay Performance Analysis of PBRS and GRBS Under Light Offered Data Load:

Subsection VI-B evaluated the performance of PBRS and GBRS for a heavy offered data load, a condition under which the source SRU's queue is highly unstable. It is important to mention that, in real life, such conditions are the norms rather than the exceptions. This is especially true since the transport infrastructure and the physical data transportation phenomenon present a rather naturally slow medium of communication and this will surely affect a source SRU's stability. Nonetheless, for the sake of completion, this section demonstrates the performance of these two schemes under stability conditions. The results are reported in Figure 3.9. Such conditions are however realized under unrealistically low offered data loads. Obviously, the stability criterion is different for each of PBRS and GBRS. In fact, under GBRS, a source SRU's queue can reach stability at much higher values of offered data load than those necessary to realize stability under PBRS. Also note that for each value of the vehicle inter-arrival times $\overline{I} \in [10; 120]$ (sec) corresponds one value of the bundle average inter-arrival time $\overline{B}$ that secures stability. Hence, for consistency purposes, the same value of $\overline{B}$ must be used for which the source SRU's queue would be stable under both PBRS and GBRS and for all of the considered values of $\overline{I}$. As a matter of fact, since stability is much more constrained under PBRS than it is under GBRS, the value of $\overline{B}$ that ensures the stability of the source SRU's queue under PBRS and for the highest value of $\overline{I} = 120$ (sec) will definitely secure the stability of the queue for GBRS and under all lower values of $\overline{I}$. The lowest such value of $\overline{B} = 700$ (sec), which is clearly unrealistic for a real life scenario.

As expected, both schemes exhibited stability performance patterns that are highly similar to those under instability conditions in the sense that GBRS performed better than PBRS. As a matter of fact, the same exact conclusions that were

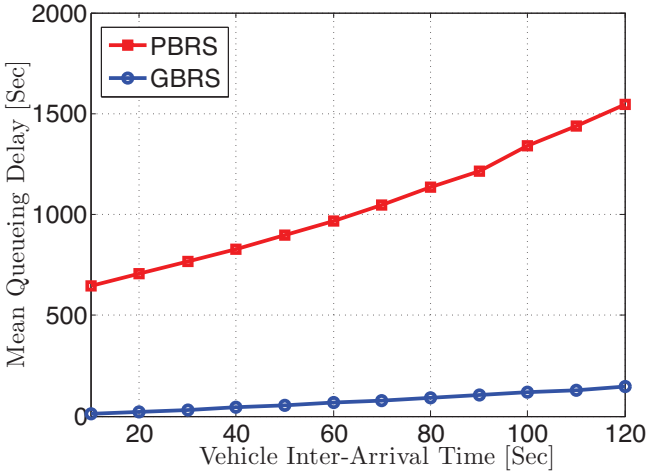

(a) Mean Queueing Delay (sec).

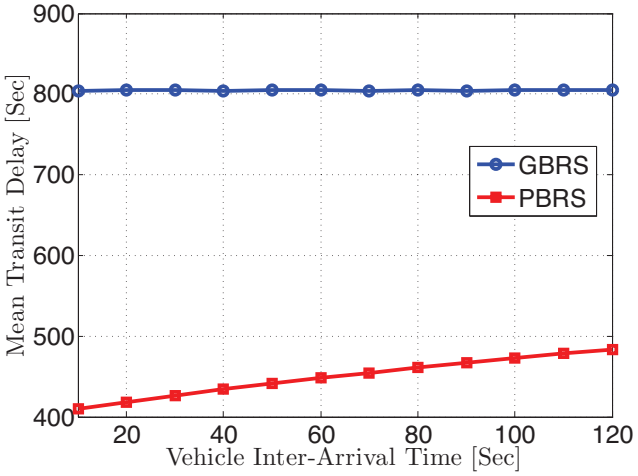

(b) Mean Transit Delay (sec).

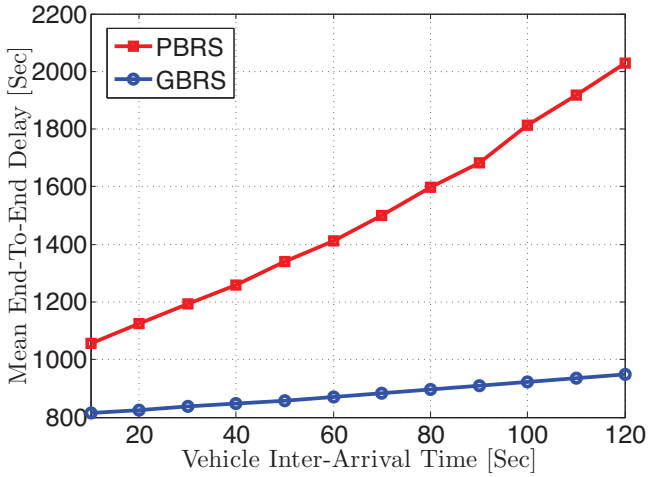

(c) Mean End-To-End Delay (sec).

Figure 3.9: Delay Performance of PBRS versus GBRS under stability conditions.

drawn in subsection 3.4.2 will apply to this case as well. It is primarily the singly bundle release per opportunity that severely degrades the performance of PBRS in terms of the queueing delay. However, the transit delay improvement that PBRS has over GBRS is remarkable. Nevertheless, the queueing delay still overshadows the transit delay and governs the performance of PBRS in terms of the end-to-end delay. In the subsequent section, an effective mechanism will be proposed to overcome the queueing delay problem. This mechanism is expected to significantly boost the performance of PBRS. This improvement will be reflected in the end-to-end delay.

Chapter 4

A Simple Free-Flow Traffic Model for Vehicular Intermittently Connected Networks

As opposed to traditional wireless ad hoc networks [75], a vehicular network exhibits volatile connectivity and has to handle a variety of network densities. For example, a vehicular network deployed over a rural roadway or within an urban area is likely to experience higher nodal densities. This is especially true during rush hours (*e.g.* 8:00 A.M. to 10:00 A.M. and 4:00 P.M. to 7:00 P.M.). However, during late night hours and whenever deployed over large highways or within scarcely populated areas, a vehicular network is expected to suffer from frequent network partitioning and repetitive link disruptions. Over the past couple of years, the networking research community has witnessed many publishable studies revolving around the connectivity analysis as well as the proposal of routing and forwarding schemes that handle the broadcast storm (*e.g.* [76, 77]) and data delivery (*e.g.* [78]) in the context of a dense vehicular network. These studies were conducted under the simplified assumption that these vehicular networks are naturally well-connected. In contrast, even

though the development of reliable, timely and resource efficient forwarding schemes that support the diverse topologies of *Vehicular Intermittently Connected Networks* (VICNs) is crucially challenging, it is believed that the immature understanding of network disruption causes and resolution procedures is persistently leading to inadequate scheme designs and inaccurate performance analysis and evaluation.

While the universally known Delay-/Disruption-Tolerant Networking's *store-carry-forward* mechanism (refer to [79]) has emerged as a highly effective solution that mitigates VICNs' link disruptions, the published performance evaluations of various VICN forwarding schemes adopting this mechanism have been shown to be inconsistent with real-life experimental observations. Ever since, the networking research community has been expressing a growing interest in uncovering the major cause of this inconsistency. Recently, several researchers have linked and proved that the reason behind this conflict between the real-world experimental observations and the theoretical analysis is the utilization of unrealistic theoretical vehicular traffic models (*e.g.* [80, 81]). Following this, every published work enclosed a customized model that attempts to emulate the realistic behaviour of vehicular traffic. The vehicular traffic is affected by a large number of random events (*e.g.* weather, road geometry, drivers' skills and habits, haphazard catastrophic incidents etc). Thus far, the open literature lacks any model that accounts for all such events. However, some of the developed models tend to have a microscopic aspect (*e.g.* [65, 82]) as they independently consider factors such as weather, road geometry, commuter's skills and habits, and so forth. These microscopic models are complex which renders them highly theoretical with limited implementation feasibility for simulations. Other models take on the macroscopic (*e.g.* [59, 83]) aspect. Macroscopic models revolve around three major traffic parameters, namely: the vehicular density, the traffic flow and vehicles' speeds. Most of the existing models deviate from reality since they are based on

highly restrictive assumptions (*e.g.* all vehicles navigate at a single constant speed, vehicles' speeds are independent from the vehicular density, etc.) tailored to their enclosing study. Ultimately, since the existing VICN forwarding schemes have different underlying traffic models, comparing their performance is not meaningful.

This chapter aims at presenting a comprehensive and traffic-theory-inspired macroscopic description of Free-flow traffic conditions (*i.e.* conditions[1] where vehicular traffic is typically characterized by low to medium vehicular density, arbitrarily high mean speeds and stable flow.) over one-dimensional uninterrupted[2] roadway segments. The purpose of this description is to introduce a generic notation for the above-mentioned three macroscopic traffic parameters and highlight the strong correlation between them. Based on this study, we propose to adopt an existing traffic model that has been developed in [37]. We refer to this model as the Free-flow Traffic Model (FTM). The reason behind adopting this model is its accuracy in capturing the dynamics of the Free-flow vehicular traffic behaviour. Nonetheless, the statistical characteristics as derived in [37] are complex and were only evaluated numerically. In this chapter, we show that a simple two-phase Coxian approximation presents itself as a highly accurate solution to work around this problem.

4.1 Vehicular Traffic Analysis

4.1.1 Free-Flow Traffic Characteristics:

Consider a roadway segment $[AB]$ such as the one depicted in Figure 4.1. $[AB]$ has a length L_{AB} (*meters*). Let l_v be the mean vehicle length. The *capacity* of

[1]Note that, under such conditions, delay tolerance becomes a major requirement for successful data delivery. This is because low to medium vehicular density coupled with high vehicle speeds causes the network to become sparse and subject to frequent link disruptions.

[2]No grade intersections, traffic lights, STOP signs, direct access to adjoint lands, bifurcations, etc.

$[AB]$ defined herein as the maximum number of vehicles that may be simultaneously present within $[AB]$ is $C_{AB} = \frac{L_{AB}}{l_v}$ $(vehicles)$, [27]. The mean *vehicular density*, ρ_v $\left(\frac{vehicles}{meter}\right)$, is defined as the mean number of vehicles per unit length. Thus, the maximum vehicular density is $\rho_{max} = \frac{C_{AB}}{L_{AB}} = \frac{1}{l_v}$. The *vehicular flow rate*, μ_v $\left(\frac{vehicles}{second}\right)$, is defined as the mean number of vehicles passing a fixed point on $[AB]$ per unit time[3]. Without loss of generality, this fixed point is assumed to be the entry point to the segment (*i.e* point A). In the sequel, the event of a vehicle entering $[AB]$ at point A is referred to as a *vehicle arrival*. Therefore, μ_v is interpreted as the *vehicle arrival rate* whose maximum is denoted by μ_{max}. Let S_{max} denote the speed limit over the segment $[AB]$.

The observation of $[AB]$ begins at a certain point in time t_0 (*e.g.* very early morning) set as the origin of the time axis (*i.e.* $t_0 = 0$) where $[AB]$ is empty (*i.e.* no vehicles are navigating over $[AB]$, $\rho_v = 0$ and $\mu_v = 0$). After some time, vehicles start arriving to $[AB]$ causing ρ_v to gradually increase with time. μ_v also exhibits a gradual stable[4] increase as a function of ρ_v. However, there exists a critical density value ρ_c that, once reached, vehicle platoons start forming all over the road segment $[AB]$. This indicates that: *a*) $[AB]$ has become considerably congested and *b*) the vehicular flow has attained its maximum μ_{max}. At this point, $[AB]$ becomes highly unstable (see [27]) since the slightest traffic perturbation may either re-stabilize the traffic flow or cause a transition into a state of over-forced flow where μ_v starts decreasing while ρ_v increases further. Eventually, at ρ_{max}, $\mu_v = 0$ indicating that $[AB]$ is experiencing a traffic jam. From the point of view of vehicular ad-hoc networks (VANETs), the formation of an end-to-end path between an arbitrary pair of nodes becomes highly probable whenever the vehicular density is high (*i.e.* $\rho_c \leq \rho_v \leq \rho_{max}$) regardless if those nodes are fixed (*e.g.* stationary roadside units) or moving along

[3]In this chapter time is measured in units of *seconds*

[4]The flow of vehicles into and out of $[AB]$ are equal.

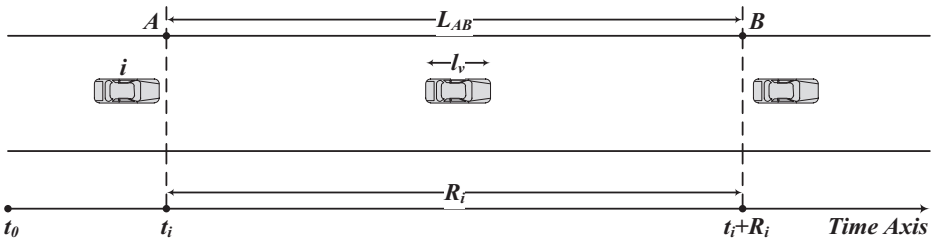

Figure 4.1: Free-flow vehicular traffic over the roadway segment $[AB]$.

the road segment (*i.e.* vehicles equipped with wireless devices). In this situation, delay tolerance is no longer a requirement and typical wireless protocols can be used over inter-vehicular-enabled VANETs to establish a multi-hop connectivity between a particular data source and destination. Obviously, this is not the case whenever the road segment is operating under Free-flow traffic conditions (*i.e.* $0 < \rho_v < \rho_c$) where the network becomes sparse and prone to link disruptions. Therefore, cases of over-forced vehicular traffic are ignored in this present study.

As shown in Figure 4.1, an arbitrary vehicle i with speed s_i enters $[AB]$ at time t_i, resides within $[AB]$ for a period $R_i = \frac{L_{AB}}{s_i}$ and exits at time $e_i = t_i + R_i$. Subsequently, vehicle $i+1$ with speed s_{i+1} arrives at time t_{i+1}, resides within $[AB]$ for a period R_{i+1} and departs at time e_{i+1}. In traffic theory, the *time headway* is defined as the time interval between successive vehicles crossing the same reference point on a road segment, [27]. In the present study, it is assumed that the reference point is the entry point to $[AB]$ (*i.e.* point A). Thus, the time headway becomes equivalent to the vehicle inter-arrival time that is denoted by $I = t_{i+1} - t_i$. Selecting a distribution for I is a delicate task that has to be handled carefully.

In [84], the authors have conducted thorough experiments over highways surrounding the city of Madrid in Spain. They have collected large sets of realistic traces during two separate time intervals, namely: *a*) Rush hours from 8:30 A.M until 9:00 A.M and *b*) Non-rush hours from 11:30 A.M until 12:00 P.M. After thorough analysis of their collected data sets, the authors found that I is best modelled

by a weighted Exponential-Gaussian distribution mixture. Indeed, this finding is of notable importance. In fact, this model particularly accounts for the inter-vehicular behavioural dependencies under dense traffic conditions and, furthermore, correctly characterizes I irrespective of the time of the day during which an arbitrary roadway segment is observed. Nevertheless, our primary objective in this chapter is to acquire knowledge about the statistical characteristics of the vehicular traffic behaviour under strict free-flow conditions. For this purpose, we need only to consider non-rush hours. That is late night and early morning hours from 7:00 P.M to 8:00 A.M as well as mid-day hours from 10:00 A.M. to 4:00 P.M. The authors of [76] and [85] have also conducted real-life experiments during these hours on the $I-80$ freeway in California, United States. The realistic data traces they have obtained show that the vehicle inter-arrival time during non-rush hours is exponentially distributed. In addition, the analysis presented in [76] shows that, during these hours and particularly whenever the vehicular flow is below 1000 vehicles per hour, the inter-vehicular distance is relatively large. In other words, vehicles navigating on a roadway segment appear to be isolated and hence, the vehicle arrivals to an arbitrary geographical reference point become independent and identically distributed (I.I.D.). This has also been confirmed in [84].

Inspired by this last observation, we have conducted thorough simulations using the Simulation for Urban MObility (SUMO) simulator. SUMO is a microscopic simulator that provides realistic vehicular mobility traces for use as input for other vehicular networking simulators. The same scenario was simulated for different vehicular flow intensities all of which, however, are less than 1000 vehicles per hour. A well defined geographical reference point was defined for all these simulations and vehicle arrival times were to this reference point were computed. The difference between two consecutive vehicle arrival times gives one sample of the vehicle inter-arrival time.

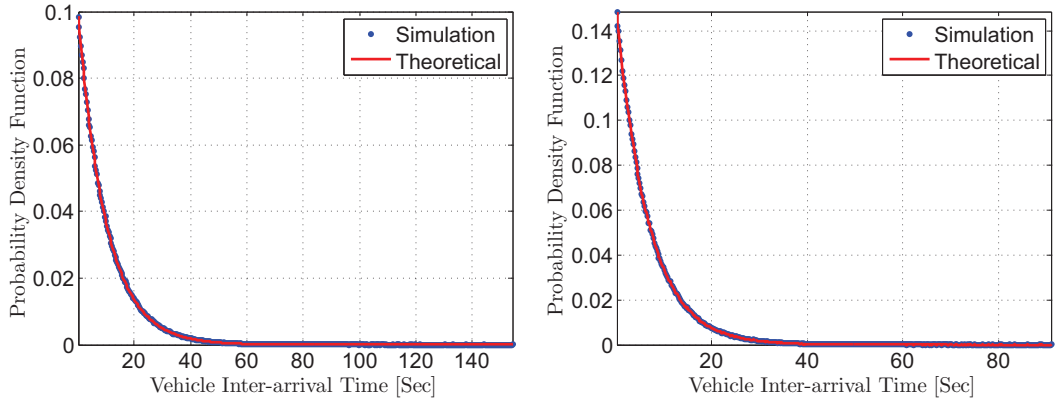

(a) $\mu_v = 0.1\,(\frac{vehicle}{second})$. (b) $\mu_v = 0.15\,(\frac{vehicle}{second})$.

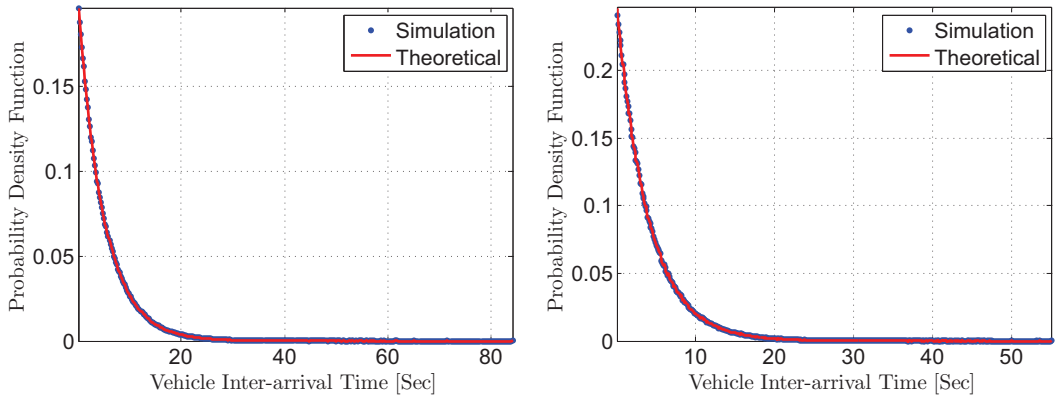

(c) $\mu_v = 0.2\,(\frac{vehicle}{second})$. (d) $\mu_v = 0.25\,(\frac{vehicle}{second})$.

Figure 4.2: Vehicle inter-arrival time probability density function for different flow rate values. Note that the utilized unit is $(\frac{vehicles}{second})$.

The conducted simulations spanned a period of time that is long enough to collect 10^5 inter-arrival time samples per simulation. The results of four simulation scenarios are reported herein in Figure 4.2. These scenarios are selected in such a way that their corresponding μ_v values uniformly cover the range of possible flow rates under Free-flow traffic conditions. This figure plots the cumulative distribution function of the collected data samples together with its theoretical counter part. It is, indeed, a tangible proof that I is exponentially distributed. Note that the mean vehicle inter-arrival time, $\overline{I} = E[I]$, is inversely proportional to the vehicle arrival rate μ_v.

It follows that the probability density function of I can be expressed as:

$$f_I(t) = \frac{1}{\mu_v} e^{-\frac{t}{\mu_v}} \text{ , for } t \geq 0 \tag{4.1}$$

Denote by $\overline{S}$ the mean of vehicle speeds observed over $[AB]$. It is established in [27] that:

$$\overline{V} = V_{max}\left(1 - \frac{\rho_v}{\rho_{max}}\right) \tag{4.2}$$

Define $\overline{R} = \frac{L_{AB}}{\overline{S}}$ as the mean vehicle residence time within $[AB]$ and $\overline{N}$ as the mean number of vehicles in $[AB]$. Hence, the following relationship is established using *Little's Law*, [86]:

$$\mu_v = \frac{\overline{N}}{\overline{R}} = \frac{\overline{N} \cdot \overline{V}}{L_{AB}} = \rho_v \cdot \overline{V} = -\frac{V_{max}}{\rho_{max}}\rho_v^2 + V_{max}\rho_v \tag{4.3}$$

Equation (4.3) is the fundamental traffic relationship, [27]. From (4.3) it is clear that $\mu_v = 0$ at both $\rho_v = 0$ and $\rho_v = \rho_{max}$. Also, the maximum flow rate $\mu_{max} = \frac{V_{max}\rho_{max}}{4}$ occurs at the critical density value $\rho_v = \frac{\rho_{max}}{2} = \rho_c$. The critical speed is defined as $V_c = \overline{V}|_{\rho_v = \rho_c} = \frac{V_{max}}{2}$. Recall that this study considers only Free-flow traffic conditions (*i.e.* $\rho_v \in \left[0; \frac{\rho_{max}}{2}\right]$). According to [27], under Free-flow traffic conditions, the speed $v_i = v$ $(i > 0)$ of an arbitrary arriving vehicle i is a normally distributed random variable with a probability density function given by:

$$f_V(v) = \frac{1}{\sigma_V\sqrt{2\pi}} e^{-\left(\frac{v-\overline{V}}{\sigma_V\sqrt{2}}\right)^2} \tag{4.4}$$

The authors of [87] assume justifiably that $\sigma_V = k\overline{V}$ and that $v \in [V_{min}; V_{max}]$, where $V_{min} = \overline{V} - m\sigma_V$ and the two-tuple (k, m) depend on the ongoing traffic activity over the observed roadway segment and are determined based on experimental data. Accordingly, in the rest of this chapter a truncated version of $f_V(v)$ in (4.4) shall be

adopted. It is defined as:

$$f_V^t(v) = \frac{f_V(v)}{\int_{V_{min}}^{V_{max}} f_V(v)dv} = \frac{2f_V(v)}{\text{erf}\left(\frac{V_{max}-\overline{V}}{\sigma_V\sqrt{2}}\right) - \text{erf}\left(\frac{V_{min}-\overline{V}}{\sigma_V\sqrt{2}}\right)} \tag{4.5}$$

for $V_{min} \leq v \leq V_{max}$. Furthermore, a seminal study conducted in [88] together with extensive real-life experimentations and data acquisition over numerous roadways show that, v_i is constantly maintained during the vehicle's entire navigation period on the road. Let $F_V^t(\cdot)$ and $F_R(\cdot)$ denote the respective cumulative distribution functions of the vehicle's speed and residence time. It can be easily shown that:

$$F_R(\tau) = 1 - F_V^t\left(\frac{L_{AB}}{\tau}\right) = 1 - \frac{\zeta}{2}\left[1 + \text{erf}\left(\frac{\frac{L_{AB}}{\tau} - \overline{V}}{\sigma_V\sqrt{2}}\right)\right] \ , \tau \in \left[\frac{L_{AB}}{V_{max}}; \frac{L_{AB}}{V_{min}}\right] \tag{4.6}$$

where $\zeta = 2\left[\text{erf}\left(\frac{V_{max}-\overline{V}}{\sigma_V\sqrt{2}}\right) - \text{erf}\left(\frac{V_{min}-\overline{V}}{\sigma_V\sqrt{2}}\right)\right]^{-1}$.
Hence the vehicle's residence time has a probability density function that is expressed as:

$$f_R(r) = \frac{\zeta \cdot L_{AB}}{r^2\sigma_V\sqrt{2\pi}} e^{-\left(\frac{\frac{L_{AB}}{r}-\overline{V}}{\sigma_V\sqrt{2}}\right)^2} \ , r \in \left[\frac{L_{AB}}{V_{max}}; \frac{L_{AB}}{V_{min}}\right] \tag{4.7}$$

4.1.2 Free-flow Traffic Model (FTM):

Under Free-flow traffic conditions, the road segment $[AB]$ experiences low to medium vehicle arrival rates (from (4.3), $0 \leq \mu_v \leq \mu_{max}$) while the observed vehicle speeds are high (from (4.2), $V_c \leq \overline{V} \leq V_{max}$), [27, 87, 88]. Hence, the probability that $[AB]$ witnesses a traffic jam density under such conditions is zero. In light of the above, and following the guidelines of the work in [37], $[AB]$ can be modelled as an $M/G/\infty$ queueing system where: *i*) vehicle arrivals follow a Poisson process with

parameter μ_v, *ii*) the number of busy servers at time t is identical to the number of vehicles within $[AB]$ at time t which is denoted by $N(t)$ and *iii*) the busy period of an arbitrary server i is equivalent to the residence time of vehicle i within $[AB]$ whose probability density function is given in (4.7).

At this level, for the purpose of rendering this chapter self-contained and for completion purposes, the derivations of the statistical characteristics of this model are repeated below.

From [72], it can be proven that the number of vehicles within $[AB]$ is Poisson distributed with a parameter $\mu_v \overline{R}$ as follows. Define:

- $P_n(t) = Pr[N(t) = n]$.
- $A_j(t) = Pr[j \text{ vehicles arrived in } (0,t)] = \frac{(\mu_v t)^j e^{-\mu_v t}}{j!}$.
- $P_{n|j}(t) = Pr\left[N(t) = n \middle| j \text{ arrivals in } (0,t)\right]$.

Therefore:

$$P_n(t) = \sum_{j=0}^{\infty} P_{n|j}(t) \cdot A_j(t) \tag{4.8}$$

The probability that an arbitrary vehicle i that arrived at time t_i is found within $[AB]$ at time t is $1 - F_R(t - t_i)$. Recall that vehicle arrivals follow a Poisson process. Hence, the distribution of the vehicle arrival times conditioned by j arrivals during time interval $(0,t)$ is identical to the uniform distribution of j points over $(0,t)$. Accordingly, the probability that any of the j vehicles that arrived in $(0,t)$ is found within $[AB]$ at time t is given by:

$$q(t) = \int_0^t [1 - F_R(t - t_i)] \frac{dt_i}{t} = \frac{1}{t} \int_0^t [1 - F_R(t_i)] dt_i \tag{4.9}$$

Consequently, the probability that a vehicle that arrived to $[AB]$ during the time

interval $(0, t)$ would have departed from $[AB]$ at time t is:

$$1 - q(t) = \frac{1}{t} \int_0^t F_R(t_i) dt_i \tag{4.10}$$

Knowing $q(t)$, it is easy to show that:

$$P_{n|j}(t) = \begin{cases} \binom{j}{n} [q(t)]^n [1 - q(t)]^{j-n} & , n \leq j \\ 0 & , n > j \end{cases} \tag{4.11}$$

Using (4.11), equation (4.8) can be re-written as:

$$\begin{aligned} P_n(t) &= \sum_{j=n}^{\infty} \binom{j}{n} [q(t)]^n [1 - q(t)]^{j-n} \cdot \frac{(\mu_v t)^j e^{-\mu_v t}}{j!} \\ &= e^{-\frac{t}{\mu_v}} \sum_{j=n}^{\infty} \frac{\left[\frac{q(t)}{\mu_v}\right]^n}{n!} \cdot \frac{\left[\frac{1-q(t)}{\mu_v}\right]^{j-n}}{(j-n)!} \\ &= \frac{[\mu_v t \cdot q(t)]^n e^{-\mu_v t}}{n!} \sum_{j=0}^{\infty} \frac{[\mu_v t \cdot (1 - q(t))]^j}{j!} \\ &= \frac{[\mu_v t \cdot q(t)]^n e^{-\mu_v t \cdot q(t)}}{n!} \end{aligned} \tag{4.12}$$

Notice that $\lim_{t\to\infty} [t \cdot q(t)] = \overline{R}$. Let $N = \lim_{t\to\infty} N(t)$. Thus, the limiting probability of having $N = n$ vehicles within $[AB]$ is:

$$P_n = \lim_{t\to\infty} [P_n(t)] = \frac{\left(\mu_v \overline{R}\right)^n e^{-\mu_v \overline{R}}}{n!} \tag{4.13}$$

At this stage, recall that the probability density function of R is given in (4.7). Thus:

$$\overline{R} = \int_0^{\infty} r \cdot f_R(r) dr = \int_0^{\infty} \frac{K \cdot L_{AB}}{r\sigma_V\sqrt{2\pi}} e^{-\left(\frac{\frac{L_{AB}}{r} - \overline{V}}{\sigma_V\sqrt{2}}\right)^2} dr \tag{4.14}$$

The complex integral in (4.14) has no closed-form solution. In [37] it was evaluated numerically. At this point, we recall that the squared coefficient of variation $c_v^2 = \frac{\sigma_R^2}{\mu_R^2}$ captures the degree of variability of R where σ_R^2 is the variance of R and μ_R^2 is the square of its mean. Simple numerical analysis show that $c_v^2 > 1$. Hence, following the recommendation of [73], we approximate $f_R(r)$ by a two-phase Coxian density function $f_R^{Cox}(r)$ that is given by:

$$f_R^{Cox}(r) = m_1 \cdot \mu_1 e^{-\mu_1 r} + (1 - m_1) \cdot \mu_2 e^{-\mu_2 r} \tag{4.15}$$

where $\mu_1 = 2\mu_R$ and $\mu_2 = \frac{\mu_1}{c_v^2}$ and $m_1 = 1 + \frac{\mu_1}{2c_v^2(\mu_1 - \mu_2)}$. Let $\widetilde{R}$ denote an approximated version of $\overline{R}$ computed as:

$$\widetilde{R} = \int_0^\infty r \cdot f_R^{Cox}(r) dr = \frac{m_1}{\mu_1} + \frac{1 - m_1}{\mu_2} \tag{4.16}$$

It follows that an approximated version of P_n in (4.13) is denoted by $\widetilde{P_n}$ and is expressed as:

$$\widetilde{P_n} = \frac{\left(\mu_v \widetilde{R}\right)^n e^{-\mu_v \widetilde{R}}}{n!} \tag{4.17}$$

where $\overline{R}$ is substituted by $\widetilde{R}$. Also, let $\widetilde{N}$ represent the approximated version of $\overline{N}$. Hence:

$$\widetilde{N} = \sum_{n=0}^{\infty} n \cdot \widetilde{P_n} = \mu_v \widetilde{R} \tag{4.18}$$

4.2 Numerical Analysis and Simulations

A Java-based discrete event simulator was developed to examine the validity and accuracy of the approximations proposed for the FTM model. The model's characterizing metrics were evaluated for a total of 10^7 vehicles and averaged out over multiple simulator runs to ensure the realization of a 95% confidence interval. The

following input parameter values were assumed: *i*) $\rho_v \in [0.0005; 0.01]$, *ii*) $L_{AB} = 200$ and *iii*) $(k, m) = (0.3, 3)$.

Figures 4.3(a) through 4.3(e) plot $f_R(r)$ together with $f_R^{Cox}(r)$ as given respectively in (4.7) and (4.15) as well as their simulated counterparts. Similarly, Figures 4(a) through 4(e) plot P_n as given in (4.13) concurrently with its approximation $\widetilde{P_n}$ and their simulated counterparts. The accuracy of $f_R^{Cox}(r)$ and that of $\widetilde{P_n}$ were respectively tested for all values of the vehicular density in the range $[0.0005; 0.01]$. The results corresponding to five values of ρ_v in the range $[0.0022; 0.01]$ are shown. These results constitute tangible proofs of the validity and high accuracy of the established approximations. This is especially true since Figures 5(a) and show that the highest Mean Squared Error (MSE) resulting from the approximation of $f_R(r)$ by $f_R^{Cox}(r)$ is of the order of 10^{-7} and Figure 5(b) shows that the largest (MSE) resulting from the approximation of P_n by $\widetilde{P_n}$ is of the order of10^{-2}.

Finally, extensive simulations were conducted to evaluate the approximated mean vehicle residence time, and the mean number of vehicles within the road segment. Figures 6(a) and 6(b) show an increase of the mean vehicle's residence time and the mean number of vehicles within $[AB]$ as a function of ρ_v. This is explained as follows. As ρ_v increases, the mean vehicle speed decreases. Concurrently, the flow of vehicles increases. As a result, $[AB]$ will experience faster vehicle arrivals and the arriving vehicles will be spending more time within $[AB]$.

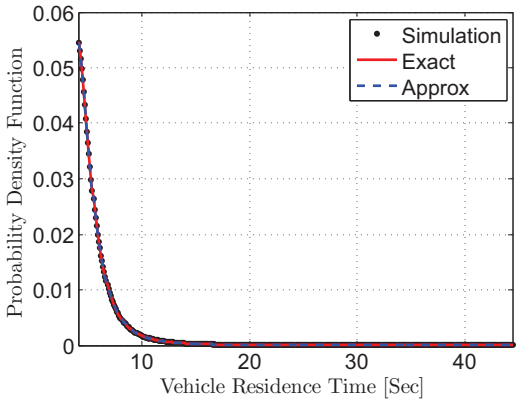

(a) $\rho_v = 0.0022\ (\frac{vehicle}{meter})$.

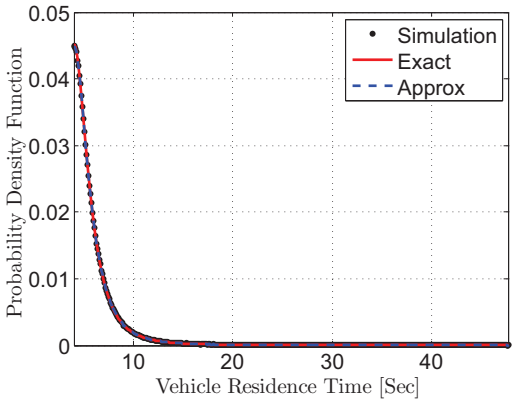

(b) $\rho_v = 0.0035\ (\frac{vehicle}{meter})$.

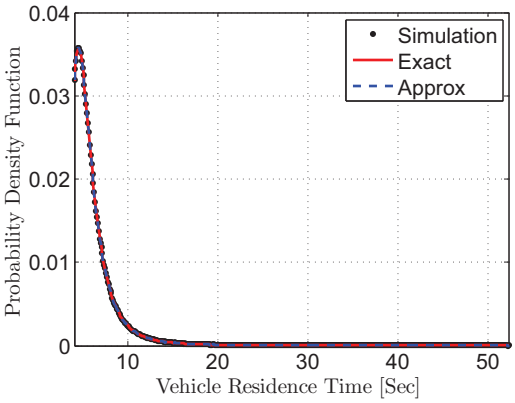

(c) $\rho_v = 0.0052\ (\frac{vehicle}{meter})$.

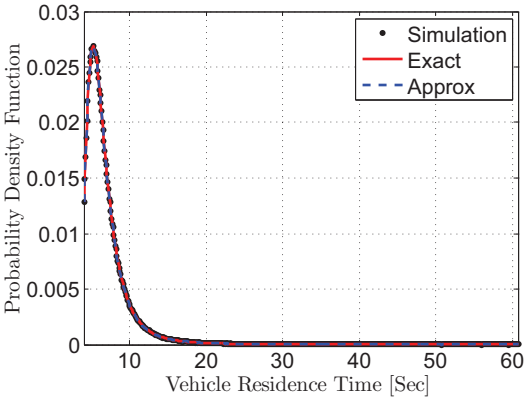

(d) $\rho_v = 0.0075\ (\frac{vehicle}{meter})$.

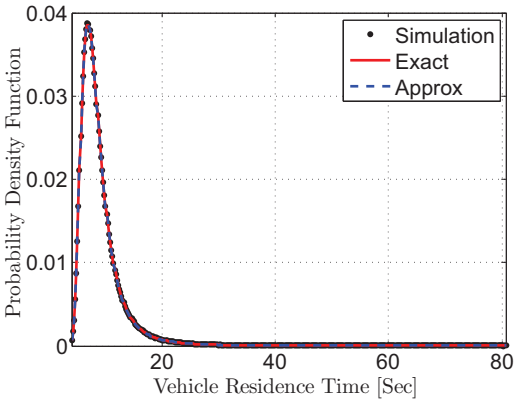

(e) $\rho_v = 0.01\ (\frac{vehicle}{meter})$.

Figure 4.3: $f_R(r)$ V.S. $f_R^{Cox}(r)$ for different values of ρ_v.

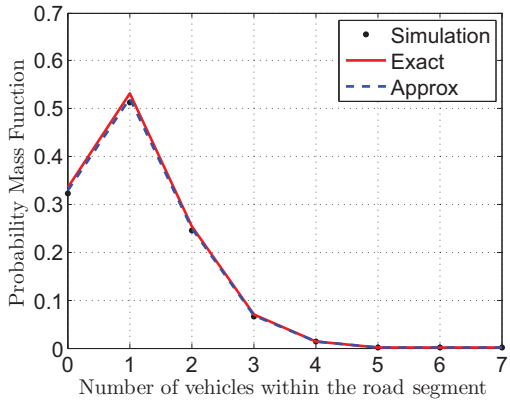

(a) $\rho_v = 0.0022$

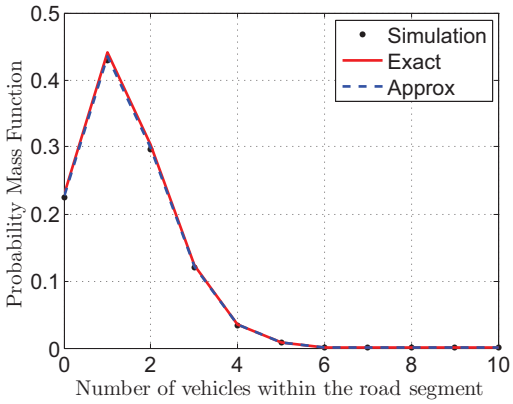

(b) $\rho_v = 0.0035\ (\frac{vehicle}{meter})$

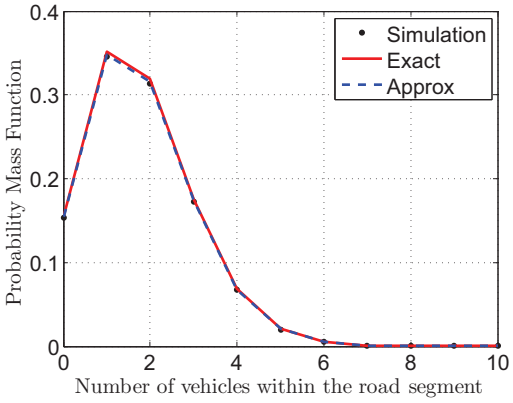

(c) $\rho_v = 0.0052$

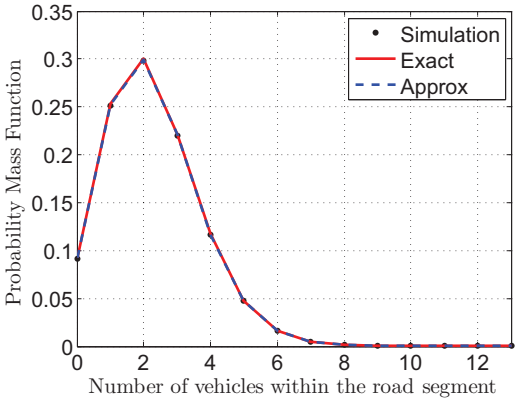

(d) $\rho_v = 0.0075$

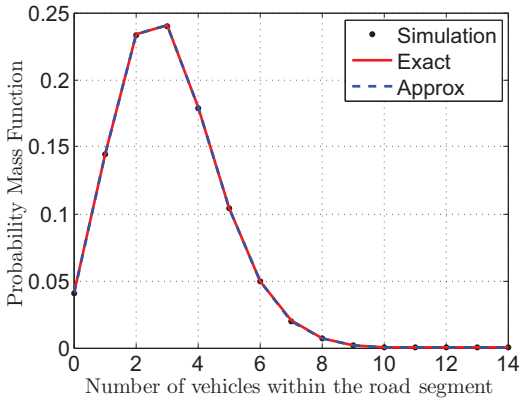

(e) $\rho_v = 0.01$

Figure 4.4: $f_R(r)$ V.S. $f_R^{Cox}(r)$ for different values of ρ_v.

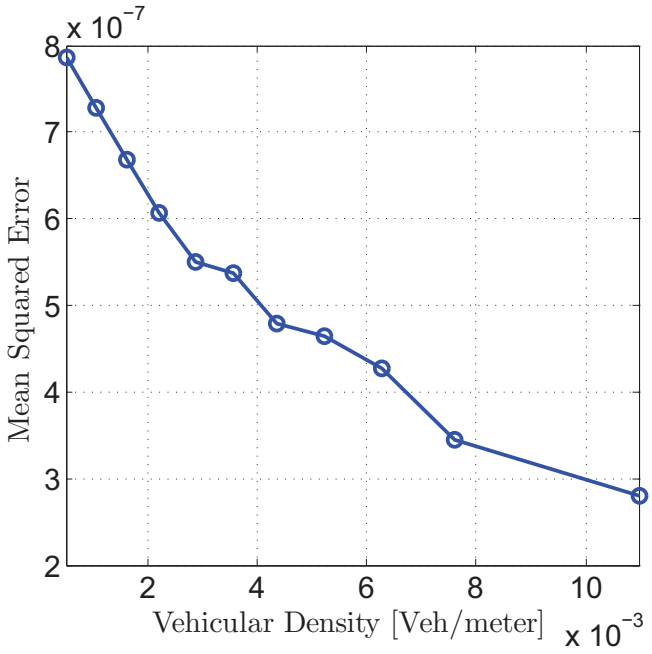

(a) R

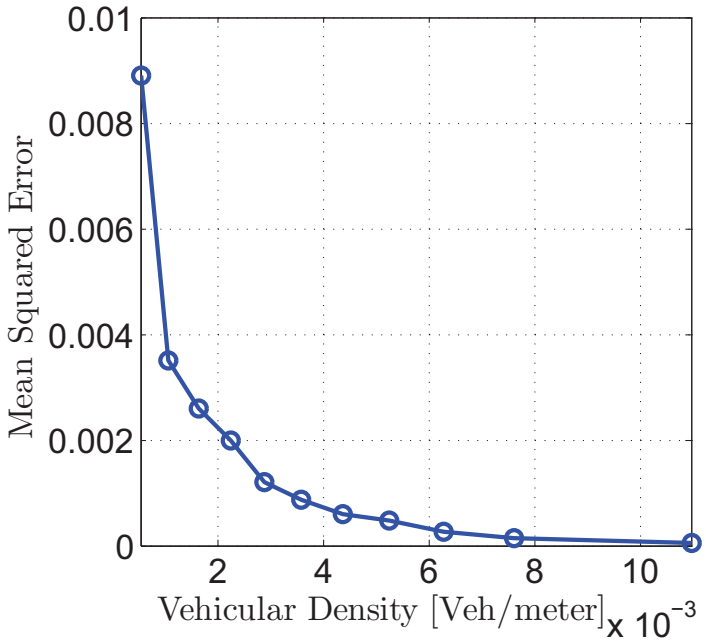

(b) N

Figure 4.5: Mean Squared Errors (percentage) for $0.01 \leq \rho_v \leq 0.1$.

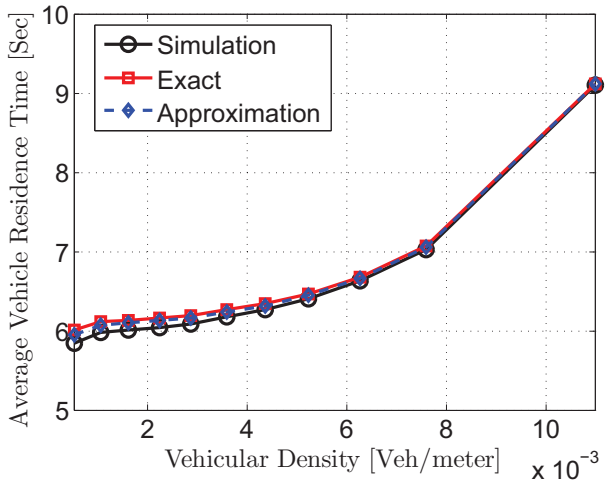

(a) $\overline{R}$ and $\widetilde{R}$ versus ρ_v.

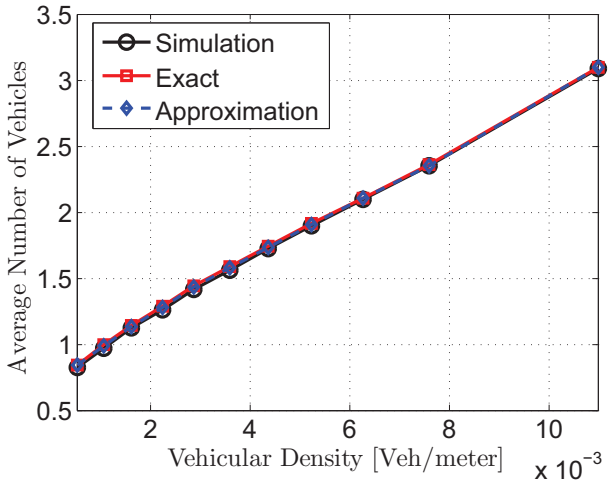

(b) $\overline{N}$ and $\widetilde{N}$ versus ρ_v.

Figure 4.6: Variations of R and N as a function of ρ_v.

Chapter 5

A Probabilistic And Traffic-Aware Bulk Bundle Release Scheme For Intermittently Connected Roadside Communication Networks

In Chapter 3, two bundle release schemes were proposed, namely: *a*) The Probabilistic Bundle Release Scheme (PBRS) and *b*) The Greedy Bundle Release Scheme (GBRS). Under both of these two schemes and similar to the typical Internet packet-like forwarding, the source SRU releases only a single bundle per opportunity. It was then observed that the limited release of a single bundle per vehicle is one of the major causes of the significant increase of the bundle queueing delay and hence has a considerable impact on the performance of these two schemes. In fact, the arrival rate of vehicles and their speeds are the two fundamental impact factors on

the performance of PBRS and GBRS. However these two factors are uncontrollable from a network operator's point of view since vehicles arrive at completely random times and have random speeds. Alternatively, the strategy of bundle release can be wisely adjusted to become more efficient and achieve better overall performance. This is the primary objective of the Bulk Bundle Release-enabled (BBR) versions of PBRS and GBRS that are presented in this chapter. These two new schemes are referred to respectively as the Probabilistic Bundle Release Scheme with Bulk Bundle Release (PBRS-BBR) and the Greedy Bundle Release Scheme with Bulk Bundle Release (GBRS-BBR).

Particularly, in the context of the networking scenario illustrated in Figure 3.1, observe that the source SRU S has a range $d_C = 200$ $(meters)$. Therefore an arriving vehicle i with speed v_i will reside in the range of S for a period of time $D_i = \frac{d_C}{v_i}$ known as vehicle i's *residence time* or *dwell time*. Assume that both, the source SRU and the vehicle, implement a variant of the 802.11 protocol where the transmitted data units have a maximum size of 1500 $(bytes)$. Consequently, if the utilized transmission rate is as low as 1 $(Mbps)$, then the transmission of a bundle of the maximum size would require 12 $(msec)$. In the worst case scenario, the fastest possible vehicle navigating at speed limit *i.e.* 50 $\left(\frac{meters}{second}\right)$ will reside in the range of S for a time period $D_i = 4$ $(seconds)$. Under PRBS and GBRS, only a single bundle is cleared out per release opportunity. As such, there will be 3.988 $(seconds)$ of wasted vehicle residence time during which no bundle is released.

In order to efficiently compensate for the wasted vehicle residence time, PBRS-BBR and GBRS-BBR will enable the source SRU to release a bulk of bundles[1] per opportunity. That is, whenever a vehicle i enters the range of S, this latter becomes aware of its speed and instantly computes its residence time D_i. Therefore, as long

[1]A group of bundles released to an in-range vehicle is referred to as a *bulk of bundles* or simply a *bulk*.

as S has bundles in its queue, it will keep on clearing them out starting from the instant vehicle i arrives up until either the vehicle exits its communication range or its queue is emptied. As a result, it is expected that the average bundle queueing delay and therefore the average bundle end-to-end delivery delay be significantly reduced. Founded on the Free-flow Traffic Model (FTM) studied in Chapter 4, a mathematical framework is setup to analyze the network performance achieved under PBRS-BBR in terms of queueing, transit and end-to-end delay metrics. At this level, note that since SFTM suggests the use of a different probability distribution for the vehicle speeds than the uniform distribution used in Chapter 3. Consequently, for the purpose of completion and consistence, the formulas pertaining to the bundle release probability introduced in Chapter 3 will be re-derived herein. The performance of GBRS-BBR will serve as a benchmark.

5.1 Probabilistic Bundle Relaying Scheme with Bulk Bundle Release

In the ICRCN scenario depicted in Figure 3.1, communication is to be established between the source SRU S and destination SRU D. S has a coverage range that spans a distance d_C of the highway. S and D are separated by a distance $d_{SD} \gg d_C$. Under PBRS-BBR, S releases bulks only to the relatively fast vehicles in order to ensure a minimal transit delay to D. In this section, a mathematical model is formulated to represent the source S operating under PBRS-BBR.

5.1.1 Mathematical Formulation and Basic Notations:

The source S becomes aware of the speed v_i of an arbitrary vehicle i only at the arrival instant t_i of the vehicle. Hence, with a probability $P_{br,i}$, S immediately starts

releasing a bulk of bundles to vehicle i. With a probability $1 - P_{br,i}$, S retains the bulk for a better subsequent release opportunity. If the bulk is released to the i^{th} vehicle, it will be successfully delivered at the instant $d_i = t_i + \frac{d_{SD}}{v_i}$. Otherwise, if it is released to the $(i+1)^{th}$ vehicle, it will be successfully delivered at the instant $d_{i+1} = t_{i+1} + \frac{d_{SD}}{v_{i+1}}$. Recall that $I_{i+1} = t_{i+1} - t_i$ represents the $(i+1)^{th}$ vehicle inter-arrival time. It follows that a better subsequent release opportunity occurs whenever $d_{i+1} < d_i \Rightarrow I_{i+1} + \frac{d_{SD}}{v_{i+1}} < \frac{d_{SD}}{v_i}$ where I_{i+1} and v_{i+1} are the only unknowns. Before deriving a closed-form expression for the bundle release probability $P_{br,i}$, the following assumptions are made:

- $A1$: Vehicle inter-arrival times have a probability density function $f_I(t)$ as given in equation (4.1).
- $A2$: Vehicle speeds have a probability density function $f_V^t(s)$ as given in equation (4.5).
- $A3$: A vehicle's speed remains constant during its entire navigation period on the road.

5.1.2 Conditional Bundle Release Probability:

The probability of retaining a bulk given that $s \leq S_i < s + ds$ can be expressed as:

$$Pr\left[d_{i+1} < d_i \middle| v \leq v_i < v + dv\right] = Pr\left[I_{i+1} + \frac{d_{SD}}{v_{i+1}} < \frac{d_{SD}}{v_i} \middle| v \leq v_i < v + dv\right] \quad (5.1)$$

Let R be the event of a bulk release. Thus, the conditional bundle release probability $P_{br,i}(s)$ is:

$$P_{br,i}(v) = Pr\left[R \middle| v \leq v_i < v + dv\right] = 1 - Pr\left[\Omega < \frac{d_{SD}}{v_i} \middle| v \leq v_i < v + dv\right] \quad (5.2)$$

Where $T_i = \frac{d_{SD}}{v_{i+1}}$ and $\Omega = I_{i+1} + T_i$ are two defined random variables with respective probability density functions $f_T(t)$ and $f_\Omega(t)$. The probability density function of I_{i+1} is $f_I(t)$. Using assumption $(A2)$, it is shown that:

$$f_T(t) = \frac{\zeta \cdot d_{SD}}{t^2 \sigma_V \sqrt{2\pi}} \exp\left[-\left(\frac{\frac{d_{SD}}{t} - \overline{V}}{\sigma_V \sqrt{2}} \right)^2 \right], \text{ for } t \in \left[\frac{d_{SD}}{V_{max}}; \frac{d_{SD}}{V_{min}} \right] \tag{5.3}$$

Since $I_{i+1} \in [0; +\infty]$ and $T \in \left[\frac{d_{SD}}{V_{max}}; \frac{d_{SD}}{V_{min}} \right]$ then $\Omega \in \left[\frac{d_{SD}}{V_{max}}; +\infty \right]$. Let $f_\Omega(t)$ denote the probability density function of Ω. It is given by the convolution of the two density function $f_I(t)$ and $f_T(t)$. Nonetheless, the remarkable complexity of the resulting convolution integral results in having no closed-form expression for $f_\Omega(t)$. Therefore, we propose (and justify) to approximate this distribution by an m-harmonic Fourier series whose parameters are determined using the *Least Squares Fitting* criterion. This approximation has the advantages of: *i*) being highly accurate for all investigated traffic conditions and *ii*) presenting relatively simple closed-form expressions for both $f_\Omega(t)$ and $P_{br,i}$. The approximated version of $f_\Omega(t)$ is:

$$\widetilde{f_\Omega^m}(t) = \begin{cases} \sum_{j=0}^{m} [\varphi_j \cos(j\omega t) + \psi_j \sin(j\omega t)] & , \frac{d_{SD}}{V_{max}} \leq t \leq \frac{d_{SD}}{V_{min}} \\ 0 & , \text{Otherwise} \end{cases} \tag{5.4}$$

where φ_j and ψ_j are the magnitude components ($\forall j = 1, 2, ..., m$) and ω is the angular frequency. φ_j, ψ_j and ω were chosen to minimize the Mean Square Error (MSE) given by:

$$\overline{\varepsilon^2} = \int_0^{+\infty} [f_\Omega(t) - \widetilde{f_\Omega^m}(t)]^2 dt \tag{5.5}$$

The above least-squares nonlinear curve fitting problem is solved using the *Gauss-Newton Numerical Algorithm*, [89]. Thorough numerical analysis showed that a value

of $m > 8$ in equation (5.4) caused $\overline{\varepsilon^2}$ to decrease marginally. Consequently, throughout this chapter, 8-harmonic Fourier functions are used to approximate $f_\Omega(t)$ for different values of the flow rate in each of the two previously identified traffic states. Figure 5.1 (upper) plots $f_\Omega(t)$ versus the $\widetilde{f_\Omega^8}(t)$ counterparts for the different flow rate values. The numbers close to each of the curves indicate the flow rate value corresponding to that curve. Figure 5.1 (lower) plots the mean squared error corresponding to each of the density function pairs. The largest observed error value is of the order of 10^{-9} proving the validity and accuracy of the approximations. Let $\widetilde{F_\Omega^m}(\tau)$ denote the m-component cumulative distribution function of Ω. It is expressed as:

$$\widetilde{F_\Omega^m}(\tau) = \sum_{j=0}^{m} \left(\frac{\varphi_j}{j\omega} \left[\sin(j\omega\tau) - \sin\left(j\omega \frac{d_{SD}}{V_{max}} \right) \right] - \frac{\psi_j}{j\omega} \left[\cos(j\omega\tau) - \cos\left(j\omega \frac{d_{SD}}{V_{max}} \right) \right] \right) \tag{5.6}$$

Define $\delta = \frac{1}{\widetilde{F_\Omega^m}\left(\frac{d_{SD}}{V_{min}}\right)}$. At this point, equation (5.2) can be rewritten as:

$$P_{br,i}(v) = 1 - \frac{\int_{\frac{d_{SD}}{V_{max}}}^{\frac{d_{SD}}{v}} \widetilde{f_\Omega^m(t)} dt}{\int_{\frac{d_{SD}}{V_{max}}}^{\frac{d_{SD}}{V_{min}}} \widetilde{f_\Omega^m(t)} dt} = 1 - \frac{\widetilde{F_\Omega^m}\left(\frac{d_{SD}}{v}\right)}{\widetilde{F_\Omega^m}\left(\frac{d_{SD}}{V_{min}}\right)} = 1 - \delta \widetilde{F_\Omega^m}\left(\frac{d_{SD}}{v}\right) \tag{5.7}$$

The probability of R, the event of a bulk release can be expressed as:

$$P_{br} = \int_{V_{min}}^{V_{max}} \left[P_{br,i}(v) \cdot f_V^t(v) \right] dv = \int_{V_{min}}^{V_{max}} \frac{\zeta \cdot P_{br,i}(v)}{\sigma_V \sqrt{2\pi}} \exp\left[-\frac{(v - \overline{V})^2}{2\sigma_V^2} \right] dv \tag{5.8}$$

Let $g_{P_{br}}(v) = \frac{\zeta \cdot P_{br,i}(v)}{\sigma_V \sqrt{2\pi}} \exp\left[-\frac{(v-\overline{V})^2}{2\sigma_V^2} \right]$. This function becomes highly complex after the substitution of $P_{br,i}$ by its expression in (5.7). Therefore, the same earlier-employed approximation technique is used once again to find a valid approximation for (5.8).

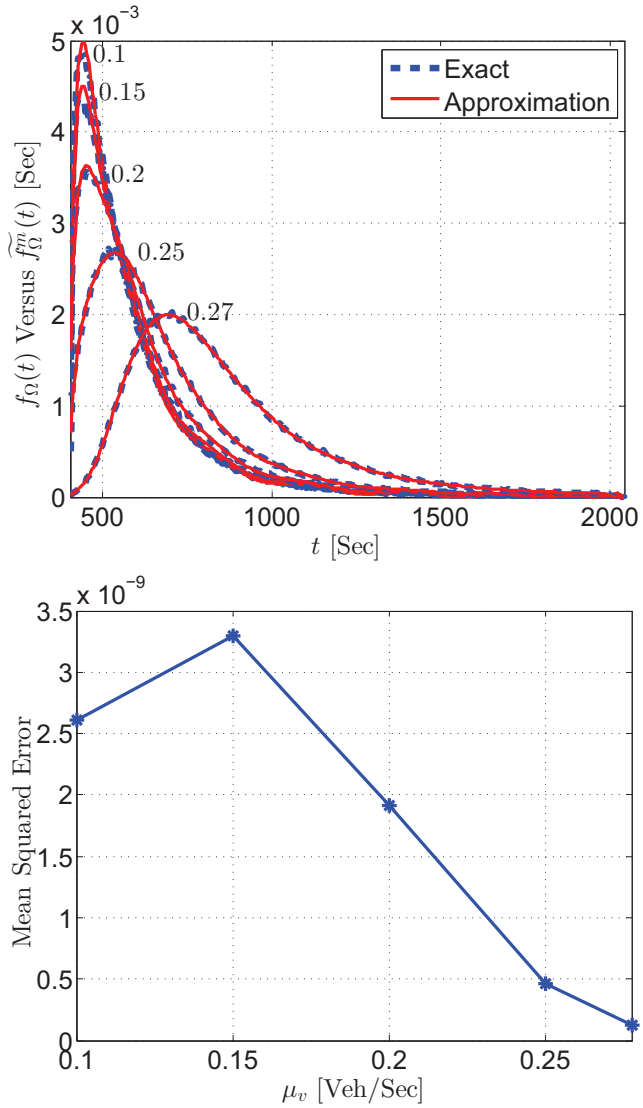

Figure 5.1: Exact versus approximated probability density function of Ω for different flow rates under both stable and unstable traffic conditions.

$g_{P_{br}}(v)$ can justifiably be approximated by an m-component mixture of Normal distributions as:

$$\widetilde{g^{m}_{P_{br}}}(v) = \sum_{j=1}^{m} \frac{1}{\sigma_j\sqrt{2\pi}} \exp\left[-\frac{(v-\mu_j)^2}{2\sigma_j^2}\right] \tag{5.9}$$

From Figure 5.2 (upper) it is concluded that $\widetilde{g^{2}_{P_{br}}}$ (*i.e.* $m = 2$) is highly accurate. The numbers close to each of the curves indicate the flow rate value corresponding to that curve. Figure 5.2 (lower) shows that the highest MSE is of the order 10^{-9}. Using (5.9), equation (5.8) is re-written as:

$$P_{br} = \frac{1}{2}\sum_{j=1}^{m}\left[\text{erf}\left(\frac{V_{max}-\mu_j}{\sigma_j\sqrt{2}}\right) - \text{erf}\left(\frac{V_{min}-\mu_j}{\sigma_j\sqrt{2}}\right)\right] \tag{5.10}$$

Having derived the probability of bundle release, the focus is now turned towards modelling and analyzing the behaviour of S under PBRS-BBR. This is done in the next section.

5.2 Bundle End-to-End Delay Analysis Under PBRS-BBR

Following the above description of the networking scenario and the mechanism of PBRS-BBR, throughout the delivery process, an incoming bundle M at S is subject to two types of delay, namely: *a*) $Q_D(M)$ being the queueing delay at S and *b*) $T_D(M)$ being the transit delay or, in other words, the travel time of the vehicle carrying M from S to D. As a result, the overall end-to-end delivery delay of M can be expressed as $E_D(M) = Q_D(M) + T_D(M)$. Let $\overline{Q_D}$, $\overline{T_D}$ and $\overline{E_D}$ denote respectively the average bundle queueing, transit and end-to-end delays. In order to determine $\overline{E_D}$, both $\overline{Q_D}$ and $\overline{T_D}$ have to be evaluated first. The remaining of this section is dedicated for the mathematical derivation of these two delay factors. Note that throughout the

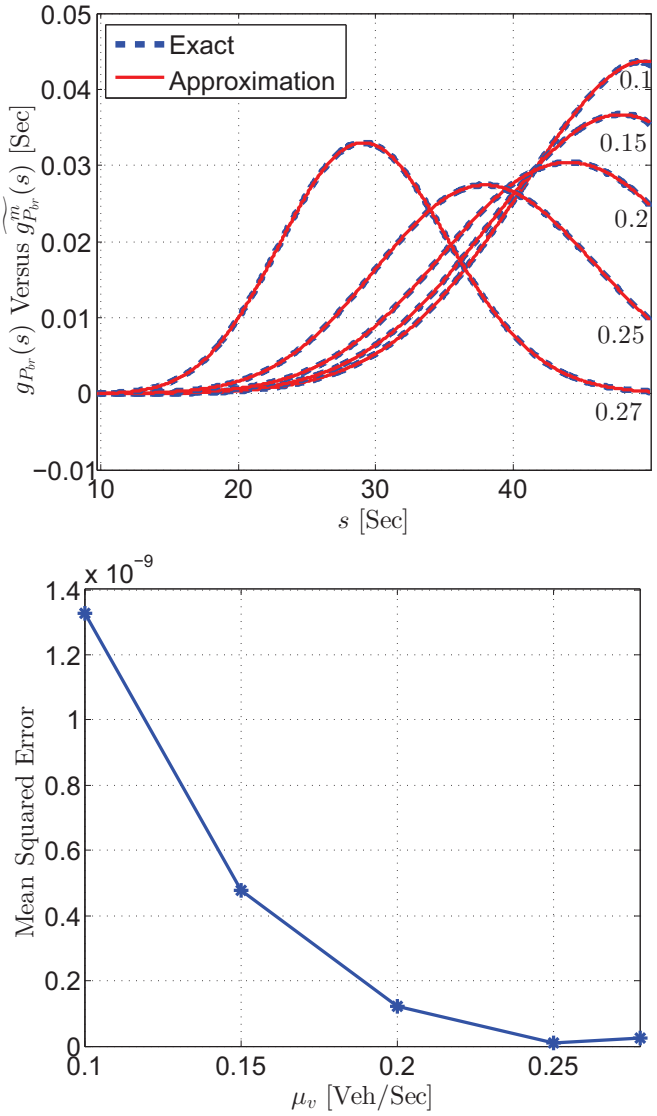

Figure 5.2: Exact versus approximated $g_{P_{br}}(s)$ functions for different flow rates under both stable and unstable traffic conditions.

below delay analysis it is assumed that S is equipped with an infinite buffer. Bundle arrivals to S follow a Poisson process with parameter $\lambda\left(\frac{bundles}{second}\right)$. All bundles have a fixed size of b $(bytes)$. S transmission rate is denoted by T_R (bps). Consequently, the transmission time of a single bundle is $\tau = \frac{8b}{T_R}$ $(seconds)$.

5.2.1 Derivation of $\overline{Q_D}$:

In order to derive $\overline{Q_D}$, a queueing model is developed to describe the behaviour of S under PBRS-BBR. The resolution of this model leads to the computation of the average number of bundles in S's buffer and therefore $\overline{Q_D}$ is computed using *Little's Theorem*, [86].

Using standard notation, let the number of bundles in S's buffer observed at an arbitrary instant be represented by a random variable N that takes on discrete values $n = 0, 1, 2, ...$ N is also adopted as the state variable of the queueing process that describes the behaviour of S's buffer contents. Let $P_n = Pr[N = n]$ denote the long-term probability that N takes on a particular value n. Without loss of generality, assume that at a random observation instant, S's buffer is found to be in state n. At this level, an incoming bundle to S causes an upward state transition (*i.e.* from state $N = n$ to state $N = n+1$) to which corresponds a transition rate that is equivalent to the bundle arrival rate λ. In contrast, the arrival of a vehicle to S causes downward state transitions that are more complex as compared to their upward counterparts. This complexity stems from the dependence of that vehicle's *bundle admissibility* on the vehicle's dwell time; that being if the arriving vehicle was selected as a bundle carrier from S to D.

Definition: The bundle admissibility K_i of a vehicle i represents the total number of bundles that vehicle can successfully receive from S during its corresponding dwell

time.

Upon the arrival of a vehicle i, S determines its speed v_i and computes $P_{br,i}(v_i)$ based on which it decides whether or not to select this vehicle to carry bundles to D. If vehicle i is selected, then S computes its dwell time $\frac{C}{v_i}$ and hence determines its *bundle admissibility* as $\frac{C}{v_i\tau}$. In this chapter, it is considered that each bundle is an atomic entity that cannot be fragmented. Therefore, K_i can only take on positive discrete values. However, the quantity $\frac{C}{v_i\tau}$ is obviously not discrete. Hence, K_i is justifiably assigned the value $\lfloor\frac{C}{v_i\tau}\rfloor$. Notice that, since S_i is bounded by V_{min} and V_{max}, therefore K_i will also be bounded by $K_{min} = \lfloor\frac{C}{V_{max}\tau}\rfloor$ and $K_{max} = \lfloor\frac{C}{V_{min}\tau}\rfloor$. In the sequel it will be considered that $K_i = k$ such that $K_{min} \leq k \leq K_{max}$. At this point, it is important to highlight the existence of a well determined range of vehicle speeds $(V_{low}^k; V_{up}^k]$ in such a way that, if S_i falls within that range, then $K_i = k$. In fact, $V_{low}^k = \frac{C}{(k+1)\tau}$ and $V_{up}^k = \frac{C}{k\tau}$. Let π_k denote the joint probability that vehicle i moving at speed $v_i = v$ is selected for bundle release and has a bundle admissibility of $K_i = k$. It is given by:

$$\pi_k = \int_{\frac{C}{(k+1)\tau}}^{\frac{C}{k\tau}} P_{br,i}(v) \cdot f_V^t(v)dv \text{ , for } k \in [K_{min}; K_{max}] \tag{5.11}$$

Now, in light of the above, since k is directly dependent on v, therefore downward transitions to many different states are possible from a given state n. Indeed, the fact that $K_{min} \leq k \leq K_{max}$ leads to having $K_{max} - K_{min} + 1$ potential downward transitions originating at state n. Furthermore, there exists $K_{max} - K_{min} + 1$ downward transitions originating from upper states of the queueing process (as will be shown further below) and sinking into state n. Note that the rate associated with a downward transition as a result of the arrival of a vehicle i whose bundle admissibility is $K_i = k$ can be expressed as $\mu_k = \mu_v\pi_k$ where $\sum_{k=K_{min}}^{K_{max}} \mu_k = \mu_v$. At this stage, the ground has been prepared to illustrate the flows into and out of state n and hence

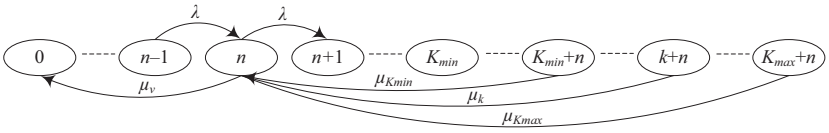

(a) Case 1: $0 < n \leq K_{min}$.

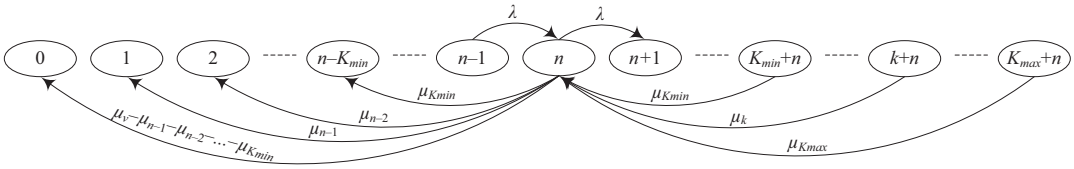

(b) Case 2: $K_{min} < n \leq K_{max}$.

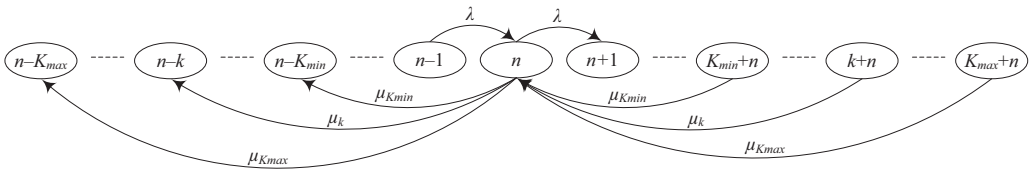

(c) Case 3: $n > K_{max}$.

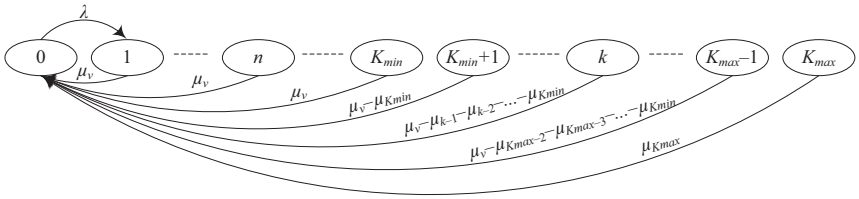

(d) Case 4: $n = 0$.

Figure 5.3: State transition rate diagrams showing the transitions into and out of state n $(n = 0, 1, 2, ...)$.

derive the appropriate balance equations. Four cases can be distinguished, namely: *a)* $0 < n \leq K_{min}$, *b)* $K_{min} < n \leq K_{max}$, *c)* $n > K_{max}$ and finally *d)* $n = 0$. On one hand, it is obvious from Figures 5.3(a) through 5.3(c) that cases (a) through (c) lead to establishing the same balance equation:

$$(\lambda + \mu_v)P_n = \lambda P_{n-1} + \sum_{k=K_{min}}^{K_{max}} \mu_k P_{n+k} \text{ , for } n > 0 \tag{5.12}$$

On the other hand, the balance equation pertaining to case (d) is given by:

$$\lambda P_0 = \mu_v \sum_{n=1}^{K_{min}} P_n + \sum_{n=K_{min}+1}^{K_{max}-1} \sum_{k=n}^{K_{max}} \mu_k P_n \tag{5.13}$$

Let $P(z) = \sum_{n=0}^{\infty} z^n P_n$ denote the p.g.f of N. Using equation (5.12) and following a similar approach to the one described in [72], $P(z)$ can be expressed as:

$$P(z) = \frac{N(z)}{D(z)} = \frac{\lambda^{-1} \sum_{k=K_{min}}^{K_{max}} \sum_{n=0}^{k} \left(z^n P_n\right) \mu_k z^{K_{max}-k} - \left(1 + \mu_v \lambda^{-1}\right) z^{K_{max}} P_0}{z^{K_{max}+1} - \left(1 + \mu_v \lambda^{-1}\right) z^{K_{max}} + \lambda^{-1} \sum_{k=K_{min}}^{K_{max}} \mu_k z^{K_{max}-k}} \tag{5.14}$$

Let $\alpha(z) = z^{K_{max}+1}$ and $\beta(z) = -\left(1 + \mu_v \lambda^{-1}\right) z^{K_{max}} + \lambda^{-1} \sum_{k=K_{min}}^{K_{max}} \mu_k z^{K_{max}-k}$. Following a similar argument to the one presented in [72], it is found that, whenever S is operating under stability conditions, then $\left|\beta(z)\right| > \left|\alpha(z)\right|$. Furthermore, using *Rouché's Theorem*, it is found that $D(z) = \alpha(z) + \beta(z)$ and $\alpha(z)$ have the same number of zeros in the range $\left|z\right| < 1 + \epsilon$. As such, since $\alpha(z)$ has $K_{max} + 1$ zeros in $\left|z\right| < 1 + \epsilon$, then $D(z)$ also has $K_{max} + 1$ zeros in this range. Observe from (5.14) that, of these $K_{max}+1$ zeros, exactly one of them occurs at $\left|z\right| = 1$, $K_{max}-1$ of them are such that $\left|z\right| < 1$ and only one denoted by z^* is such that $\left|z^*\right| > 1$. At this point,

$P(z)$ being the z-transform of a probability distribution, it must analytic in the range $\left|z\right| \leq 1$ indicates that the $K_{max} - 1$ zeros of $D(z)$ whose respective magnitudes are less than or equal to 1 are also the zeros of $N(z)$ and hence will cancel each other. As a result, after appropriate manipulation of $P(z)$, its inversion leads to having:

$$P_n = \left(1 - \frac{1}{z^*}\right)\left(\frac{1}{z^*}\right)^n \ , \ n \geq 0$$

Accordingly, the average number of bundles in S's buffer is $\overline{N} = \sum_{n=0}^{\infty} nP_n$. Finally, the average bundle queueing delay is computed from *Little's Theorem* as:

$$\overline{Q_D} = \frac{\overline{N}}{\lambda} \tag{5.15}$$

5.2.2 Derivation of $\overline{T_D}$:

PBRS-BBR is a scheme developed to allow the release of a bulk of bundles B, to a selected vehicle. Truly, $T_D(B)$, the transit delay of B, is equivalent to the ratio of the travel distance to the speed of the selected vehicle. At the bundle level, $T_D(M)$, the transit delay of a particular bundle $M \in B$ is equivalent to $T_D(B)$. Nonetheless, one must carefully observe that the average bundle transit delay is not equivalent to the average bulk transit delay. This follows from the fact that the number of bundles constituting each of the released bulks potentially differs from one bulk to the other. Hence, *length biasing* plays a major role in this regard and has to be accounted for adequately. The following example serves the purpose of a better explanation.

Example: Consider that two bulks B_i and B_j composed respectively of x_i and x_j bundles have been released to two vehicle i and j with respective speeds v_i and v_j. The respective transit delays of these two bundle bulks are $T_D(B_i) = \frac{d_{SD}}{v_i}$

and $T_D(B_j) = \frac{d_{SD}}{v_j}$. Hence, the average bulk transit delay would be equivalent to $\frac{T_D(B_i)+T_D(B_j)}{2} = \frac{d_{SD}(v_i+v_j)}{2v_iv_j}$. However, since vehicle i received x_i bundles and vehicle j received x_j bundles, hence the average bundle transit delay will be $\overline{T_D} = \frac{d_{SD}(x_iv_j+x_jv_i)}{v_iv_j(x_i+x_j)}$. Note that the weighing by the bulk sizes x_i and x_j is the kind of length biasing that has to be considered.

Let $f_{v_c}(v)$ denote the probability density function of the speed of a vehicle whose numerical index is i_n and which is carrying a randomly targeted bundle n. Resorting to the typical ergodicity arguments, $f_{v_c}(v)$ can be expressed as:

$$f_{v_c}(v)dv = \lim_{m\to\infty} \frac{\sum_{n=1}^{m} U_{i_n}(v, v+dv)}{m} \tag{5.16}$$

where $U_{i_n}(v, v+dv)$ is an indicator function which is equal to 1 if the speed of vehicle i_n falls within the range $(v, v+dv)$ and 0 otherwise. At this level, in order to account for the above-mentioned length biasing, the number of bundles carried by vehicle i_n is introduced into the expression of $f_{v_c}(v)$ and (5.16) refined to become:

$$f_{v_c}(v)dv = \lim_{m\to\infty} \frac{\sum_{r=1}^{i_m} x_r U_r(v, v+dv)}{m} \tag{5.17}$$

where $U_r(v, v+dv)$ being indicator function which is equal to 1 if the speed of vehicle whose numerical index is r falls within the range $(v, v+dv)$ and is equal to 0 otherwise, and x_r is the number of bundles carried by vehicle r. Note that $x_r = 0$ either if, at the time of its arrival, vehicle r navigating at speed v_r was selected to carry bundles to D but S's buffer was empty, or if vehicle r was not selected to carry bundles to

D. Since $i_m \xrightarrow[m\to\infty]{} \infty$, (5.17) can be re-written as:

$$f_{v_c}(v)dv = \lim_{m\to\infty} \left(\frac{\sum_{r=1}^{i_m} x_r U_r(v, v+dv)}{i_m} \cdot \frac{i_m}{m} \right) = \frac{\overline{X}(v) \cdot f_V^t(v)dv}{\overline{X}} \tag{5.18}$$

where $f_V^t(v)$ is given in (4.5), $\overline{X}(v)$ is the expected size of a bulk of bundles that is carried by a vehicle navigating at speed v (*i.e.* the length biasing factor) and $\overline{X}$ is the expected size of a bulk of bundles that is carried by an arbitrarily selected vehicle. Given that vehicle arrivals follow a Poisson process and that a bulk of bundles is released to a vehicle r navigating at speed v with probability $P_{br,r}(v)$, therefore:

$$\overline{X}(v) = \left[\sum_{n=1}^{K_r} nP_n + \sum_{n=K_r+1}^{\infty} K_r P_n \right] P_{br,r}(v) \tag{5.19}$$

where K_r is the bundle admissibility of vehicle r and P_n is the steady-state probability of S's buffer being in state n. As such:

$$\overline{X} = \int_{V_{min}}^{V_{max}} \overline{X}(v) \cdot f_V^t(v)dv \tag{5.20}$$

This concludes the derivation of $f_{v_c}(v)$ which can now be utilized to compute the average bundle transit delay as:

$$\overline{T_D} = \int_{V_{min}}^{V_{max}} \frac{d_{SD}}{s} f_{v_c}(v)dv \tag{5.21}$$

Remark: A Greedy Bundle Release Scheme with Bulk Bundle Release (GBRS-BBR) will be used as a benchmark. Under GBRS-BBR, a bulk of bundles is released to every arriving vehicle. The same above analysis applies to GBRS-BBR with $P_{br,i} = P_{br} = 1$.

5.3 Simulation and Numerical Analysis

An in-house Java-based discrete event simulator was developed to examine the performance of PBRS-BBR and GBRS-BBR in terms of the average bundle queueing delay, $\overline{Q_D}$, the average bundle transit delay, $\overline{T_D}$ and the average bundle end-to-end delay, $\overline{E_D}$. Each of the two schemes is simulated under Free-flow vehicular traffic conditions. The delay metrics were evaluated for a total of 10^7 bundles and averaged out over multiple simulator runs to ensure the realization of a 95% confidence interval. The following input parameter values were assumed: *i*) the vehicle flow rate $\mu_v \in [0.1; 0.27] \left(\frac{Vehicles}{second}\right)$, *ii*) the bundle arrival rate $\lambda = 1 \left(\frac{Bundles}{second}\right)$, *iii*) the source-destination distance $d_{SD} = 20000$ $(meters)$, *iv*) the maximum allowable speed$S_{max} = 50 \left(\frac{meters}{second}\right)$, the transmission rate of the source *v*) $T_R = 1$ $(Mbps)$ and *vi*) the coverage range of the source $C = 200$ $(meters)$. Figures 5.4(a) through 5.4(c) concurrently plot the resulting theoretical curves of $\overline{E_D}$, $\overline{T_D}$ and $\overline{E_D}$ along with their simulated counterparts as a function of μ_v. These figures constitute tangible proofs of the validity of the earlier-presented mathematical analysis as well as the accuracy of the developed simulator. This is particularly true given that the theoretical curves in all of the three plots almost perfectly overlap with their simulated counterparts. The rest of this section contrasts the performance of the PBRS-BBR with that achieved by GBRS-BBR.

Figure 5.4(a) shows that GBRS-BBR outperforms PBRS-BBR in terms of $\overline{Q_D}$. In fact, a source SRU S employing GBRS-BBR releases bulks to every arriving vehicle. Hence, during a single vehicle inter-arrival period, this will not allow the accumulation of too many newly incoming bundles. Under PBRS-BBR, the source often witnesses several vehicle arrivals before releasing a bulk to the most suitable one. Accordingly, this has the effect of: *i*) increasing the queueing delays experienced by existing bundles and *ii*) forcefully exposing the newly incoming bundles to extended queueing

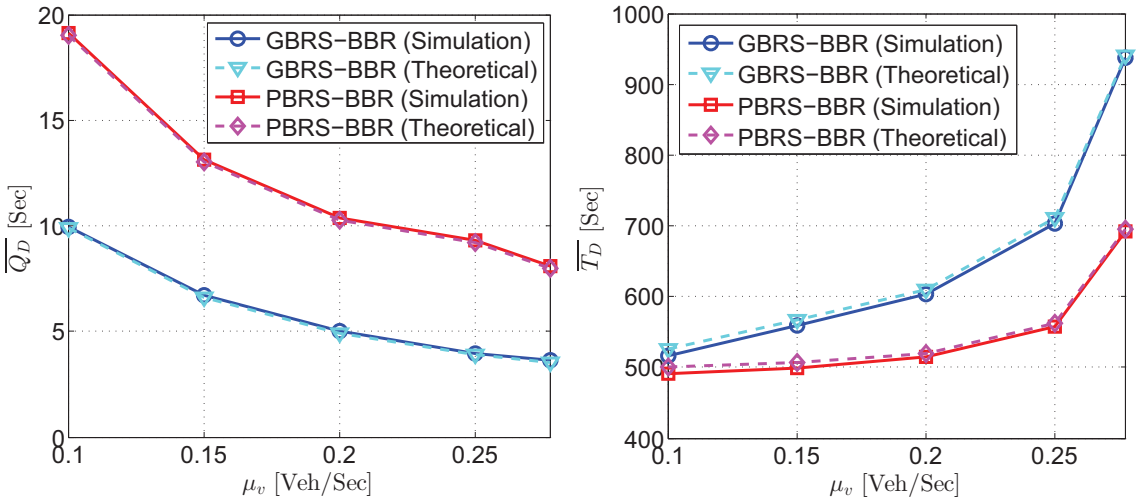

(a) Mean Queueing Delay.

(b) Mean Transit Delay.

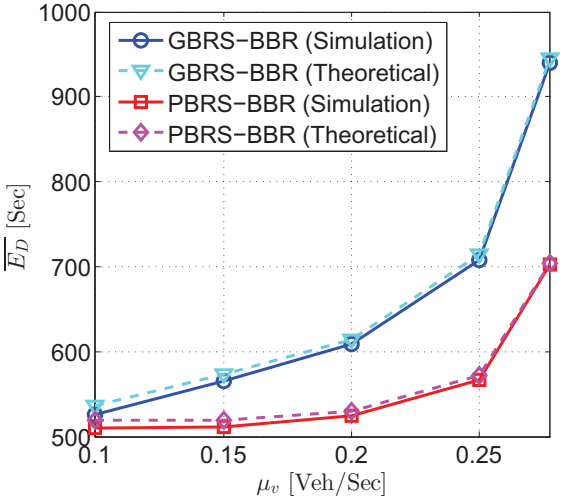

(c) Mean End-To-End Delay.

Figure 5.4: Performance evaluation of PBRS-BBR and GBRS-BBR under Free-flow vehicular traffic conditions.

periods. Notice, however, that $\overline{Q_D}$ is a decreasing function of μ_v. As μ_v increases the vehicle inter-arrival time decays but the probability of fast vehicle arrivals increases. Hence, both PBRS-BBR and GBRS-BBR are able to release bundles faster.

On a transit delay level, PBRS-BBR outperforms GBRS-BBR as shown in Figure 5.4(b). By design, PBRS-BBR selects the relatively fast vehicles so as to achieve the minimum possible transit delays while GBRS-BBR does not differentiate between fast and slow vehicles and releases a bulk to every arriving vehicle. Observe that, as μ_v increases the vehicular density also increases thus causing a decay in the average speed. As a result, the bundle transit delay is an increasing function of μ_v.

Now observe that the queueing delay improvement of GBRS-BBR over its probabilistic counterpart ranges from a few seconds to almost ten seconds while the transit delay improvement of PBRS-BBR over GBRS-BBR ranges from a couple of tens to more than two hundred seconds. It follows that queueing delays are completely overshadowed by transit delays. Hence, on the overall end-to-end delay level, PBRS-BBR clearly outperforms GBRS-BBR. This fact is reflected in Figure 5.4(c).

Finally, it is important to mention the fact that vehicle speeds and hence their residence periods within the source SRU's coverage range are totally uncontrollable by the SRU. This actually imposes a limitation on the capability of the SRU in clearing out bundles. As a matter of fact, an SRU cannot release bundles to a vehicle more than that vehicle's bundle admissibility. Now, the arrival of bundles to the SRU is also outside of the control of the SRU itself and clearly depends on the intensity of user service demands. Hence, note that, if the offered load to the SRU increases beyond what the SRU can release to vehicles given its data transmission rate, then the SRU will experience a serious case of buffer instability. This is especially true since the bundle queueing delay will exhibit a rapid irregular increase. Consequently, PBRS-BBR, irrespective of its ability to decrease transit delays, will not be able to

overcome this phenomenon. It may seem that GBRS-BBR, under such conditions, will prevail. However, in reality it will not because, then, the delay it achieves, although finite, is quite significant to the point that this scheme becomes inefficient. In fact, at this point, two-hop VICNs present marginal utility in data communication from one SRU to another unless offline data is being transferred with high delay tolerance. Recall that, the analysis presented herein assumes the utilization of the IEEE 802.11 protocol with 200 meters transmission range and 1 Mbps transmission rate. Nevertheless, the advances in wireless communications technology come to the rescue as the recently developed IEEE 802.11p (refer to [17]) standard for vehicular environment offers very high transmission rates of up to 27 ($Mbps$). It, as well, enlarges the SRU's coverage range to almost 1 (Km). This remarkably stabilizes the source SRU's queue even in situations where the offered data traffic load is very high. Equipping the SRU with IEEE 802.11p comes at no additional cost but has the above described benefits. Under such conditions, PBRS-BBR will still outperform GBRS-BBR.

Chapter 6

Delay-Optimal Data Delivery In Intermittently Connected Roadside Communication Networks

This chapter presents a Delay-Optimal Data Delivery scheme (DODD) which aims at achieving delay-optimal bundle delivery in the context of the ICRCN scenario illustrated in Figure 6.1 while relaxing the complete/partial knowledge assumptions. This, indeed, is a challenging task whose resolution is founded on top of a revolutionary knowledge acquisition philosophy that leverages the concept of *Virtual Space* (refer to [42]) for the purpose of augmenting the source SRU S with a mechanism that allows for only necessary retransmissions of bundle copies to faster arriving vehicles securing their earlier delivery.

More precisely, under DODD, incoming bundles to S are initially enqueued in its Main Buffer (MB) according to their order of arrival. As time goes by, vehicles enter

the coverage range of (*i.e.* arrive to) S. Following the First-In-First-Out (FIFO) service strategy, S releases a bundle to every arriving vehicle. Copies of all the released bundles are retained in S's VS and each copy is associated a decremental expiry timer upper bounded by the travel time to D of the initial vehicle carrying it. Without loss of generality, upon the arrival of a new vehicle, S acquires knowledge of its speed and determines its travel time to D. Knowing the residual expiry times of all the bundle copies in its VS, S determines if the newly arriving vehicle may contribute in delivering any of the unexpired virtual copies to D faster than their corresponding earlier carriers. Consequently, all those copies found to benefit from a faster delivery achieved by the newly arriving vehicle are retransmitted to that vehicle and their expiry timers are updated. Next, one original bundle is transmitted to the new vehicle from the MB (if available) and its copy enqueued in the VS with the appropriate expiry timer set. Every expiring virtual copy is deleted and its allocated buffer space is freed. Finally, a bundle is considered as received by D as soon as its first copy arrives to D. All subsequently arriving copies are discarded. At this point, it is important to note that, in contrast to [42], here the expiry timers of virtual copies are stochastic and dynamically updated according to the turn of events (*i.e.* arrivals of vehicles constituting faster delivery opportunities). Hence, the primary objective of this chapter is to lay out a mathematical model that characterizes the behaviour of a source SRU S under DODD, evaluate its performance as well as the achieved bundle end-to-end delay. In addition to highlighting the efficiency of DODD in considerably reducing the overall bundle end-to-end delay as compared to existing schemes, the mathematical model presented in this chapter, in general, and particularly the analysis pertaining to the bundle residence time in the virtual space are of generic integral significant that expands to what is beyond the specific context of delay-optimal data delivery in intermittently connected roadside communication

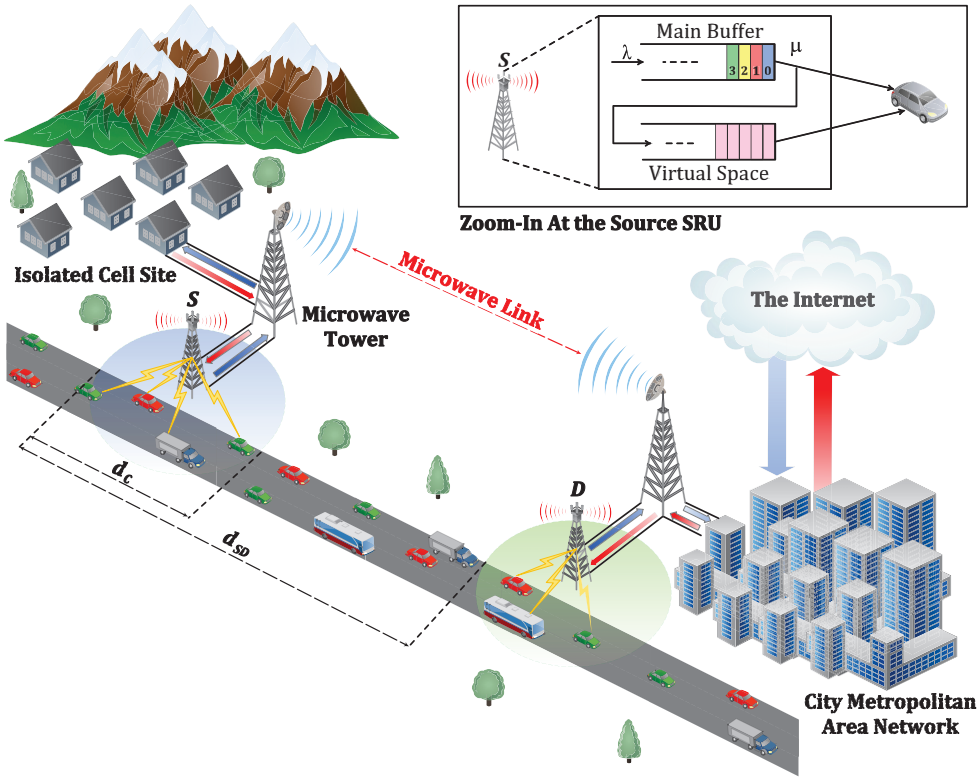

Figure 6.1: Intermittently Connected Roadside Network Scenario.

networks. As a matter of fact, this theoretical foundation may set the ground floor for the analysis of general systems. Consequently, any further results that can be derived have a potential significance and utility for other fields.

6.1 A Discrete-Time Variant of FTM

This section lays out a discrete-time variant of the FTM vehicular mobility model presented in Chapter 4. Recall that vehicles are assumed to navigate over an uninterrupted roadway segment $[SD]$ of length d_{SD} $(meters)$ as shown in Figure 6.1. $[SD]$ is assumed to operate under low-to-medium vehicular traffic conditions and time is subdivided into mini-slots of size τ $(seconds)$. Let K_v denote the number of slots that elapses between two consecutive vehicle arrivals. Following the guidelines presented

in Chapter 4, K_v can be drawn from a geometric distribution given by:

$$f_{K_v}(k) = q(1-q)^k \text{ , for } k \geq 0 \tag{6.1}$$

where $q = \mu_v \tau$ denotes the probability that a vehicle arrives at the end of a mini-slot and μ_v is the vehicle flow rate ($\frac{vehicles}{second}$). Also from Chapter 4, vehicle speeds are independent and identically distributed in the range $[V_{min}; V_{max}]$. These speeds are drawn from a truncated Normal distribution having an average $\overline{V}$, a standard deviation σ_V. Moreover, vehicles maintain their speeds constant during the entire navigation period over d_{SD}. The travel time from S to D of an arbitrary vehicle j with speed v_j is a random variable defined as $T_j = \frac{d_{SD}}{v_j}$ and whose probability density function $f_T(t)$ defined over the range $t \in \left[\frac{d_{SD}}{V_{max}}; \frac{d_{SD}}{V_{min}}\right]$ is expressed in equation (4.5). Let $L_j = l = \lceil \frac{T_j}{\tau} \rceil$ ($l \in \mathbb{Z}^+$) represent the discrete time equivalent of T_j. L_j is respectively lower and upper bounded by $L_{min} = \lceil \frac{d_{SD}}{\tau V_{max}} \rceil$ and $L_{max} = \lceil \frac{d_{SD}}{\tau V_{min}} \rceil$. It can be easily shown that, the probability mass function of L_j can be expressed as:

$$\begin{aligned}
f_L(l) &= \int_{(l-1)\tau}^{l\tau} f_T(t)dt \\
&= \int_{(l-1)\tau}^{l\tau} \frac{\zeta d_{SD}}{t^2 \sigma_V \sqrt{2\pi}} \exp\left[-\left(\frac{\frac{d_{SD}}{t} - \overline{V}}{\sigma_V\sqrt{2}}\right)^2\right] dt \\
&= \int_{\frac{d_{SD}}{l\tau}}^{\frac{d_{SD}}{(l-1)\tau}} \frac{\zeta d_{SD}}{\frac{d_{SD}^2}{v^2}\sigma_V\sqrt{2\pi}} \exp\left[-\left(\frac{v - \overline{V}}{\sigma_V\sqrt{2}}\right)^2\right] \left(-\frac{d_{SD}}{v^2}\right) dv \\
&= -\zeta \int_{\frac{d_{SD}}{l\tau}}^{\frac{d_{SD}}{(l-1)\tau}} \frac{1}{\sigma_V\sqrt{2\pi}} \exp\left[-\left(\frac{v - \overline{V}}{\sigma_V\sqrt{2}}\right)^2\right] dv \\
&= \frac{\zeta}{2}\left[\text{erf}\left(\frac{\frac{d_{SD}}{l\tau} - \overline{V}}{\sigma_V\sqrt{2}}\right) - \text{erf}\left(\frac{\frac{d_{SD}}{(l-1)\tau} - \overline{V}}{\sigma_V\sqrt{2}}\right)\right], \text{ for } l \in [L_{min}; L_{max}]
\end{aligned} \tag{6.2}$$

where ζ is a normalization constant (refer to Chapter 4 for more details).

6.2 Behavior of The Source SRU Under DODD

In this section, the behavior of the source SRU S under DODD is described according to a time progressive turn of events.

6.2.1 Preliminaries:

For the purpose of describing S's behavior under DODD, three major points must be elaborated as follows:

1. In the context of the VICN scenario illustrated in Figure 6.1, the events of interest are: a) bundle arrivals to S's MB, b) vehicle arrivals to S, c) bundle departures from S's MB d) creation and storage of bundle copies in S's VS, e) retransmission of bundle copies and f) vehicle arrivals to D (*i.e.* delivery of bundles/copies).

2. The IEEE 802.11p standard is used for vehicle-to-SRU communication. In order to reduce the communication overhead, the IEEE 802.11p standard provides no procedures for associating newly arriving vehicles to the SRU [17]. However, the bundle delivery mechanism proposed in this chapter requires the SRU to learn the parameters of arriving vehicles in order to adequately process original bundle releases as well as necessary bundle retransmissions. Hence, a connection setup between the SRU and a newly arriving vehicle becomes necessary. To establish such a connection, one option is to enable every arriving vehicle to send out a Connection Setup Request (CSR) as soon as it can sense the presence of an SRU. In this CSR, the vehicle includes its arrival slot and speed. CSRs being very short and instantaneously transmittable bundles, they incur minimal communication overhead, [48].

3. Without loss of generality, assume that vehicle j arrives to S during an arbitrary

slot s_j, ($s_j \in \mathbb{Z}^+$). Upon receiving a CSR from that vehicle, S becomes aware of its arrival slot s_j and its speed, v_j and hence determines the time slot $d_j = s_j + L_j$ during which this vehicle will arrive to D. L_j is the number of time slots during which vehicle j will travel the distance d_{SD}.

Definition: The *vulnerability period* of vehicle j is the period of time during which S may witness the arrival of an arbitrary vehicle $j+i$ ($i \geq 1$) that is capable of reaching D before vehicle j does. It is:

$$\widetilde{\nu_p}(j) = L_j - L_{min} \ , \forall L_j \in [L_{min}; L_{max}] \tag{6.3}$$

Recall that the minimum number of slots a vehicle may consume in travelling the distance d_{SD} is L_{min}. Observe that only the fastest possible vehicle may achieve this minimal travel time. Therefore, on one hand, if $L_j = L_{min}$, then $\widetilde{\nu_p}(j) = 0$. This means that any subsequently arriving vehicle with a travel time that is even as low as L_j will not be able to reach D before vehicle j. On the other hand, if $L_j > L_{min}$, then $\widetilde{\nu_p}(j) > 0$. During this vulnerability period, S may possibly witness the arrival of a subsequent vehicle $j+i$ ($i \geq 1$) within an arbitrary time slot s_{j+i} ($s_{j+i} > s_j$). This vehicle may happen to achieve a low enough travel time L_{j+i} in such a way that it will reach D before vehicle j does. Let $f_{\nu_p}(k)$ denote the probability mass function of $\widetilde{\nu_p}(j)$. Knowing that L_{min} is a constant value, it becomes clear that:

$$f_{\nu_p}(k) = f_L(k + L_{min}) \ , \text{for } k \in [0; L_{max} - L_{min}] \tag{6.4}$$

where $f_L(l)$ is given in equation (6.2) for $l \in [L_{min}; L_{max}]$. Now, let $R_j(s_{j+i}) = d_j - s_{j+i}$ denote the residual travel period of vehicle j at the end of time slot s_{j+i}. Thus, for vehicle $j+i$ to reach to D before vehicle j, it is necessary that

the following condition be satisfied:

$$d_i < R_j(s_{j+i}) \ , \forall i \in \{i \geq 1 \big| s_{j+i} > s_j \text{ and } L_{j+i} \in [L_{min}; L_{max}] \text{ and } d_{j+i} = s_{j+i} + L_{j+i}\}. \tag{6.5}$$

According to all of the above, the behavioral description of S may now be laid out next.

6.2.2 Detailed Description of S's Behavior Under DODD:

With no loss of generality, assume that, upon the arrival of vehicle j, S finds in its MB some original bundles that have arrived earlier in time. However, its VS is empty. In servicing the original bundles (*i.e.* opportunistically releasing them to arriving vehicles), S follows the First-In-First-Out (FIFO) strategy. Before releasing the front bundle of its MB, say M_y, to vehicle j, S determines d_j and $\widetilde{\nu_p}(j)$ being respectively vehicle j's arrival slot to D and its vulnerability period. Depending on the value of $\widetilde{\nu_p}(j)$, S may engage in two different actions:

- ***Case* 1** ($\widetilde{\nu_p}(j) = 0$)**:**

  As shown in Figure 6.2, this situation will arise only whenever $L_j = L_{min}$. Therefore, S immediately releases M_y to vehicle j without holding any copy of it for future retransmissions. This behaviour is justified by the fact that, as explained earlier, no subsequent vehicle will be able to reach D before vehicle j does. Hence, the end-to-end delay of M_y in this case is:

$$E_D\left(M_y \Big| \widetilde{\nu_p}(j) = 0\right) = Q_{mb}(M_y) + L_j = Q_{mb}(M_y) + L_{min} \tag{6.6}$$

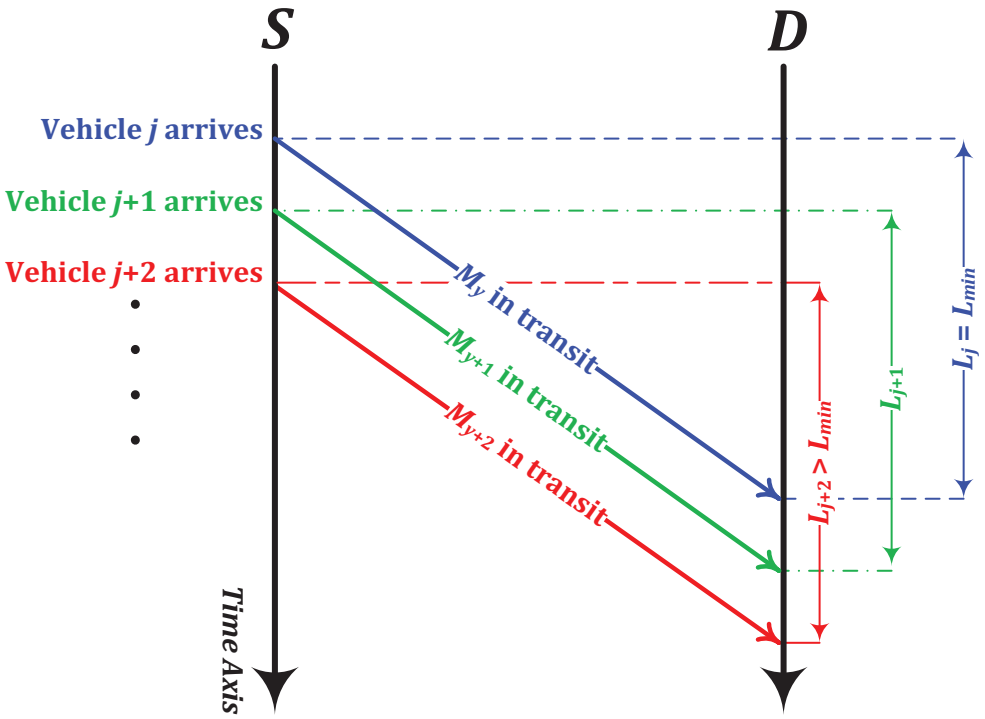

Figure 6.2: Time-progressive SRU behavior in case 1 of section 6.2.2.

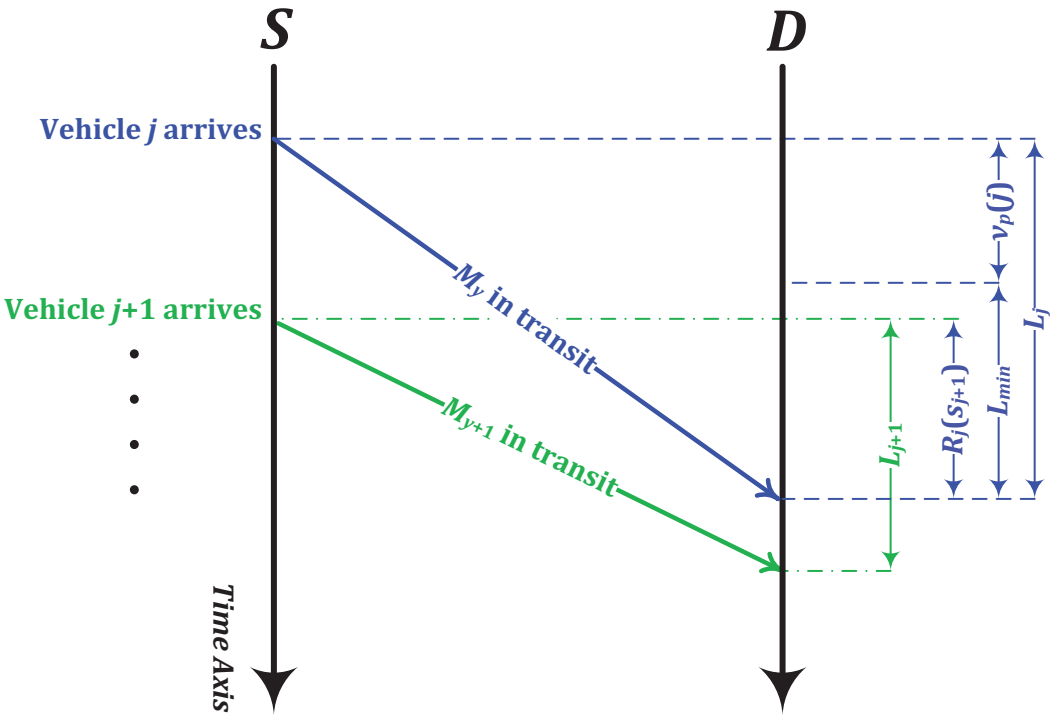

Figure 6.3: Time-progressive SRU behavior in case 2.1 of section 6.2.2.

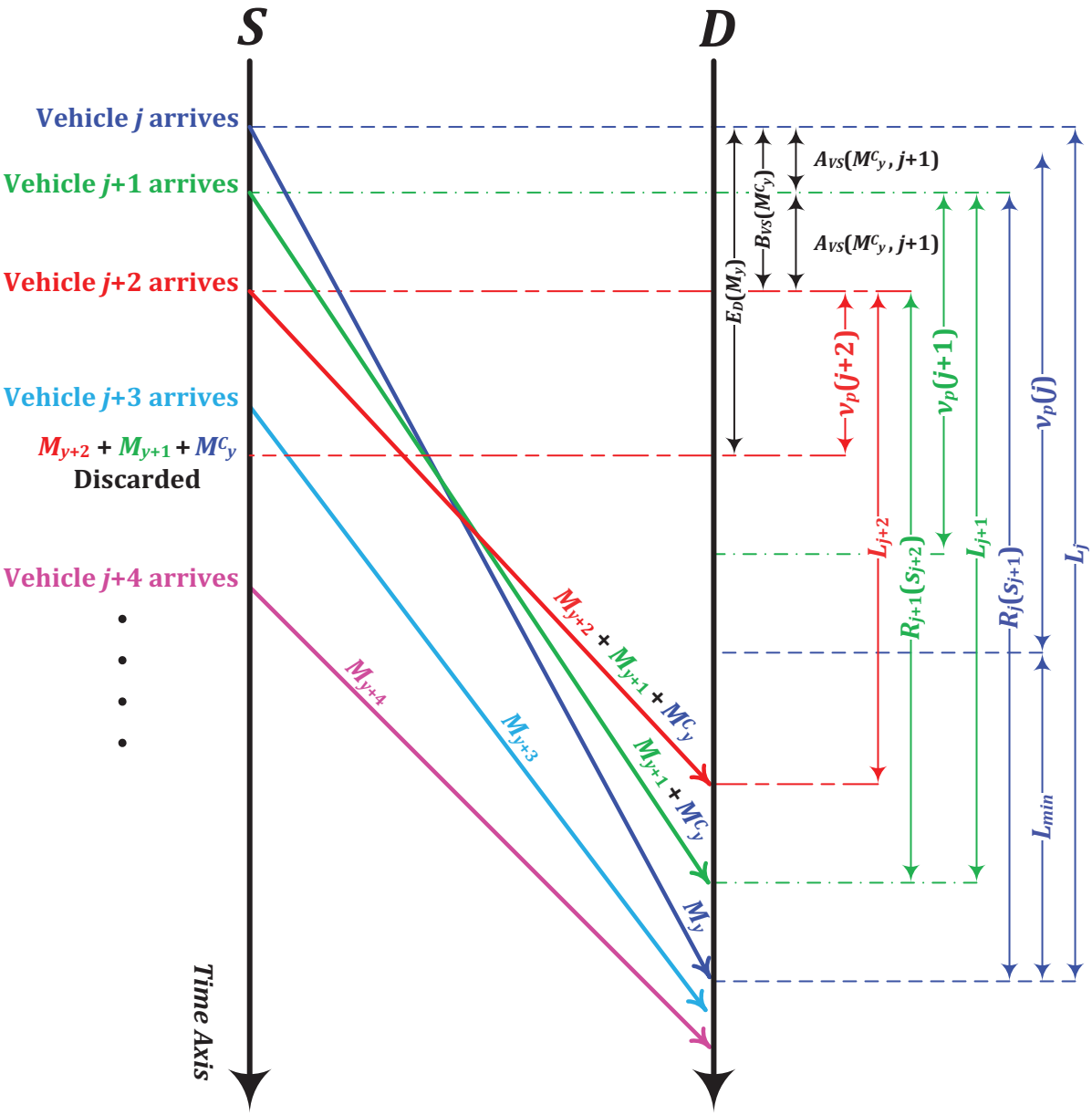

Figure 6.4: Time-progressive SRU behavior in case 2.2 of section IV.

where $Q_{mb}(M_y)$ is the queueing delay of bundle M_y in S's MB.

- ***Case 2*** **($\widetilde{\nu}_p(j) > 0$):**

  This occurs whenever $L_j > L_{min}$. In this case, S duplicates M_y, associates to the resulting copy, M_y^C, an initial expiry timer $E_t(M_y^C) = \widetilde{\nu}_p(j)$ and enqueues it into the VS. Then, S releases M_y to vehicle j. At this level, two sub-cases may arise depending on the number of vehicles X that arrive during $\widetilde{\nu}_p(j)$. These two sub-cases are laid out as follows:

  - **Case 2.1 ($X = 0$):**

    Clearly, as shown in Figure 6.3, since no vehicle arrives during the vulnerability period of vehicle j, then:

    $$E_D\left(M_y \middle| \widetilde{\nu}_p(j) > 0, X = 0\right) = Q_{mb}(M_y) + \underbrace{\widetilde{\nu}_p(j) + L_{min}}_{L_j} \tag{6.7}$$

  - **Case 2.2 ($X = x$ with $x > 0$):**

    In this sub-case, of these x arriving vehicles, some may possibly contribute to achieving earlier deliveries of M_y^C to D while the others will not. Upon the arrival of these latter, S will just decrement $E_t(M_y^C)$ by one time slot. Now, consider the arrival of an arbitrary one of the X vehicles, say vehicle $j + i$, that satisfies condition (6.5) and achieves a transit delay of L_{j+i}. In this case, as shown in Figure 6.4, S decreases M_y^C's expiry timer to $E_t(M_y^C) = \widetilde{\nu}_p(j + i)$, and retransmits M_y^C to vehicle $j + i$. This process may repeat an arbitrary number of times until eventually no further arriving vehicle will satisfy condition (6.5). From there on, surely $E_t(M_y^C) = 0$ since, only then, no matter how fast the newly arriving vehicle is, it will not be able to achieve an earlier delivery of M_y^C to D. In other words, the

last vehicle to which M_y^C was retransmitted became invulnerable. Consequently, S will discard M_y^C from its VS. Let i^* denote the numerical index of that vehicle. At this point, computing the bundle end-to-end delay as simply the sum of the queueing delay in S's MB and the transit delay of vehicle i^* is certainly incorrect. This is due to the fact that such computation overlooks the additional delays $A_{vs}(M_y^C, r)$ $(j+1 < r \leq i^*)$ spent by M_y^C in S's VS until the arrival of vehicle i^*. As such:

$$E_D\left(M_y \middle| \widetilde{\nu_p}(j) > 0, X = x, j < i^* \leq j + x\right) = Q_{mb}(M_y) + \sum_{r=j+1}^{i^*} A_{vs}(M_y^C, r) + L_{i^*} \tag{6.8}$$

Note that a very special case is whenever none of the arriving x vehicles contributes to achieving earlier deliveries of M_y^C to D. In other words, $i^* = j$. Only then:

$$E_D\left(M_y \middle| \widetilde{\nu_p}(j) > 0, X = x, i^* = j\right) = Q_{mb}(M_y) + L_j \tag{6.9}$$

In general, at an arbitrary time slot s_j, upon the arrival of a vehicle j, S may find a number N_{vs} of bundle copies in its VS. The corresponding originals of these copies have been sent earlier with N_{vs} *vulnerable* vehicles (*i.e.* vehicles $j - N_{vs}$, $j - N_{vs} + 1$, $j - N_{vs} + 2$, ..., $j - 1$) (otherwise the copies would have been already cleared). Hence, for each of the N_{vs} vehicles that happens to arrive to D after vehicle j, its corresponding virtual bundle copy in S's VS is retransmitted to vehicle j followed by a sequence of expiry timers and vulnerability periods updates.

In addition, vehicle j will also pick up, from S's MB one original bundle (assumed available since S is operating under saturation conditions), the copy of which is enqueued in S's VS with the appropriate expiry timer associated to it. Throughout vehicle j's vulnerability period, alternative better vehicles may have arrived to S. In

addition to their own original bundles, these better vehicles would also pick up from S's VS a copy of vehicle j's bundle as well as a subset (or proper subset) of bundle copies corresponding to any vulnerable and relatively worse vehicle. As vehicle j (respectively any other vehicle) crosses its own vulnerability period, all the bundle copies it carries are cleared at S and their occupied space freed.

6.2.3 Further Observations:

In light of the above description of S's behavior under DODD, some additional facts can be observed as explained below:

1. Had S had complete *a priori* knowledge of the arrivals of subsequent vehicles presenting delivery opportunities of bundle M_y to D that are earlier than that of vehicle j, then it would have further retained bundle M_y and released it to the best one of these vehicles. Assuming, as in the above case 2.2, that vehicle i^* is the one that achieves the earliest delivery of M_y to D, then the factor $\sum_{r=j+1}^{i^*} A_{vs}(M_y^C, r)$ in E_D can be interpreted as the additional queueing delay that M_y would have spent in S's MB until the arrival of vehicle i^*.

2. Ultimately, every arriving vehicle to D will attempt to deliver all the bundles it is transporting from S. However, D will consider as redundant all bundles whose copies have already been delivered by earlier arriving vehicles. Hence, it will discard all such bundles. Nevertheless, in some scenarios, under poor channel conditions and high error rates, redundant copies become beneficial as they may be interpreted as minimal-delay retransmissions that contribute to the increase of the message delivery ratio. Such cases are currently outside the scope of this chapter and will be considered as future work.

6.3 Modeling And Analysis of The Source SRU Under DODD

Following of the earlier description of the source SRU S and its behaviour under DODD, this section has the following objectives: a) develop a mathematical model for S's MB and hence the corresponding average bundle queueing delay Q_{mb}, b) compute the average bundle buffering time in S's VS, c) derive the average bundle transit delay and finally d) derive the average bundle delivery (*i.e.* end-to-end) delay. The modeling of S as well as the analysis of its behavior and the evaluation of its achievable performance under DODD are conducted in light of the below-listed classical assumptions:

6.3.1 Basic Assumptions:

- $A1$: Time is discretized into mini-slots of length τ ($seconds$) each.
- $A2$: Events can only occur at the end of these mini-slots.
- $A3$: Both the MB and the VS of S have infinite size.
- $A4$: The transmission rate of S is T_R ($Mbps$).
- $A5$: The bundle size is fixed to b ($bytes$).
- $A6$: Bundle arrivals follow a Poisson process with rate $\lambda \left(\frac{bundles}{second}\right)$.

6.3.2 Modeling The Source SRU's Main Buffer:

Define K_b to be the number of slots that elapse between two consecutive bundle arrivals to S's MB. Based on assumptions $A1$, $A2$ and $A6$, K_b is geometrically distributed with a parameter $p = \lambda\tau$. A typical queueing system is composed of a queue

where arriving customers wait until they get served and a server where customers receive service. In the context of the networking scenario depicted in Figure 6.1, it is considered that S's MB's front position is the server and subsequent positions constitute the queue. A bundle occupying the front position of S's MB departs from that MB upon the arrival of a vehicle to which that bundle is released. At this point, it is worthwhile to note that the bundle transmission time is negligible as compared to the inter-arrival time of vehicles. Since the IEEE 802.11p protocol is employed for V2S communication, consider the worst case where the transmitted bundle's size is equal to the maximum transmission unit (MTU) size (*i.e.* 1500 *bytes*). The minimum transmission rate of S under 802.11p is 3 (*Mbps*). Consequently the worst case bundle transmission time is 4 (*milli-second*). As discussed in Chapter 4, the minimum vehicle inter-arrival time under free-flow traffic conditions is 3.6 (*seconds*). Hence, it is assumed justifiably that the bundle transmission is instantaneous. As such, the bundle service time, in this case, becomes equivalent to the amount of time a bundle waits at the front position of S's MB for a vehicle to arrive. As mentioned in section III, the inter-arrival time of vehicles is K_v and is geometrically distributed with parameter $1-q$. In light of the above, S's MB may be modelled as a $Geo(p)/Geo(q)/1$ queue. Such a queueing system has been widely studied in the open literature. In order to avoid redundancy, the reader is referred to [72] for further details. Nonetheless, one of the relevant parameters evaluated throughout the analysis presented in [72] is the average number of customers in the system which is equivalent to the average number of bundles in S's MB in this chapter. Let N_{mb} denote the number of bundles in S's MB. Following the analysis in [72], the probability mass function of N_{mb} is

given by:

$$\pi_n = Pr[N_{mb} = n] = \begin{cases} 1-\rho & \text{, for } n = 0 \\ \frac{1-\rho}{1-q}\left[\frac{\rho(1-q)}{1-p}\right]^n & \text{, for } n \geq 1 \end{cases} \tag{6.10}$$

where $\rho = pq^{-1}$. Denote by $\overline{N_{mb}}$ the average number of bundles in S's MB which is derived as:

$$\overline{N_{mb}} = \sum_{n=1}^{\infty} n\pi_n = \frac{\rho(1-p)}{1-\rho} \tag{6.11}$$

Finally, using *Little's Formula*, the average queueing delay in S's MB is given by:

$$\overline{Q_{mb}} = p^{-1}\overline{N_{mb}} \tag{6.12}$$

$\overline{Q_{mb}}$ constitutes the first factor of the overall bundle delivery delay. The following section has the objective of determining the residency period of a bundle's copy in S's VS.

6.3.3 Bundle Buffering Time In The Virtual Space:

Let $B_{vs}(M_y^C)$ and $\overline{B_{vs}}$ denote respectively the buffering time of bundle copy M_y^C in S's VS and its average value. In light of the description of S's behavior in section 6.2.2, B_{vs} depends on four parameters, namely: *a)* $\widetilde{\nu_p}(j)$ being the vulnerability period of vehicle j, *b)* X being the number of vehicles arriving during $\widetilde{\nu_p}(j)$, *c)* n being the number of arriving vehicles out of X that contribute to the minimization of the delivery delay of bundle M_y and *d)* i^* being the numerical index of the ever last vehicle that achieves the earliest delivery of M_y^C to D. For instance, whenever $\widetilde{\nu_p}(j) = 0$, (*i.e.* in section 6.2.2 case 1), S will not enqueue a copy of the released bundle in its VS. Hence, $B_{vs}(M_y^C) = 0$ and $\overline{B_{vs}} = 0$. This occurs with a probability

$Pr[\widetilde{\nu_p}(j) = 0] = f_{\nu_p}(0)$. Otherwise, with a probability $1 - f_{\nu_p}(0)$, $\widetilde{\nu_p}(j) > 0$. Thus, a bundle copy M_y^C is enqueued into S's VS and the total amount of time that it spends there is controlled by S only as long as the last vehicle to which M_y^C was retransmitted remains vulnerable. This matter has been well elaborated in cases 2.1 and 2.2 of section 6.2.2. In the sequel, each of these cases is analyzed separately. For this purpose, assume that $\widetilde{\nu_p}(j) = \nu$ such that $\nu \in [1; L_{max} - L_{min}]$ and recall that $X = x$ is the total number of vehicles that arrive during ν. These vehicles will arrive at the end of arbitrary x slots. Hence, the probability mass function of X is given by:

$$f_X(x) = Pr[X = x] = \binom{\nu}{x} q^x (1-q)^{\nu - x}, \text{ for } 0 \leq x \leq \nu \tag{6.13}$$

Case 2.1: From equation (6.7), it can be perceived that:

$$B_{vs}\left(M_y^C \middle| \widetilde{\nu_p}(j) = \nu, X = 0\right) = \widetilde{\nu_p}(j) \tag{6.14}$$

This is especially true since, during the entire $\widetilde{\nu_p}(j)$, M_y^C was waiting in S's VS but S has witnessed no vehicle arrivals at all. As such:

$$\begin{aligned}
E\left[B_{vs} \middle| \widetilde{\nu_p}(j) = \nu, X = 0\right] &= E\left[\widetilde{\nu_p}(j)\right] \\
&= \sum_{k=0}^{L_{max}-L_{min}} k f_{\nu_p}(k) \\
&= \sum_{k=0}^{L_{max}-L_{min}} k f_L(k + L_{min}) \\
&= \sum_{k=L_{min}}^{L_{max}} (k - L_{min}) f_L(k) \\
&= \sum_{k=L_{min}}^{L_{max}} k f_L(k) - \sum_{k=L_{min}}^{L_{max}} L_{min} f_L(k) \\
&= \overline{L} - L_{min}
\end{aligned} \tag{6.15}$$

It follows that, for this case, the average bundle buffering time in S's VS is given by:

$$\overline{B_{vs}} = \sum_{\nu=1}^{L_{max}-L_{min}} \left(\overline{L} - L_{min}\right)(1-q)^{\nu} f_{\nu_p}(\nu). \tag{6.16}$$

Case 2.2:

A careful examination of equation (6.8) indicates that:

$$\begin{aligned} B_{vs}\left(M_y^C \middle| \widetilde{\nu_p}(j) = \nu, X = x, j < i^* \leq j + x\right) &= \sum_{r=j+1}^{i^*} A_{vs}(M_y^C, r) + \widetilde{\nu_p}(i^*) \\ &= A_{vs}(M_y^C, i^*) + \widetilde{\nu_p}(i^*) \end{aligned} \tag{6.17}$$

This exactly follows from the fact that S discards M_y^C as soon as the last vehicle to which this copy was released (*i.e.* vehicle i^*) becomes invulnerable. At this level, two major challenging problems are identified. The first problem (which is the most challenging) is to probabilistically determine i^* then, knowing i^*, the second problem is to evaluate the average bundle buffering time resulting from equation (6.17). The resolution of these two problems follows.

- **Problem 1:** *Probabilistic Determination of* i^*

  Given a positive value of $X = x$, this problem consists of deriving the probability distribution of i^* such that $j \leq i^* \leq j + x$. Among all the x arriving vehicles during ν, vehicle i^* being the one that achieves the earliest delivery of M_y^C to D, means that all the subsequently arriving $x - i^*$ vehicles are not able to beat it. Assume that vehicle i^* achieves a transit delay $L_{i^*} = l$. A vehicle u ($i^* < u < j + x$) that achieves a transit delay L_u will not be able to beat vehicle i^* if an only if:

$$L_u > L_{i^*} - K_u \Rightarrow L_u + K_u > L_{i^*} \tag{6.18}$$

where the term $K_u = \sum_{r=i^*+1}^{u} K_r$ represents the sum of all vehicle inter-arrival slot intervals from vehicle i^* to u. Note that each K_r has a probability mass function as given in (6.1). Also as mentioned in section 6.1, under Free-flow traffic conditions, vehicle inter-arrival slot intervals are independent and identically distributed. As a result, the probability mass function of K_u denoted by $f_{K_u}(k)$ is equivalent to the u-fold convolution of $f_{K_v}(k)$. Also, L_u is distributed according to equation (6.2). Now, let $\Omega = L_u + K_u$ be a random variable whose probability mass function and cumulative distribution function are respectively given by $f_\Omega(k)$ and $F_\Omega(l)$. Denote by β_u the probability that a vehicle u will not be able to beat i^*. It is given by:

$$\begin{aligned}
\beta_u &= \sum_{l=L_{min}}^{L_{max}} Pr\left[L_u + \sum_{r=i^*+1}^{u} K_r > L_{i^*} \middle| L_{i^*} = l\right] \cdot Pr[L_{i^*} = l] \\
&= \sum_{l=L_{min}}^{L_{max}} Pr\left[\Omega > L_{i^*} \middle| L_{i^*} = l\right] \cdot f_L(l) \\
&= \sum_{l=L_{min}}^{L_{max}} \left[1 - F_{\Omega|L_{i^*}}(l)\right] \cdot f_L(l) \qquad (6.19)
\end{aligned}$$

However, the complexity of f_L in (6.2) renders the derivation of $f_\Omega(k)$ as the convolution of the f_{K_u} and f_L a remarkably complex and computational resource exhaustive task that results in no closed-form solution for $f_\Omega(k)$, let along $F_\Omega(l)$. Fortunately, thorough numerical analysis have shown that β_u can be approximated with a very high accuracy whenever $K_u = \sum_{r=i^*+1}^{u} K_r$ is substituted by $\widetilde{K_u} = u\overline{K}$ where $\overline{K}$ is the average of K_r. Hence, the computation of

β_u reduces to evaluating:

$$\begin{aligned}\beta_u &= \sum_{l=L_{min}}^{L_{max}} \left[1 - Pr\left[L_u < L_{i^*} - u\overline{K}\middle| L_{i^*} = l\right]\right] \cdot Pr[L_{i^*} = l] \\ &= \sum_{l=L_{min}}^{L_{max}} \left[1 - F_{L|L_{i^*}}(l - u\overline{K})\right] \cdot f_L(l) \end{aligned} \tag{6.20}$$

Note that, the above computation of $F_{L|L_{i^*}}(l) = Pr\left[L_u < L_{i^*} - u\overline{K}\middle| L_{i^*} = l\right]$, although done numerically, is much faster and less resource expensive. This being done, the conditional probability mass function of i^* can be expressed as:

$$f_{i^*|X}(i) = Pr\left[i^* = i\middle| X = x\right] = \prod_{u=i+1}^{j+x} \beta_u \text{ , for } j \leq i \leq j + x \tag{6.21}$$

- **Problem 2:** *Evaluation of the average bundle buffering time*

  Observe in equation (6.17) that, for a particular value of i^*, all of the $A_{vs}(M_y^C, r)$ with $(j + 1 \leq r \leq i^*)$ are independent and identically distributed random variables with probability mass functions similar to the one given in equation (6.1). As a result, $A_{vs}(M_y^C, i^*)$ has a conditional probability mass function $f_{A_{vs}}(k|i^*)$, that is equal to the i^*-fold convolution of $f_{K_v}(k)$. Following the derivation procedure of [90], it can be proven that $f_{A_{vs}}(k|i^*)$ is a Pascal Distribution. For completion purposes, this derivation is as follows.

  Let, $\widehat{F_{K_v}}(s)$ denote the moment generating function of an arbitrary K_r variable $(j + 1 \leq r \leq i^*)$. It is given by:

$$\widehat{F_{K_v}}(s) = E\left[e^{sk}\right] = \sum_{k=1}^{\infty} q(1-q)^{k-1}e^{sk} = \frac{qe^s}{1 - (1-q)e^s} \tag{6.22}$$

Let $\widehat{F_{A_{vs}}}(s|i^*)$ denote the conditional moment generating function of $A_{vs}(M_y^C, i^*)$. It is given by:

$$\begin{aligned}\widehat{F_{A_{vs}}}(s|i^*) &= \prod_{r=j+1}^{i^*} \widehat{F_{K_v}}(s) \\ &= \left[\widehat{F_{K_v}}(s)\right]^{i^*} = \left(\frac{qe^s}{1-(1-q)e^s}\right)^{i^*} \\ &= q^{i^*}e^{si^*}\left(\frac{1}{1-(1-q)e^s}\right) \end{aligned} \tag{6.23}$$

Let $\omega = (1-q)e^s$ and note that:

$$\frac{d^m}{d\omega^m}\left(\frac{1}{1-\omega}\right) = m!\left(\frac{1}{1-\omega}\right)^{m+1} \text{, for } m \geq 1 \tag{6.24}$$

Therefore, equation (6.23) may be rewritten as:

$$\begin{aligned}\widehat{F_{A_{vs}}}(s|i^*) &= q^{i^*}e^{si^*}\frac{1}{(i^*-1)!}\frac{d^{i^*-1}}{d\omega^{i^*-1}}\left(\frac{1}{1-\omega}\right) \\ &= q^{i^*}e^{si^*}\frac{1}{(i^*-1)!}\frac{d^{i^*-1}}{d\omega^{i^*-1}}\sum_{m=1}^{\infty}\omega^{m-1} \\ &= q^{i^*}e^{si^*}\frac{1}{(i^*-1)!}\sum_{m=i^*}^{\infty}\frac{(m-1)!}{(m-i^*)!}\omega^{m-i^*} \end{aligned} \tag{6.25}$$

At this stage, substitution for ω leads to rewriting equation (6.25) as:

$$\begin{aligned}\widehat{F_{A_{vs}}}(s|i^*) &= \sum_{m=i^*}^{\infty} q^{i*}e^{si^*}\frac{1}{(i^*-1)!}\frac{(m-1)!}{(m-i^*)!}(1-q)^{m-i^*}e^{s(m-i^*)} \\ &= \sum_{m=i^*}^{\infty}\binom{m-1}{i^*-1}q^{i^*}(1-q)^{m-i^*}e^{sm} \end{aligned} \tag{6.26}$$

Equation (6.26) is equivalent to $E\left[e^{sm}\right]_{m=k}$. Hence, $f_{A_{vs}}(k|i^*)$ can be extracted

from equation (6.20) to be, indeed, a Pascal distribution expressed as:

$$f_{A_{vs}}(k|i^*) = \binom{k-1}{i^*-1} q^{i^*}(1-q)^{k-i^*}, \text{ for } k \geq i^* \tag{6.27}$$

At this point, the conditional average value of $A_{vs}(M_y^C, i^*)$ is given by:

$$E\left[A_{vs}(M_y^C, i^*)\middle| i^*\right] = \sum_{k=i^*}^{\infty} k \cdot f_{A_{vs}}(k|i^*) = \frac{i^*}{q} \tag{6.28}$$

Now, the average value of $E\left[\widetilde{\nu_p}(i^*)\middle| i^*\right]$ is computed. Notice that, for a particular value of i^*, the achieved transit delay by vehicle i^* is $L_{i^*} = l$. Consequently, the value of $\widetilde{\nu_p}(i^*)$ follows directly from equation (6.3) and is distributed according to equation (6.4). As a result, it can be easily proven as in equation (6.15) that:

$$E\left[\widetilde{\nu_p}(i^*)\middle| i^*\right] = \overline{L} - L_{min} \tag{6.29}$$

This being done, the conditional average value of the bundle buffering time is given by:

$$E\left[B_{vs}\middle|\widetilde{\nu_p}(j) = \nu, X = x, j < i^* \leq j + x\right] = \frac{i^*\left(\overline{L} - L_{min}\right)}{q} \tag{6.30}$$

Thus, the unconditional average value of $B_{vs}(M_y^C)$, in this case, can be expressed as:

$$\begin{aligned}\overline{B_{vs}} &= \sum_{\nu=1}^{L_{max}-L_{min}} \sum_{x=1}^{\nu} \sum_{i=j+1}^{j+x} \frac{i\left(\overline{L} - L_{min}\right)}{q} \cdot f_{i^*}(i) \cdot f_X(x) \cdot f_{\nu_p}(\nu) \\ &= \frac{\xi\left(\overline{L} - L_{min}\right)}{2q} \sum_{\nu=1}^{L_{max}-L_{min}} \sum_{x=1}^{\nu} \sum_{i=j+1}^{j+x} \left[\prod_{u=i+1}^{j+x} \beta_u\right] \binom{\nu}{x} q^x (1-q)^{\nu-x} \times \\ &\qquad \left[\operatorname{erf}\left(\frac{\frac{d_{SD}}{(\nu+L_{min})\tau} - \overline{V}}{\sigma_V\sqrt{2}}\right) - \operatorname{erf}\left(\frac{\frac{d_{SD}}{(\nu+L_{min}-1)\tau} - \overline{V}}{\sigma_V\sqrt{2}}\right)\right]\end{aligned} \tag{6.31}$$

Finally, what remains to conclude the analysis of case 2.2, is the derivation of the average bundle buffering time in S's VS under the special case pertaining to equation (6.9). This is done next. In that special case, it is clear that the bundle buffering time in S's VS is $B_{vs}\left(M_y^C \middle| \widetilde{\nu_p}(j)=\nu, X=x, i^*=j\right) = \widetilde{\nu_p}(j)=\nu$. It follows that the average value of B_{vs} in this case is given by:

$$\begin{aligned}\overline{B_{vs}} &= \sum_{\nu=1}^{L_{max}-L_{min}} \sum_{x=1}^{\nu} \nu \cdot f_{i^*}(j) \cdot f_X(x) \cdot f_{\nu_p}(\nu) \\ &= \frac{\xi}{2} \sum_{\nu=1}^{L_{max}-L_{min}} \sum_{x=1}^{\nu} \nu \left[\prod_{u=j+1}^{j+x} \beta_u\right] \binom{\nu}{x} q^x (1-q)^{\nu-x} \times \\ &\qquad \left[\operatorname{erf}\left(\frac{\frac{d_{SD}}{(\nu+L_{min})\tau} - \overline{V}}{\sigma_V\sqrt{2}}\right) - \operatorname{erf}\left(\frac{\frac{d_{SD}}{(\nu+L_{min}-1)\tau} - \overline{V}}{\sigma_V\sqrt{2}}\right)\right] \end{aligned} \quad (6.32)$$

6.3.4 Bundle Delivery Delay:

Recall that $E_D(M_y)$ being the delivery delay of a bundle M_y is given in equation (6.6). Following the analysis made in subsection V-C, this expression may be rewritten as:

$$E_D(M_y) = Q_{mb}(M_y) + B_{vs}(M_y^C) + L_{min} \quad (6.33)$$

It follows that the average bundle delivery delay is given by:

$$\overline{E_D} = \overline{Q_{mb}} + \overline{B_{vs}} + L_{min} \quad (6.34)$$

6.4 Numerical Analysis and Simulations

In this section the model laid out in section V will be verified and the performance of DODD will be evaluated in the context of the IRCN scenario illustrated in Figure 6.1. The adopted performance metric is the average bundle delivery delay The

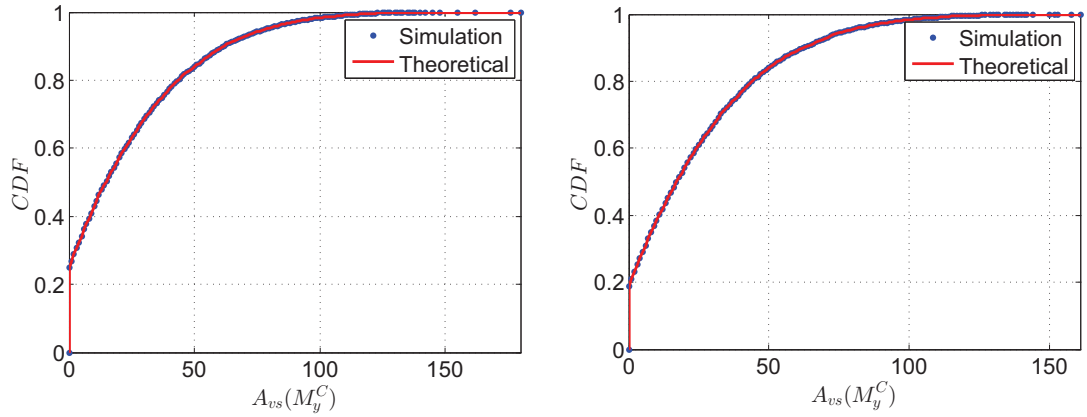

(a) $\mu_v = 0.1$.

(b) $\mu_v = 0.15$.

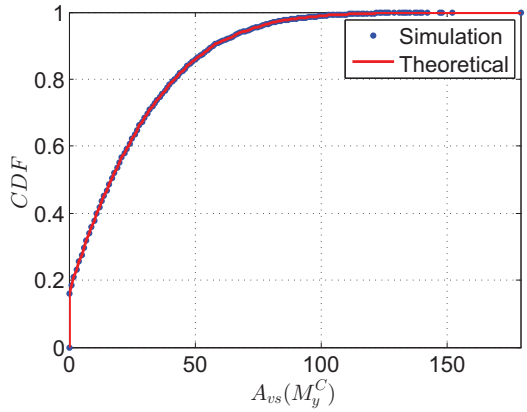

(c) $\mu_v = 0.2$.

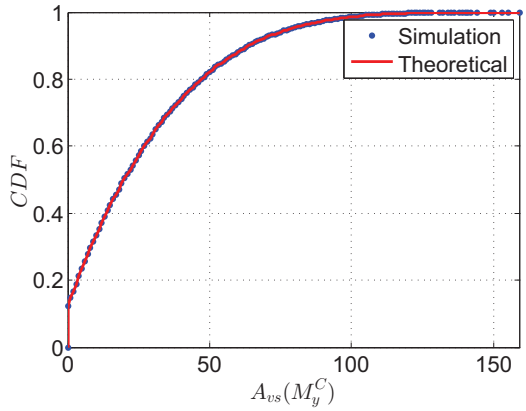

(d) $\mu_v = 0.25$.

Figure 6.5: Simulated VS Theoretical versions of the cumulative distribution function of $A_{vs}(M_y^C)$.

performance achieved by PBRS-BBR and GBRS-BBR developed in Chapter 5 will serve as benchmarks.

A Java-based discrete event simulator was developed. The adopted performance metric was evaluated for a total of 10^7 bundles and averaged out over multiple runs of the simulator to ensure that a 95% confidence interval is realized. Simulations were conducted using the following classical parameter values: *a*) mini-slot duration $\tau = 1$ $(second)$, *b*) $\mu_v \in [0.1; 0.27]$ $\left(\frac{Vehicles}{second}\right)$, *c*) $\lambda = 0.09$ $\left(\frac{Bundles}{second}\right)$, *d*) $T_R = 11$ $(Mbps)$ and *e*) $b = 1500$ $(bytes)$. Figures 6.5 and 6.6 concurrently plot the respective empirical

and theoretical cumulative density functions of $A_{vs}(M_y^C)$ and $\nu_p(i^*)$ corresponding to two values of the vehicle flow rate. Figures 6.7(a), 6.7(b) and 6.7(d) concurrently plot the respective theoretical and empirical curves of $\overline{Q_{mb}}$, $\overline{B_{vs}}$ and $\overline{E_D}$ as achieved by DODD for various values of μ_v. In addition, Figure 7(c) plots L_{min} as computed from Chapter 4 for the various values of μ_v. All of these figures constitute tangible proofs of the validity of the proposed model as well as the accuracy of the simulations. This is especially true since the empirical and theoretical curves of each of the plots almost perfectly match. In the sequel, the performance of DODD is evaluated. For this purpose, two other schemes developed in an earlier work will serve as benchmarks. These two schemes are, namely: *a*) Probabilistic Bundle Release Scheme with Bulk Bundle Release (PBRS-BBR) and *b*) Greedy Bundle Release Scheme with Bulk Bundle Release (GBRS-BBR). Figure 6.8 concurrently plots the respective curves of $\overline{E_D}$ as achieved by DODD, PBRS-BBR and GBRS-BBR. The figure shows that DODD significantly outperforms PBRS-BBR and GBRS-BBR. This is especially true since, under DODD, the utilization of the VS characterizes S with supplementary intelligence. In other words, S is now augmented with the capability of knowledge acquisition and *short-term memorization*[1] of arriving vehicles' parameters. Consequently, S may now react on the spur of the moment and according to the turn of events in such a way to perform necessary bundle retransmissions to the arriving faster vehicles. These vehicles, in turn, will guarantee deliveries of those copies to D earlier than the slower vehicles already carrying them. This is not the case whenever the BBR-enabled schemes developed in Chapter 5 are used. As a matter of fact, under these two schemes, S does not retain copies of released bundles and hence retransmissions are not possible. In addition, for instance, under GBRS-BBR, S releases a bulk of bundles for an arriving vehicle irrespective of its arrival time and

[1] S will only retain the parameters of a vehicle j carrying bundles for as long as either this vehicle did not cross its vulnerability period or all the bundles it carries have been retransmitted to subsequent faster vehicles. At this level, it becomes useless to further retain vehicle j's parameters.

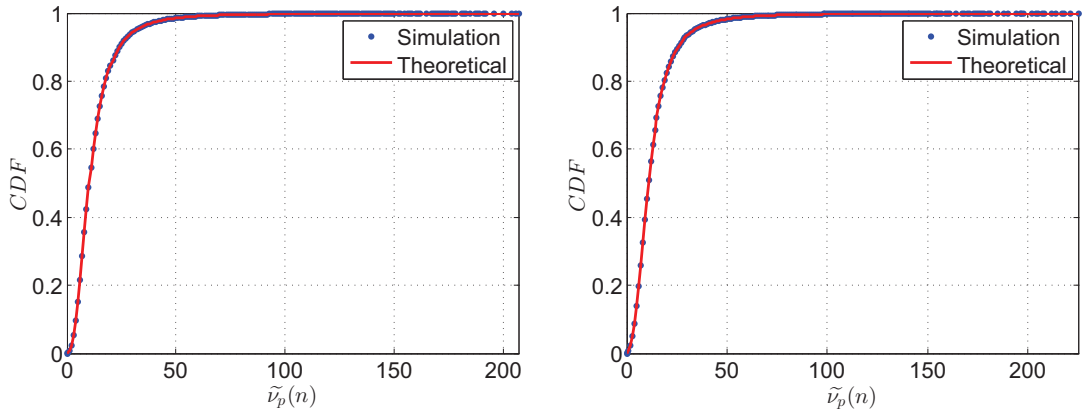

(a) $\mu_v = 0.1$. (b) $\mu_v = 0.15$.

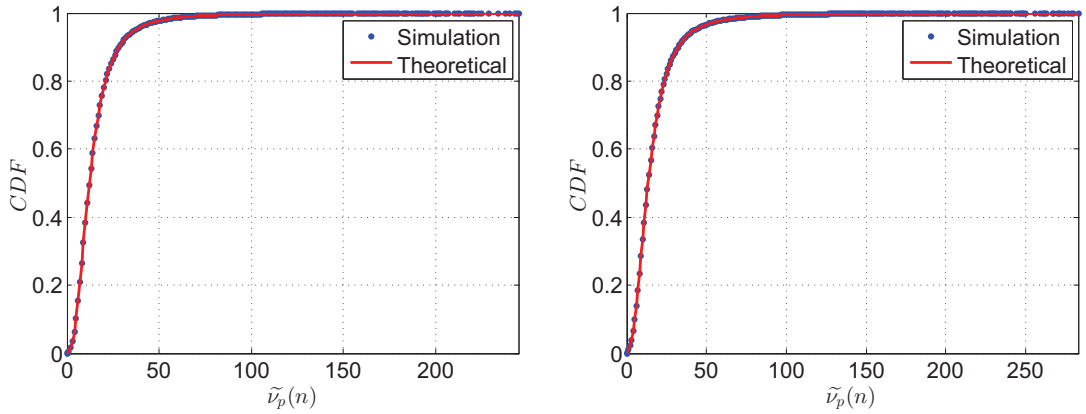

(c) $\mu_v = 0.2$. (d) $\mu_v = 0.25$.

Figure 6.6: Empirical VS Theoretical versions of the cumulative distribution function of $\nu_p(n)$.

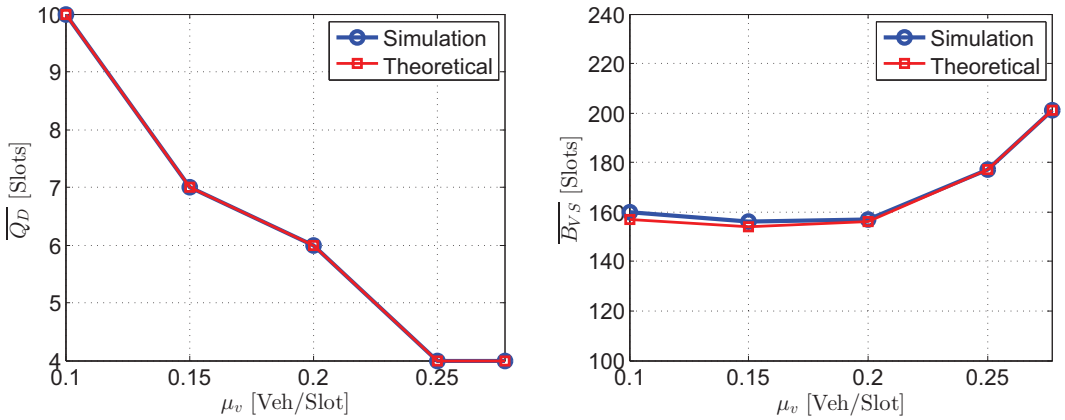

(a) Average bundle queueing delay in S's MB. (b) Average bundle buffering time in S's VS.

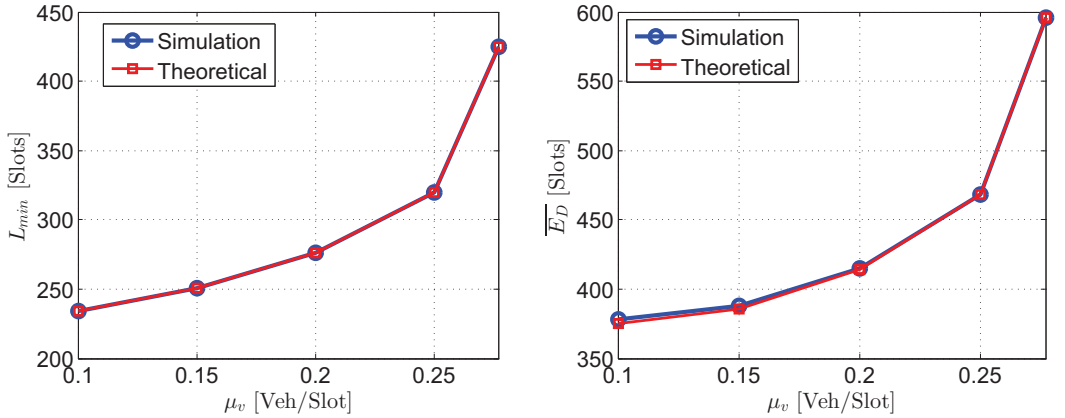

(c) Minimum transit delay under free-flow conditions. (d) Average bundle delivery delay achieved by DODD.

Figure 6.7: Comparison between theoretical and empirical results for the purpose of model validity and accuracy verification.

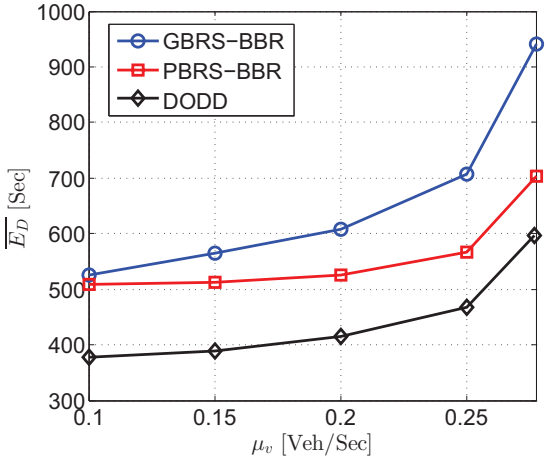

Figure 6.8: Performance evaluation of DODD versus PBRS-BBR and GBRS-BBR.

speed. This, indeed, contributes to the minimization of the average queueing delay. However, observe that, in this case, bundle bulks become equally likely to be released to fast as well as slow vehicles. At this stage, it is important to note that both the distribution of the vehicle travel time in section III and its discretized equivalent result from the use of a truncated Normal distribution for vehicle speeds with an average $\overline{V}$. Hence, it is more likely that the speed of an arriving vehicle selected to transport bundles to D be close to $\overline{V}$ rather than higher speeds. Consequently, the resulting average transit delay achieved under GBRS-BBR will be relatively high in such a way that it overshadows the low queueing delay and dominates the achieved end-to-end delay performance. This situation is improved whenever PBRS-BBR is employed. This is especially true since, under PBRS-BBR, S follows the recommendation of a probabilistic prediction parameter P_{br} indicating the degree of contribution of an arriving vehicle to the minimization of the average end-to-end delay. Consequently, S becomes selective and releases bundle bulks only to those vehicles it predicts will contribute the most to the realization of this objective. In other words, under PBRS-BBR, a bulk of bundles is released to an arriving vehicle with a probability P_{br}. With a probability $1-P_{br}$ bundles are retained until the arrival of a subsequent vehicle that is predicted to present an earlier bundle delivery opportunity to D. On one hand, it may seem that, in this case, the accumulation of more bundles in S's queue until the arrival of the suitable vehicle will increase the queueing delay. However, the BBR mechanism controls and prohibits the queueing delay from increasing significantly. On the other hand, given the probabilistic nature of PBRS-BBR, chances are that S misses some early delivery opportunities only because it predicts that subsequently arriving vehicles may, with a probability P_{br}, deliver earlier. This may turn out not to be the case. Moreover, contrary to BDS, the release decision is taken on a per bulk basis rather than on a per bundle basis. That is, once S selects a vehicle, it

keeps on releasing bundles to that vehicle until it goes out of range and hence S overlooks any earlier delivery opportunity that may arise during this time. Missing these opportunities altogether causes PBRS-BBR to achieve a rather sub-optimal transit delay and hence a sub-optimal end-to-end delay.

Chapter 7

Conclusion and Future Directions

7.1 Conclusions

Throughout this thesis, the two-hop intermittently connected roadside communication subnetwork scenario illustrated in Figure 3.1 was considered. This scenario consists of establishing delay-minimal connectivity between two stationary roadside units (SRUs), a source S and a destination D. In this thesis, the focus was on the bundle release mechanism at the source SRU and particularly on the selection process of vehicles that contribute to the minimization of the average bundle end-to-end delivery delay.

The performance of two network information unaware Internet packet-like bundle releasing schemes was investigated. The first scheme is a Greedy Bundle Release Scheme (GBRS) under which a source SRU greedily releases bundles to vehicles that enter its coverage range. The second scheme is the Probabilistic Bundle Release Scheme (PBRS) that has the luxury of holding the head-of-line bundle in the source SRU's queue while awaiting for the arrival of a relatively high speed vehicle that best contributes to the minimization of the average bundle transit delay. An extended mathematical framework was presented for the estimation of several performance

metrics such as the bundle queueing, transit and end-to-end delivery delays under both GBRS and PBRS. As opposed to several strategies found in the open literature, the mathematical study is founded on top of the unavailability of *a priori* network information and strongly capitalizes on capturing the essence of the Vehicular Delay-Tolerant Networking communication paradigm. Through extensive simulations, the performance of PBRS was compared with GBRS. Results showed that PBRS outperformed GBRS in terms of average transit delay. However, the traditional Internet packet-like relaying mechanism significantly impairs the SRU's queue stability and incurs excessive queueing delays that were found to overshadow transit delays. Theoretical and simulation results showed that, under both GBRS and PBRS, bundles suffered excessive queueing delays that rendered these two relaying strategies practically inefficient. A solution to this problem consisted of augmenting the source SRU with the capability of releasing multiple bundles to a selected vehicle throughout that vehicle's residence time. Consequently, it is observed that a selected vehicle leaving the coverage range of the source SRU would be carrying a bulk of bundles to the destination SRU. Hence, integrating the Bulk Bundle Release (BBR) option in either one of PBRS and GBRS has the objective of stabilizing the source SRU's queue and, therefore, lead to considerably improving the performance of both schemes.

At this level, before further developing and analyzing the BBR-enabled schemes, respectively PBRS-BBR and GBRS-BBR, it was observed that the functionality as well as the performance of ICRCNs similar to the one considered in this thesis are significantly correlated to the vehicular traffic behaviour irrespective of the employed bundle delivery schemes. This is especially true since the bundle delivery process is particularly dependent on the vehicle arrivals and their speeds. Therefore, a comprehensive study of the macroscopic vehicular traffic dynamics constituted the incentive for adopting a realistic vehicular traffic model that was referred to throughout this

thesis as the Free-flow Traffic Model (FTM). FTM represents an observed roadway segment operating under Free-flow traffic conditions using an $M/G/\infty$ queueing system. Closed form expressions for this model's characteristic parameters were developed through the introduction of a simple yet highly accurate approximation. Extensive simulations were conducted to examine the validity and accuracy of the presented approximation.

Using FTM as a building block, a queueing model was formulated to characterize a source SRU employing PBRS-BBR and its greedy counterpart and evaluate the average bundle queueing delay. In addition, mathematical analysis were presented with the objective of evaluating the average bundle transit delay and hence the average bundle end-to-end delay. A simulation study was conducted to prove the validity and accuracy of the proposed mathematical model and analysis. The performance of GBRS-BBR served as a benchmark. The reported results show that PBRS-BBR outperforms GBRS-BBR in terms of the mean end-to-end delivery delay. Nevertheless, there exists a bundle arrival rate threshold beyond which the achieved delays under PBRS-BBR will start to irregularly increase. However, under such heavy data traffic offered loads GBRS-BBR will also exhibit delays that, although finite, are very significant. At this point, TH-VICNs will exhibit marginal benefits for delay-minimal bundle deliveries and more sophisticated schemes have to be considered.

Finally, a theoretical modelling and performance evaluation is presented for a novel Delay-Optimal Data Deliver (DODD) scheme that aims at achieving a delay-minimal bundle delivery in the context of the considered ICRCN scenario. The realization of this objective is challenging especially that network information was assumed to be completely unavailable. Nevertheless, the famous retransmission mechanism used in typical data communication networks to recover from data losses and errors comes to the rescue. This mechanism together with the concept of virtual

space is adopted herein for the purpose of enabling the source to retransmit bundle copies, as necessary, to newly arriving vehicles that can secure their delivery to the destination earlier than their foregoing transporters. Extensive simulations have been conducted and constitute tangible proofs of the efficiency of DODD and its ability to considerably outperform the two earlier-developed knowledge-oblivious bundle relaying schemes respectively GBRS-BBR and PBRS-BBR. In fact, DODD improves the average bundle delivery delay achieved by GBRS-BBR by 22.15% to 36.84% and that of PBRS-BBR by 14.28% to 20.91%.

7.2 Future Work

The presented work in this thesis provided an in-depth investigation of the inter-SRU connectivity establishment problem. This problem was adequately addressed through the proposal of realistic bundle delivery schemes. The focus was on one aspect of the delivery process from the source SRU's point of view with an ultimate objective of achieving delay-optimal deliveries in a context where network information is completely unavailable. The developed chapters of this thesis, even though heavily mathematical, they narrate the story of how this objective was attained. Indeed, starting from ground zero, it was only through a gradual but yet an in-depth analysis of the problem that we were able to strengthen our knowledge and gain more insight into the development of the appropriate solutions. However, truly, there are several aspects pertaining to the same scenario that were shelved throughout our research journey. However, these are of immense interest and we will not let them go unseen. In fact, they constitute a list of problems that we will consider in the future. Below some of these problems are listed:

1. The first issue that is of interest as a future investigation is throughput. An existing work in the open literature, [53], indicates that, for an ICRCN similar

to the one considered in this thesis, the achievable best and worst case effective throughputs are respectively 4.5 and 2 *Mbps* whenever the transmission rate of the source is 11 *Mbps*. Throughout [53], the IEEE 802.11a/b was considered as a communication protocol. We believe that, in light of the latest advancements in wireless communication technology, and particularly the recent release of the IEEE 802.11p a higher effective throughput may be achievable especially under schemes augmented with the BBR extension. In addition, the open literature lacks any mathematical modelling and analysis in this context. It is therefore our interest to fill this gap and introduce novel mathematical models that have the objective of providing further insights into the throughput performance of two-hop ICRCNs. Accordingly, a mathematical framework may be setup to study the delay-throughput tradeoff if there arises any evidence that such a tradeoff may exist.

2. Spectrum unavailability and contention are stringently limiting constraints that severely affect the performance of opportunistic relaying schemes. This is especially true when considering the message delivery process at the destination SRUs. As a matter of fact, several vehicles may be present in the range of a destination SRU D with more than one of these vehicles having messages to deliver to D. If all of these vehicles simultaneously initiate message uploads to D a large amount of collisions will occur. Moreover, given the spectrum scarcity problem, there might be no readily available channels to enable all vehicles to communicate with D. In light of these observations we consider studying the dynamic variation/availability of the spectrum and investigate contention resolution as well as the possibility of spectrum sharing between various sub-networks using cognitive radios. These studies will form the basis for refining the access schemes developed in this thesis so as to maximize the message delivery ratio.

3. During medium-to-heavy vehicular traffic, the vehicular density becomes high. Therefore, there exists the possibility of establishing end-to-end paths between the source and the destination SRUs. Messages can therefore be easily routed over these paths and hence the delivery delay would decrease to an order of a couple of milliseconds. The open literature reports on several attempts to adopt typical Internet (*i.e.* TCP/IP suite) and Mobile Ad-Hoc Network (MANET) routing protocols (*e.g.* AODV, DSR, OLSR, etc.) for this purpose. Nevertheless, these attempts proved the unsuitability as well as the failure of these transport/routing protocols when for inter-vehicular communications. Therefore we will consider the development of protocols that enable inter-vehicular communications in order to achieve very low message delivery delays that are of the order of milliseconds.

Bibliography

[1] A. Pentland, R. Fletcher, and A. Hasson, "Daknet: Rethinking connectivity in developing nations," *IEEE Computer*, vol. 37, no. 1, pp. 78–83, January 2004.

[2] United Nations Department of Economic and Social Affairs, "E-government survey 2010: Leveraging e-government at a time of financial and economic crisis," 2010. [Online]. Available: http://www2.unpan.org/egovkb/documents/2010/E_Gov_2010_Complete.pdf

[3] Y. Yang, H. Hu, J. Xu, and G. Mao, "Relay technologies for wimax and lte advanced mobile systems," *IEEE Communications Magazine*, vol. 47, no. 10, pp. 100–105, October 2009.

[4] CISCO, "Cisco visual networking index: Global mobile data traffic forecast update," January 2009. [Online]. Available: http://mobiletvworld.com/documents/Global%20Mobile%20Data%20Traffic%202009.pdf

[5] Federal Communications Commission, "Connecting america: The national broadband plan," March 2005. [Online]. Available: http://www.broadband.gov/plan/#read-the-plan

[6] Motorola, "Adaptive modulation and coding," *Technical Report TR 25.848 on HSDPA.*, October 2000. [Online]. Available: http://www.3gpp.org/ftp/tsg_ran/WG1_RL1/TSGR1_17/docs/PDFs/R1-00-1395.pdf

[7] Z. Shi and C. Schlegel, "Iterative multiuser detection and error control code decoding in random cdma," *IEEE Transactions on Signal Processing*, vol. 54, no. 5, pp. 78–83, May 2006.

[8] K. Sundaresan and R. Sivakumar, "Cooperating with smartness: Using heterogeneous smart antennas in multihop wireless networks," *IEEE Transactions on Mobile Computing*, vol. 10, no. 12, pp. 1666–1680, December 2011.

[9] B. Sklar, *Digital Communications: Fundamentals and Applications*, 2nd ed. Prentice Hall PTR, 2001.

[10] J. Laneman, D. Tse, and G. W. Wornell, "Cooperative diversity in wireless networks: Efficient protocols and outage behavior," *IEEE Transactions on Information Theory*, vol. 50, no. 12, pp. 3062–3080, December 2004.

[11] Q. Zhao and B. M. Sadler, "A survey of dynamic spectrum access," *IEEE Signal Processing Magazine*, vol. 24, no. 3, pp. 79–89, May 2007.

[12] J. W. Lee, R. R. Mazumdar, and N. B. Shroff, "Joint opportunistic power scheduling and end-to-end rate control for wireless ad hoc networks," *IEEE Transactions on Vehicular Technology*, vol. 56, no. 2, pp. 801–809, March 2007.

[13] Y. S. Su, S. L. Su, and J. S. Li, "Topology-independent link activation scheduling schemes for mobile cdma ad hoc networks," *IEEE Transactions on Mobile Computing*, vol. 7, no. 5, pp. 599–616, May 2008.

[14] M. Johansson and L. Xiao, "Cross-layer optimization of wireless networks using nonlinear column generation," *IEEE Transactions on Wireless Communications*, vol. 5, no. 2, pp. 435–445, February 2006.

[15] C. F. Solution, "Reduce costs, improve coverage and convenience." [Online]. Available: http://www.cisco.com/en/US/netsol/ns941/networking_solutions_solution_category.html

[16] Federal Communications Commission, "Amendment of the commission's rules regarding dedicated short-range communications services in the 5.850-5.925 ghz (5.9 ghz band)," *Federal Register, The Daily Journal of the United States Government, FCC 03-324*, July 2006. [Online]. Available: https://www.federalregister.gov/articles/2006/09/07/E6-14795/amendment-of-the-commissions-rules-regarding-dedicated-short-range-communications-ser

[17] IEEE Standards Association, "802.11p-2010 - IEEE standard for information technology - local and metropolitan area networks - specific requirements - part 11: Wireless lan medium access control (mac) and physical layer (phy) specifications amendment 6: Wireless access in vehicular environments." [Online]. Available: http://standards.ieee.org/findstds/standard802.11p-2010.html

[18] S. Panichpapiboon and W. P. Atikom, "Connectivity requirements for self-organizing trafc information systems," *IEEE Transactions on Vehicular Technology*, vol. 57, no. 6, p. 33333340, November 2008.

[19] J. Zhao, Y. Zhang, and G. Cao, "Data pouring and buffering on the road: A new data dissemination paradigm for vehicular ad hoc networks," *IEEE Transactions on Vehicular Technology*, vol. 56, no. 6, p. 32663277, November 2007.

[20] H. Saleet, R. Langar, O. Basir, and R. Boutaba, "A distributed approach for location lookup in vehicular ad hoc networks," in *Proceedings of the IEEE International Conference on Communications*, Dresden, Germany, June 2009, pp. 1–6.

[21] H. Saleet, O. Basir, R. Langar, and R. Boutaba, "Region-based location-service-management protocol for vanets," *IEEE Transactions on Vehicular Technology*, vol. 59, no. 2, pp. 917–931, February 2010.

[22] H. Soroush, N. Banerjee, A. Balasubramanian, M. D. Corner, B. N. Levine, and B. Lynn, "Dome: A diverse outdoor mobile testbeds," in *Proceedings of the First ACM International Workshop on Hot Topics of Planet-Scale Mobility Measurments*, Krakow, Poland, June 2009.

[23] S. Panichpapiboon and W. P. Atikom, "A review of information dissemination protocols for vehicular ad hoc networks," *IEEE Communications Surveys and Tutorials*, vol. PP, no. 99, pp. 1–15, Accepted 2011.

[24] Y. Toor, P. Muhlethaler, A. Laouiti, and A. D. L. Fortelle, "Vehicle ad-hoc networks: Applications and related technical issues," *IEEE Communications Surveys and Tutorials*, vol. 10, no. 3, pp. 74–88, 2008.

[25] V. Ramaiyan, E. Altman, and A. Kumar, "Delay optimal schedule for a two-hop vehicular relay network," *Journal of Mobile Networks and Applications*, vol. 15, no. 1, February 2010.

[26] D. J. Goodman, J. Borras, N. Mandayam, and R. Yates, "Infostations: A new system model for data and messaging services," in *Proceedings of the IEEE Vehicular Technology Conference*, vol. 2, June 1997, pp. 969–973.

[27] R. P. Roess, E. S. Prassas, and W. R. McShane, *Traffic Engineering*, 3rd ed. Prentice Hall, 2004.

[28] C. A. O'Flaherty, Ed., *Transport Planning and Traffic Engineering*, 3rd ed. Elsevier, Butterworth-Heinemann, 2006.

[29] P. Perreira, A. Casaca, J. Rodrigues, J. T. V. Soares, and C. C. Pastor, "From delay-tolerant networks to vehicular delay-tolerant networks," *IEEE Communications Surveys and Tutorials*, vol. PP, no. 99, pp. 1–17, Early Access 2011.

[30] G. Karagiannis, O. Altintas, E. Ekici, G. Heijenk, B. Jarupan, K. Lin, and T. Weil, "Vehicular networking: A survey and tutorial on requirements, architectures, challenges, standards and solutions," *IEEE Communications Surveys and Tutorials*, vol. 13, no. 4, pp. 584–616, Fourth Quarter 2011.

[31] J. Luo and J. P. Hubaux, "A survey of inter-vehicle communication," *EPFL Technical Report IC/2004/24, CH-1015, Lausanne, Switzerland*, 2004.

[32] F. Qu, F. Wang, and L. Yang, "Intelligent transportation spaces: Vehicles, traffic, communications and beyond," *IEEE Communications Magazine*, vol. 48, no. 11, pp. 136–142, November 2010.

[33] M. Sichitiu and M. Kihl, "Inter-vehicle communication systems: A survey," *IEEE Communications Surveys and Tutorials*, vol. 10, no. 2, pp. 88–105, November 2008.

[34] M. G. Rubenstein, F. B. Abdesslem, M. D. D. Amorim, S. R. Cavalcanti, R. D. S. Alves, L. H. M. K. Costa, O. C. M. B. Duarte, and M. E. M. Campista, "Measuring the capacity of in-car to in-car vehicular networks," *IEEE Communications Magazine*, vol. 47, no. 11, pp. 128–136, November 2009.

[35] L. Frank and F. G. Castineira, "Using delay tolerant networks for car2car communications," in *Proceedings of the International Symposium on Industrial Electronics*, Vigo, Spain, June 2007, pp. 261–266.

[36] T. L. Willke, P. Tientrakool, and N. F. Maxemchuk, "A survey of inter-vehicle communication protocols and their applications," *IEEE Communications Surveys and Tutorials*, vol. 11, no. 2, Second Quarter 2009.

[37] M. Khabazian and M. K. M. Ali, "A performance modeling of connectivity in vehicular ad hoc networks," *IEEE Transactions on Vehicular Technology*, vol. 57, no. 4, July 2008.

[38] M. J. Khabbaz, C. M. Assi, and W. F. Fawaz, "Disruption-tolerant networking: A comprehensive survey on recent development and persisting challenges," *IEEE Communications Surveys and Tutorials*, vol. PP, no. 99, pp. 1–34, Accepted 2011.

[39] M. J. Khabbaz, W. F. Fawaz, and C. M. Assi, "Modeling and delay analysis of intermittently connected roadside communication networks," *IEEE Transactions on Vehicular Technology*, Accepted 2012.

[40] M. J. Khabbaz, W. F. Fawaz, and C. M. Assi, "A probabilistic and traffic-aware bundle release scheme for vehicular intermittently connected networks," *IEEE Transactions on Communications*, Submitted 2011.

[41] M. J. Khabbaz, H. M. K. Alazemi, and C. M. Assi, "Delay-optimal data delivery in vehicular intermittently connected networks," *IEEE Transactions on Communications*, Submitted 2012.

[42] A. G. Konheim, "A queueing analysis of two arq protocols," *IEEE Transactions on Communications*, vol. 28, no. 7, July 1980.

[43] S. Y. Wang, "Predicting the lifetime of repairable unicast routing paths in vehicle-formed mobile ad-hoc networks on highways," in *Proceedings of the International Symposium on Personal, Indoor and Mobile radio Communications*, vol. 4, Vigo, Spain, September 2004, pp. 2815 – 2819.

[44] ITS Standards Fact Sheets, "IEEE 1609 - family of standards for wireles access in vehicular environments (wave)." [Online]. Available: http://www.standards.its.dot.gov/fact_sheet.asp?f=80

[45] Research and Innovative Technology Administration, "Intelligent transportation systems report." [Online]. Available: http://ntl.bts.gov/lib/31000/31300/31334/14488_files/sec_5.htm

[46] J. Ott, *From Drive-thru Internet to Delay-Tolerant Ad-Hoc Networking.* Nova Science Publishers INC., 2007.

[47] C. M. Chou, C. Y. Li, W. M. Chien, and K. C. Lan, "A feasibility study on vehicle-to-infrastructure communication: Wifi vs. wimax," in *Proceedings of the 2009 Tenth International Conference on Mobile Data Management: Systems, Services and Middleware*, Washington D.C., United States, June 2009.

[48] A. Bohm and M. Jonsson, "Handover in ieee 802.11p-based delay-sensitive vehicle-to-infrastructure communication," *Research Report IDE-0924*, 2007.

[49] A. Bohm and M. Jonsson, "Supporting real-time data traffic in safety-critical vehicle-to-infrastructure communication," in *Proceedings of the IEEE Conference on Local Computer Networks*, October 2008, pp. 614–621.

[50] S. C. Ng, W. Zhang, Y. Zhang, Y. Yang, and G. Mao, "Analysis of access and connectivity probabilities in vehicular relay networks," *IEEE Journal on Selected Areas in Communications*, vol. 29, no. 1, January 2011.

[51] A. Abdrabou and W. Zhuang, "Probabilistic delay control and road side unit placement for vehicular ad hoc networks with disrupted connectivity," *IEEE Journal on Selected Areas in Communications*, vol. 29, no. 1, pp. 129–139, January 2011.

[52] A. Mansy, M. Ammar, and E. Zegura, "Reliable roadside-to-roadside data transfer using vehicular traffic," in *Proceedings of the IEEE International Conference on Mobile AdHoc and Sensor Systems*, October 2007, pp. 1–6.

[53] B. Petit, M. Ammar, and R. Fujimoto, "Protocols for roadside-to-roadside data relaying over vehicular networks," in *Proceedings of the IEEE Conference on Wireless Communications and Networking*, April 2006, pp. 1–6.

[54] S. Guo, M. H. Falaki, E. A. Oliver, S. U. Rahman, A. Seth, M. A. Zaharia, and S. Keshav, "Very low-cost internet access using kiosknet," *ACM SIGCOMM Computer Communication Review*, vol. 37, no. 5, October 2007.

[55] A. Einstein, "Investigations on the theory of the brownian motion," *Einstein, Collected Papers*, vol. 2, pp. 170–182, January 1956.

[56] D. B. Johnson, D. A. Maltz, and J. Broch, *DSR: The Dynamic Source Routing Protocol for Multi-Hop Wireless Ad Hoc Networks.* Ad-Hoc Networking, Addison-Wesley, 2001.

[57] V. A. Davies, "Evaluating mobility models within an ad hoc network," Master's thesis, Colorado School of Mines, 2000.

[58] F. Bai, N. Sadagopan, and A. Helmy, "The important framework for analyzing the impact of mobility on performance of routing protocols for ad-hoc networks," *Elsevier Ad Hoc Networks*, vol. 1, pp. 383–403, 2003.

[59] M. Lighthill and G. Whitham, "On kinematic waves ii: A theory of traffic flow on long crowded roads," *Royal Society A 229*, pp. 317–345, 1955.

[60] I. W.-H. Ho, K. K. Leung, and J. W. Polak, "Stochastic model and connectivity dynamics for vanets in signalized road system," *IEEE Transactions on Networking*, vol. 29, no. 1, pp. 383–403, January 2011.

[61] D. C. Gazis, R. Herman, and R. W. Rothery, "Delay optimal schedule for a two-hop vehicular relay network," *Journal of the Institute For Operations Research and Management Scenes, Operations Research 9*, pp. 545–567, August 1961.

[62] T.-F. H. R. Center, *Revised Monograph on Traffic Flow Theorys*, 2001.

[63] S. Panwai and H. Dia, "Comparative evaluation of microscopic car-following behavior," *IEEE Transactions on Intelligent Transportation Systems*, vol. 6, no. 3, pp. 314–325, 2005.

[64] M. Aycin and R. Benekohal, "Comparison of car-following models for simulation," *National Research Council Research Record No. 1678 TRB*, vol. 6, no. 3, pp. 116–127, 1999.

[65] Y. Zhang, "Scalability of car-following and lane-changing models in microscopic traffic simulation systems," Master's thesis, Louisiana State University, 2002.

[66] B. Gavish and A. G. Konheim, "Computer communication via satellites - a queueing model," *IEEE Transactions on Communications*, vol. 25, no. 1, January 1977.

[67] A. Einstein, "Performance of protocols in the satellite channel," *L.R.I.*, vol. 2, January 1979.

[68] D. Towsley and J. Wolf, "On the statistical analysis of queue lengths and waiting times for statistical multiplexors with arq retransmission schemes," *IEEE Transactions on Communications*, vol. 27, no. 4, pp. 693–702, April 1979.

[69] D. Towsley, "The stutter go back-N arq protocol," *IEEE Transactions on Communications*, vol. 27, no. 6, June 1979.

[70] A. Jeffrey and D. Zwillinger, Eds., *Gradshteyn and Ryzhik's Tables of Integrals, Series and Products*, 7th ed. 3251 Riverport Ln, Maryland Heights, MO 63043, United States: Academic Press, 2007.

[71] M. Abramowitz and I. A. Stegun, Eds., *Handbook of Mathematical Functions With Formulas, Graphs, and Mathematical Tables*, 10th ed. Washington, D.C. 20402: National Bureau of Standards, Superintendent of Documents, U.S. Government Printing Office, 1972.

[72] L. Kleinrock, *Queueing Systems Volume I: Theory.* Wiley Interscience, 1975.

[73] D. R. Cox, "A use of complex probabilities in the theory of stochastic processes," *Mathematical Proceedings of the Cambridge Philosophical Society*, vol. 51, no. 2, pp. 313–319, April 1955.

[74] L. Garcia, *Probability, Statistics, and Random Processes for Electrical Engineering*, 3rd ed. Upper Saddle River, NJ 07458: Prentice Hall, 2008.

[75] O. K. Tonguz and G. Ferrari, *Ad Hoc Wireless Networks: A Communication-Theoretic Perspective*, 7th ed. John Wiley & Sons, 2006.

[76] N. Wisitpongphan, O. Tonguz, J. Parikh, F. Bai, P. Mudalige, and V. Sadekar, "On the broadcast storm problem in ad hoc wireless networks," in *Proceedings of the International Conference on Broadband Communication Networks and Systems*, San Jose, C.A., United States, October 2006.

[77] M. Torrent-Moreno, D. Jiang, and H. Hartenstein, "Broadcast reception rates and effects of priority access in 802.11-based vehicular ad-hoc networks," in *Proceedings of the ACM International Workshop on Vehicular AdHoc Networks*, Philadelphia, United States, October 2004.

[78] W. Zhao, M. Ammar, and E. Zegura, "A message ferrying approach for data delivery in sparse mobile ad-hoc networks," in *Proceedings of the ACM Mobile AdHoc Networking and Computing*, Philadelphia, United States, 2004, pp. 187–198.

[79] K. Fall, "A delay-tolerant network architecture for challenged internets," *Intel Research Berkley*, 2003.

[80] R. Baumann, S. Heimlicher, and M. May, "Towards realistic mobility models for vehicular ad-hoc networks," in *Proceedings of the International Conference on Computer Communications (INFOCOM)*, Anchorage, Alaska, May 2007.

[81] J. Yoon, M. Liu, and B. Noble, "Random waypoint considered harmful," in *Proceedings of the International Conference on Computer Communications (INFOCOM)*, San Francisco, United States, April 2003.

[82] N. Wisitpongphan, F. Bai, P. Mudalige, V. Sadekar, and O. Tonguz, "Routing in sparse vehicular ad hoc wireless networks," *IEEE Journal on Selected Areas in Communications*, vol. 25, no. 8, October 2007.

[83] S. A. Kulkarni and G. R. Rao, "Vehicular ad hoc network mobility models applied for reinforcement learning routing algorithm," *Contemporary Computing (Springer)*, vol. 95, pp. 230–240, October 2010.

[84] M. Gramaglia, P. Serrano, J. A. Hernandez, M. Calderon, and C. J. Bernardos, "New insights from the analysis of free flow vehicular traffic in highways," in

Proceedings of the International Symposium on a World of Wireless, Mobile and Multimedia Networks, Lucca, Italy, June 2011.

[85] P. M. N. Wisitpongphan, F. Bai and O. K. Tonguz, "On the routing problem in disconnected vehicular ad-hoc networks," in *Proceedings of the International Conference on Computer Communications (INFOCOM)*, 2007.

[86] J. Little, "A proof of the queueing formula: $l = \lambda w$," *Operations Research 9*, vol. 3, pp. 383–387, 1961.

[87] M. Rudack, M. Meincke, and M. Lott, "On the dynamics of ad hoc networks for inter-vehicles communications (ivc)," in *Proceedings of the International Conference on Wireless Networks*, Las Vegas, USA, June 2002.

[88] J. H. Banks, "Freeway speed-flow-concentration relationships: More evidence and interpretations," *Transportation Research Board, Transportation Research Record 1225*, 1989.

[89] C. Abou-Rjeily and M. Bkassini, "On the error and outage performance of coherent uwb systems over indoor wireless channels," in *Proceedings of the Vehicular Technology Conference*, Ottawa, Canada, October 2010.

[90] C. Rose, "Derivation of pascal distribution," November 2007. [Online]. Available: http://www.winlab.rutgers.edu/~crose/541_html/pascal.pdf